

A CHITINOZOAN ANALYSIS OF CORE IGS-527 TO HELP REFINE THE UPPER ORDOVICIAN – LOWER SILURIAN BIOSTRATIGRAPHY OF THE USA MIDCONTINENT

Wiebe Degraeuwe

Student number: 01308741

Promotor: Prof. Dr. Thijs Vandenbroucke

Co-promotor: Dr. Patrick McLaughlin

Jury: Prof. Dr. Stephen Louwye, Prof. Dr. David Van Rooij

Master's dissertation submitted in partial fulfilment of the requirements for the degree of master in geology

Academic year: 2018-2019

Preface

First of all, I would like to thank my promotor, Prof. Dr. T. Vandenbroucke, for giving me the opportunity to work on this topic, for the help during the long journey this master thesis was and for guiding me in the right direction, especially with the determination of the chitinozoans. I would also like to thank my co-promotor, Dr. P. McLaughlin, for providing me with the isotope curves and additional data and giving me new insights by answering all of my questions. Julie De Weirdt deserves a special thanks for answering all of my questions, processing a few samples, checking my text and guiding me through my thesis. Also a big thank you to Tim De Backer for getting me started with photoshop so I did not had to watch hours of tutorials on the internet and to Sabine Van Cauwenberghe for helping me with the lab work. Thanks to Renaat Desaville for coating all of my samples.

Finally, I would like to thank my parents for believing in me and helping wherever they could, my friends and my girlfriend for being patient with me during these long weeks and giving me courage when I needed it.

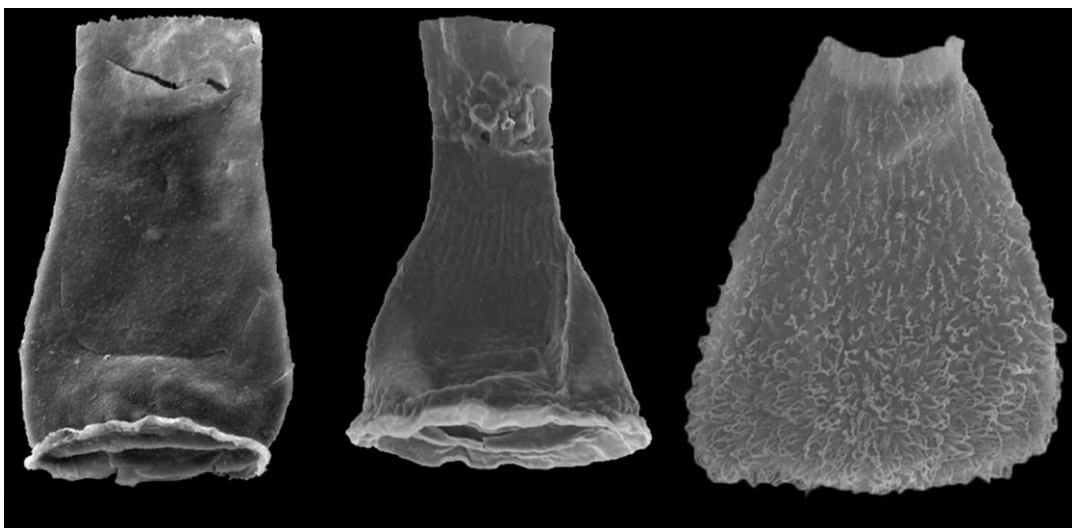
Story of my research

When I graduated from high school, I had to choose what I was going to study here at Ghent University. It was clear for me that it would be something scientific, but what exactly I did not know. I was always very interested in animals and plants so biology seemed like a good path to follow. Also the world itself appealed to me, how everything originated, how seas and mountains formed, volcanoes and so on. Then someone told me about geology, which I had not heard of before. I did some research and signed up for it. So here I am, a few years later, writing my master thesis to get my degree of Master of Science in Geology. This thesis brings my interest for both biology and geology together.

What I love about this thesis, and micropalaeontology in general, is the fact that we can get a lot of information just from microfossils, such as chitinozoans, that are only a few micrometers in size. Although they are millions of years old, they are well preserved and you can use these tiny animals to build the stratigraphy of an area. This is really something magnificent. The fact that it has been unknown for a long time what they are and the animals that produced them still are unknown makes it even more stunning.

A master thesis like this one gives you a good idea of how research 'in the real world' is done. It was fun to start from scratch, even if the core was already collected prior to my involvement in the project, and to conduct my own research. I enjoyed being in the lab dissolving all the samples, picking the chitinozoans and even though the SEM at Ghent University was not state of the art anymore and the room was very hot on warm and sunny days, I enjoyed being there taken pictures of my samples. The identification of the specimens was a slow process and sometimes frustrating. There are so many different species and so many details you have to take into account, but this made it even more rewarding each time I made a correct identification.

My master thesis is only a small part of a larger project including many thesis's like this one and projects by researchers in different countries. All of these pieces of the puzzle may lead to more important breakthroughs in our understanding of the Upper Ordovician and lower Silurian stratigraphy of the US Midcontinent and Earth's processes in general. I can only have much respect to all the scientists who work on this topic and contribute to unraveling the complex history of the Earth.



Abstract

A large-scale stratigraphic framework for the Midcontinent of the USA is currently being constructed by collecting and comparing data from multiple scientific fields. Recent studies have focused on the Upper Ordovician, while not much research has been done on the lower Silurian biostratigraphy. In this context, core IGS-527 was sampled in Carrol County, Indiana, providing a section that could cover the Upper Ordovician and lower Silurian strata of the Illinois Basin. Creating such a stratigraphic framework can improve our understanding about the redox state of the paleo-oceans, stable isotope excursions and associated (mass) extinction events.

In this study, a chitinozoan biostratigraphic framework was constructed from core IGS-527 based on 22 samples yielding 4151 specimens of which 2339 were identified down to species level. These were assigned to 31 different species. Using this framework, we investigate if core IGS-527 indeed covers the Upper Ordovician-lower Silurian interval and we try to provide an age for the samples. Stable carbon isotope analysis of the core revealed the tail end of the Hirnantian Carbon Isotopic Excursion (HICE) and the Paroveja Excursion from Ainsaar et al. (2010). Correlations are made with Upper Ordovician and lower Silurian sections across north America for which the chitinozoan biostratigraphy has already been established. Correlation with the Maquoketa Group in Wisconsin, the Cincinnati Arch Region in Ohio and the Vauréal and Ellis Bay formations on Anticosti Island showed a discrepancy between the bio- and chemostratigraphical observations and requires further research. This study seems to confirm that core IGS-527 indeed covers the Upper Ordovician-lower Silurian interval and that the ages of the samples largely correspond with the age of the provisional lithostratigraphic units and chemostratigraphy.

Table of contents

Preface	3
Story of my research	4
Abstract	5
1. Introduction	8
1.1. Rationale	8
1.2. Research questions.....	9
1.3. Research objectives	10
1.4. The Ordovician world.....	10
1.4.1. Palaeogeography	10
1.4.2. Palaeoclimate and palaeoceanography.....	11
1.5. The Silurian world.....	12
1.5.1. Palaeogeography	12
1.5.2. Palaeoclimate and palaeoceanography.....	14
1.6. Upper Ordovician chronostratigraphy	14
1.6.1. Sandbian Stage ($458.4 \pm 0.9 - 453.0 \pm 0.7$).....	15
1.6.2. Katian Stage ($453.0 \pm 0.7 - 445.2 \pm 1.4$).....	15
1.6.3. Hirnantian Stage ($445.2 \pm 1.4 - 443.8 \pm 1.5$).....	15
1.6.4. Regional stratigraphic units	15
1.7. lower Silurian chronostratigraphy	16
1.7.1. Regional stratigraphic units	17
1.8. Geological setting	17
1.8.1. Structural setting and history of the Illinois Basin	17
1.8.2. Core location	18
1.9. Lithostratigraphy	19
1.9.1. Upper Ordovician lithostratigraphy	19
1.9.2. lower Silurian lithostratigraphy.....	20
1.9.3. Provisional lithostratigraphy of core IGS-527	21
1.9.3.1. Sexton Creek Limestone	21
1.9.3.2. Cape La Croix Shale.....	22
1.9.3.3. Fernvale Formation.....	22
1.9.3.4. Liberty Formation.....	23
1.10. Carbon Isotope Excursions.....	23
1.10.1. General overview.....	23
1.10.2. Upper Ordovician carbon isotope excursions	23
1.10.3. lower Silurian carbon isotope excursions	25
1.10.4. Stable carbon isotope curve of core IGS-527.....	26
1.11. Biostratigraphy.....	27

1.11.1.	Upper Ordovician biostratigraphy	27
1.11.1.1.	Graptolites and conodonts	27
1.11.1.2.	Chitinozoans	28
1.11.2.	lower Silurian biostratigraphy	28
1.11.2.1.	Graptolites and conodonts	28
1.11.2.2.	Chitinozoans	30
2.	Methodology	31
2.1.	Chitinozoans	31
2.1.1.	Morphology and structure	31
2.1.2.	Biological interpretation and systematic position	32
2.1.3.	Classification	33
2.1.4.	Biostratigraphic value	33
2.2.	Core sampling	33
2.3.	Sample selection	34
2.4.	Sample preparation	34
2.5.	Picking and light microscopy	35
2.6.	Scanning Electron Microscopy (SEM) imaging	35
2.7.	Palynological identification	35
3.	Results	37
3.1	Overview	37
3.2.	Stratigraphic ranges of selected species	40
3.3.	Systematic palaeontology	41
3.3.1.	Alphabetical list	41
3.3.2.	Systematics	41
4.	Discussion	42
4.1.	Assemblages	42
4.2.	Correlations	42
4.2.1.	Correlation with the Maquoketa Group of Indiana (De Boodt, 2018)	42
4.2.2.	Correlation with the Maquoketa Group of Wisconsin (De Backer, 2017)	43
4.2.3.	Correlation with the Arbuckle Mountains, Oklahoma	44
4.2.4.	Correlation with the Fernvale of Tennessee (Meyvisch, 2018)	46
4.2.5.	Correlation with the Cincinnati Arch, Ohio	48
4.2.6.	Correlation with Anticosti Island	49
4.2.7.	Correlation with western Illinois (core Principia #4)	51
4.2.8.	Correlation with Nevada	52
5.	Conclusions	54

1. Introduction

1.1. Rationale

This master dissertation is part of a larger research project between the Department of Geology of the Ghent University, Dr. Patrick McLaughlin (Indiana Geological and Water Survey, IGWS) and Dr. Poul Embso (United States Geological Survey, USGS). The intention of the research project is to shed a light on the interplay of processes within the ancient Earth's system in geochemistry, palaeogeography, oceanography and climatology and how these interactions induced major palaeobiological events such as the Late Ordovician mass extinction (LOME). The Upper Ordovician-lower Silurian stratigraphic record from eastern North America is used in order to resolve this complex puzzle. This stratigraphic succession is preserved across a wide geographic area, stretching from the US Midcontinent all the way to the east coast. The first step in this process is to untangle the stratigraphy of the succession, which includes solving a range of the standing stratigraphic issues (see below), using a holostratigraphic methodology. By combining facies analysis, stable carbon isotope chemostratigraphy, astrochronology and biostratigraphic occurrences of index fossils such as graptolites, conodonts and chitinozoans, a larger-scale picture is emerging. Previous work across these disciplines, including datasets from drill cores and road cuts from all over the eastern North American continent resulted in a (provisional) sequence stratigraphic model for the Illinois Basin (Fig. 1; Patrick McLaughlin (Pers. Comm.)). This model acts as a solid foundation for further research, from which to build an advanced understanding of the distribution of the strata, both in time and in space, and from which their local and global correlation can be improved.

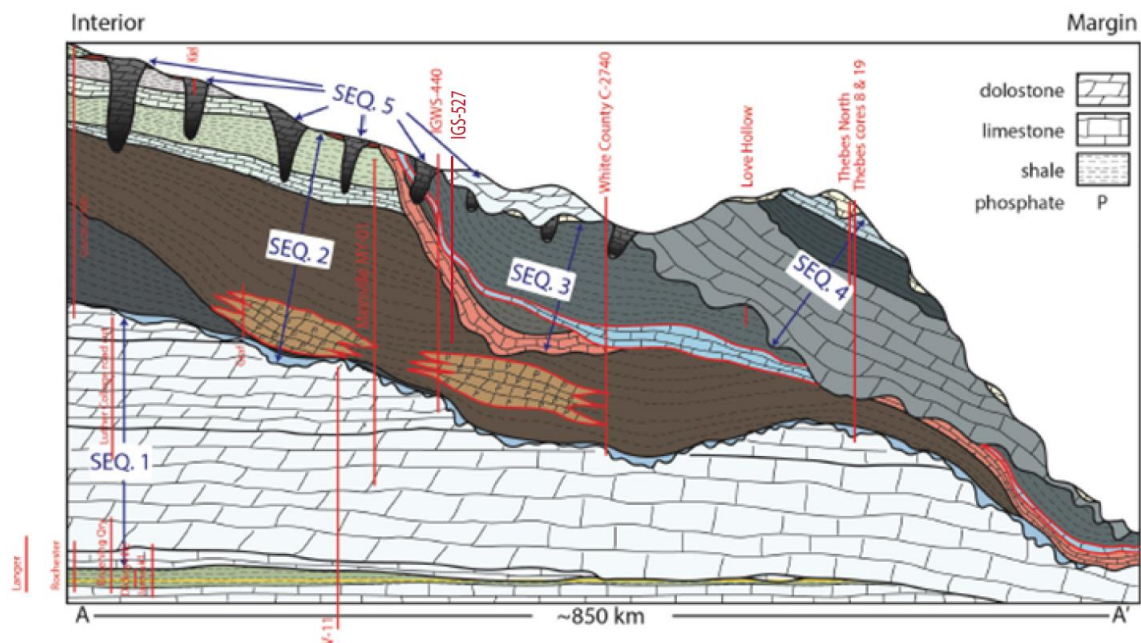


Figure 1: Sequence stratigraphic model of the Illinois Basin. 5 sequences are indicated in blue, sections and cores analysed by the UGent group are indicated in red (e.g. Gardner Kiln core (De Backer, 2017), core IGWS-440 (De Boodt, 2018), cores MY-14 and BV-11 (Velleman, 2016), Langer core (Bas, 2017), James #1 and Bruening quarry sections (De Waele, 2018), White County C-2740 core (Meyvisch, 2018) and core IGS-527 (this study)). Modified from Patrick McLaughlin (Pers. Comm.).

However, a series of questions remain that need to be solved. A preferred tool to address these stratigraphic questions uses trends in stable carbon isotope chemostratigraphy (McLaughlin et al., 2012), as these provide high-resolution correlations across facies. However, it is difficult to use this method on its own because very few stable carbon isotope excursions have a unique signature that can be used to discriminate it from other, similar excursions of comparable amplitude and signature (Bergström et al., 2010). Therefore, this technique should be used in combination with a biostratigraphical approach, which does provide a unique signal (Kaljo et al., 2007). A historical biostratigraphic framework in place of some of the units under scrutiny, palynomorphs (organic

walled microfossils) now are being extensively studied by the research group, as they can improve the current biostratigraphic resolution. This master thesis is part of this focused effort. By combining all of the different stratigraphic methods, the resolution and certainty of the final model will improve and will give additional insights and higher certitude about the palaeo-environmental conditions during the Late Ordovician and early Silurian, and the contemporaneous events (extinctions and radiations) that shaped the evolution of Palaeozoic life.

In this context, a high-resolution Upper Ordovician and lower Silurian biostratigraphy is currently being developed, by analyzing the palynological content of a selection of cores in and around the Illinois Basin. This effort so far has focused on the Upper Ordovician. The research is conducted at the Department of Geology of Ghent University and encompasses several PhD projects and master dissertations (including this one). For his master dissertation, Velleman (2016) studied two cores from the Cincinnati Arch region: BV-11 and MY-14 (Upper Sandbian to Katian). He correlated the two cores and studied the chitinozoan assemblages that he could relate to four stable carbon isotope excursions identified by Bergström et al. (2010) (early Katian Guttenberg isotope carbon excursion (GICE), Kope, Fairfiew and Waynesville). This allowed him to anchor the carbon isotope excursions to his chitinozoan biostratigraphy. His research was extended by De Backer (2017) and Bas (2017). De Backer studied the Gardner Kiln core, piercing through the Maquoketa Group (Upper Katian), located in the Michigan Basin area in Wisconsin. He discovered rich and excellently preserved chitinozoan assemblages from the Maquoketa Group that he could position against the Waynesville excursion and the overlying Whitewater isotope excursion. Bas (2017) studied the Langer core (Upper Ordovician Galena Group) from the Upper Mississippi Valley in western Wisconsin. She could correlate the chitinozoan assemblages of the core with the GICE present in the section she analyzed. Her study formed the basis of a Katian biostratigraphy in the Wisconsin area. De Boodt (2018) studied the palynological content of the IGWS-440 core from Newton County, north-western Indiana. She tried to assess the age of the Upper Ordovician Maquoketa Group in this region more accurately. The lower part of her core resembled the (Richmondian) Maquoketa Group as studied by De Backer (2017) in his Gardner Kiln core. Based on chitinozoan assemblages in the upper part of her core, she was able to make correlations with the Katian Sylvan Shale of Oklahoma and the lower Ellis Bay Formation of Anticosti Island. Meyvisch (2018) studied the Mannie Shale from the Appalachian Basin and the Cape La Croix Shale from the Illinois Basin and he suggested a possible equivalence between them. He also correlated these two shales with the Sylvan shale of the Arbuckle Mountains in Oklahoma. Other studies to establish an Upper Ordovician biostratigraphic framework of the US Midcontinent include the master dissertation of De Waele (2018).

Once a valid and detailed stratigraphic framework for the US Midcontinent is built, it will enable the research team to investigate hypotheses about the redox state of the palaeo-oceans during the late Ordovician and a lower Silurian. Oceanic anoxic events (OAE's) of the Mesozoic oceans are known to record major changes in the palaeoceanographic and climatic state of the Earth and represent major disturbances in the global carbon cycle (Jenkyns, 2010). Recent studies on the end-Ordovician (Hirnantian) $\delta^{13}\text{C}_{\text{carb}}$ excursion (De Weirtdt et al., 2016; De Weirtdt et al., 2017; Hammerlund et al., 2012; Vandenbroucke et al., 2015) and on Silurian $\delta^{13}\text{C}_{\text{carb}}$ excursions of the Telychian, Sheinwoodian and Pridoli suggest that this is also the case for some Palaeozoic stable carbon isotope excursions (Embsø et al., 2010; McLaughlin et al., 2012; Vandenbroucke et al., 2015). The fact that many of these Palaeozoic stable isotope excursions coincides with (mass) extinction events makes it a topic of interest amongst researchers.

1.2. Research questions

Recent studies have focused on building and enhancing the chitinozoan biostratigraphy of the Upper Ordovician in NW Indiana (De Boodt, 2018), NW Wisconsin (De Backer, 2017), Anticosti Island, Quebec (Achab et al., 2013), central Nevada and Arctic Canada (Soufiana and Achab, 2000b), but not much research has been done on the lower Silurian biostratigraphy. This study will focus on enhancing the Upper(most?) Ordovician and especially the lower Silurian biostratigraphical

framework for the Indiana region of the US Midcontinent. Core IGS-527 in northern Indiana has the potential to cover this current gap in our framework, as indicated by its (trace)elemental composition and its stable carbon isotope chemostratigraphy (Patrick McLaughlin, Pers. Comm.). The tail end of the HICE and the Paroveja excursion of Ainsaar et al. (2010) are identified in the $\delta^{13}\text{C}$ curve of core IGS-527 (Patrick McLaughlin, Pers. Comm.). He also provided a provisional lithostratigraphy of the core, including the following units (from bottom to top of the core): Liberty Formation, Fernvale Limestone Formation, Cape La Croix Shale and Sexton Creek Formation.

Although this initial assessment suggest a preliminary stratigraphy for core IGS-527, a number of specific questions remain:

- Does the core indeed covers the Upper Ordovician-lower Silurian interval that is so far missing in the chitinozoan biostratigraphic framework for the USA Midcontinent? What assemblages do the samples contain in this interval? Can the other assemblages be correlated to those of parallel studies in the wider area?
- What is the age of the samples retrieved from core IGS-527? Do these ages align with or confirm the provisional lithostratigraphy and chemostratigraphy of McLaughlin?
- One of the most interesting units in this context is the Fernvale Limestone Formation (524-531 ft depth). It was unexpected to find this unit (or a facies very much like it?) this far east, and so far is the only record of this unit in Indiana. Can we confirm it has similar assemblages to this unit in its type area?
- What is the age of the peculiar laminated facies, the provisional Cape La Croix Shale, at the base of what is currently referred to as the Sexton Creek Formation?

1.3. Research objectives

Core IGS-527 provides a section that covers Upper Ordovician and lower Silurian strata of the Illinois Basin. In this master dissertation, I will try to assess the age of these strata as accurately as possible by correlating the observed chitinozoan assemblages with known and previously described Upper Ordovician and lower Silurian assemblages found at other locations, and by correlating with the provided isotope excursions.

The objectives of this master dissertation are:

- To make an assessment of the chitinozoan assemblages present in the core
- To correlate this core with other sections based on chitinozoan biostratigraphy
- To build a biostratigraphic framework based on chitinozoans for the Upper Ordovician-lower Silurian for core IGS-527
- To identify assemblages that can be correlated with other sections, and especially identify (uppermost Ordovician?) assemblages that may be missing from (these specific intervals of) the current stratigraphic framework
- To assess, biostratigraphically, the (potential) presence of the Fernvale Limestone Formation in northern Indiana

1.4. The Ordovician world

1.4.1. Palaeogeography

The Ordovician period is characterized by large amounts of tectonic activity, volcanism and important plate dispersion. The plate tectonic setting in the Middle Ordovician (ca. 460 Ma) shows that there are four major palaeocontinents present: Baltica, Gondwana, Laurentia and Siberia (Fig. 2). In between those four major continents, smaller micropalaeocontinents, e.g. Avalonia, were present (Torsvik and Cocks, 2016). At the start of the Ordovician, the major oceans were at their widest (Cocks and Torsvik, 2002).

The northern hemisphere was occupied by the vast Panthalassic Ocean and the landmasses were mostly concentrated in the southern hemisphere. Laurentia consisted mainly of North America, Greenland and parts of Scotland and Ireland and was separated from Gondwana (South America) and Baltica by the Lapetus Ocean (Fig. 2; Cocks and Torsvik, 2002, 2011; Achab and Paris, 2007).

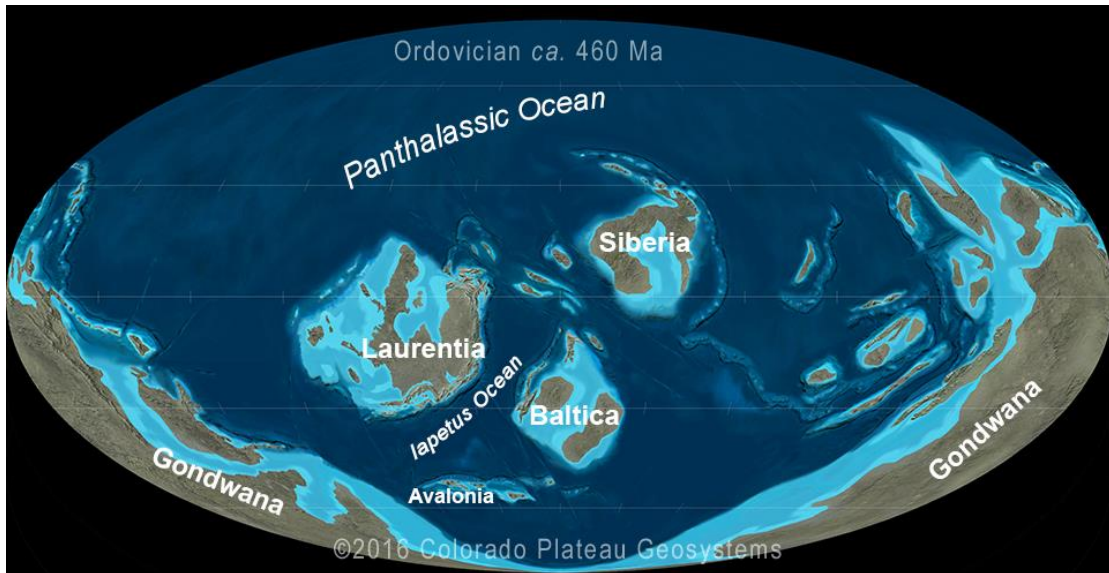


Figure 2: Palaeogeographic reconstruction of the Earth during the Middle Ordovician (ca. 460 Ma). The major continents and oceans are indicated. From Meyvisch (2018), modified from the original picture at <http://deeptimemaps.com/global-series-thumbnails>.

The largest palaeocontinent was Gondwana, which stretched from the South Pole all the way to the equator (Fig. 2). The Gondwanan core consists of present day Africa, Arabia, Madagascar, Greater India, most of Antarctica, most of Australia, New Guinea and most of South America (Cocks and Torsvik, 2002). Avalonia was part of the NW margin of Gondwana, but split off due to rifting at the end of the Cambrian and beginning of the Ordovician (Prigmore et al., 1997). Avalonia drifted rapidly northward and collided with Baltica at the Ordovician-Silurian transition (Torsvik et al., 1992). During this period, the Rheic Ocean between Gondwana and Avalonia was at its widest (Cocks and Torsvik, 2002).

Baltica moved rapidly from the cool temperate climate zone around 50°S towards warmer temperate latitudes, reaching about 40°S in the mid-Darriwilian (Middle Ordovician) (Torsvik et al., 2012). This movement was the result of the opening of the Rheic Ocean and happened simultaneous with the closure of the Lapetus Ocean and the Tornquist Ocean. They are located respectively between Laurentia, Baltica and Avalonia (Fig. 2) and between Baltica and Avalonia (Torsvik and Rehnström, 2003). The closing of the Tornquist Ocean and collisions of terranes and volcanic arcs along this Laurentian margin created the Taconic orogeny (Torsvik and Cocks, 2016).

1.4.2. Palaeoclimate and palaeoceanography

The Ordovician is not only characterized by volcanism and tectonic activity, but also by high sea levels, perhaps even the highest in the Phanerozoic (Nielssen, 2004), and are estimated to be 100-200 m higher than today (Haq and Schutter, 2008). It was also a period of major climatic changes and fluctuations. The Lower and Middle Ordovician were previously considered to have experienced greenhouse climate conditions with only a short and intense glaciation event in the Hirnantian (uppermost Ordovician). This is based on Lower and Middle Ordovician data suggesting high relative global sea levels and light marine $\delta^{18}\text{O}_{\text{Carb}}$ -values from limestones and brachiopod shells (Brenchley et al., 1994).

Other authors challenge the idea of a warm greenhouse Ordovician period. Based on sequence stratigraphy and stable isotope data, they suggested that there was a steady cooling of the climate throughout the Ordovician which already started before the Hirnantian glaciation (Pope and Read, 1998; Saltzman and Young, 2005; Dabard et al., 2015; Nardin et al., 2011; Bennett et al., 2018).

Recent studies show that the atmospheric CO₂ content was probably much lower than previously proposed (Rothman, 2002; Vandenbroucke et al., 2010a; Pancost et al., 2013) and that ocean temperatures reached modern-like values as early as the Middle Ordovician (Trotter et al., 2008; Vandenbroucke et al., 2010b).

Based on conodont O-isotope data, Trotter et al. (2008) argued that there was a steady cooling trend through the Early Ordovician reaching modern equatorial temperatures that were sustained throughout the Middle and Late Ordovician. Based on stable carbon isotope data of benthic fossils, Rasmussen et al. (2016) observed an overall temperature decrease of 4-5°C across the Dapingian-Darriwilian (Middle Ordovician), which according to them represents a shift in the sea floor temperature. They concluded that this temperature drop represents a major ocean cooling and a shift from greenhouse to icehouse conditions, causing a major glacioeustatic sea level drop and that the onset of the icehouse conditions already started around the Early-Middle Ordovician boundary.

The cooling of the climate during the Ordovician resulted in vast widespread continental ice sheets and a major ice cap on Gondwana at the end of the Ordovician. This was confirmed by recent studies of Pohl et al. (2016). They used an Earth system model with an innovative coupling method between ocean, atmosphere and land ice accounting for climate and ice sheet feedback processes. More specifically a Fast Ocean Atmosphere Model (FOAM) with Community Climate Model version 2 (CCM2) as the atmospheric component and Ocean Model version 3 (OM3) as the ocean module. Sea ice was simulated with the aid of thermodynamics of the National Center for Atmospheric Research's (NCAR) Climate System Model 1.4.

Based on boundary conditions predicated on a wide range of suggested Ordovician *p*CO₂ values (3-24), their models suggest that Gondwana was covered by a single ice sheet extending from the South Pole (North Africa) to the tropics (South Africa) during the latest Ordovician, under a *p*CO₂ regime from 8 to 3 PAL. This Ordovician ice sheet emerged in two discrete phases. During the first phase, the continental ice sheet appeared suddenly in a warm climate and covered Gondwana from the South Pole to midpalaeolatitudes, as from a *p*CO₂ threshold of 16-12 PAL. It was only during the second phase when the atmospheric CO₂ levels dropped further, that the temperatures dropped steeply (tropical SST dropped by ~ 8°C) and sea ice extended to the tropics (South Africa). This marked the onset of the Hirnantian glacial maximum. Combining the GCM output with sedimentological, geochemical and micropalaeontological data, Pohl et al. (2016) suggested that the first step of the Ordovician ice sheet growth occurred already at the Darriwilian (Middle Ordovician), which was also suggested by Rasmussen et al. (2016). All this evidence leads to the paradigm of an 'early Palaeozoic Ice Age' (EPI) (Page et al., 2007) and that glacial onset predated Late Ordovician climate cooling (Pohl et al., 2016).

1.5. The Silurian world

1.5.1. Palaeogeography

As mentioned before, Avalonia and Baltica collided at the Ordovician-Silurian transition around 443 Ma (Torsvik et al., 1992) and during this period, the Rheic Ocean was at its widest (Fig. 3). The combined landmasses of Avalonia and Baltica collided with Laurentia and formed the major continent of Laurussia. This collision caused the Caledonian Orogeny, a major event with complex sequences of tectonic events (Cocks and Torsvik, 2002; Torsvik and Cocks, 2013).

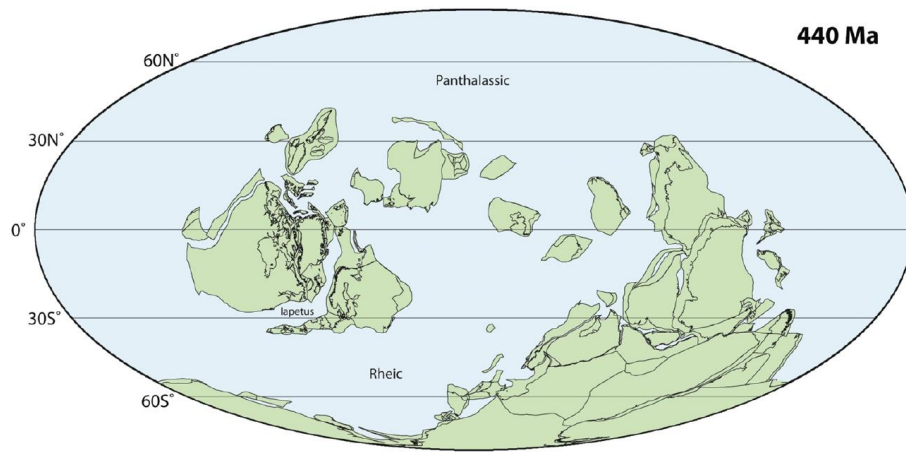


Figure 3: Palaeogeographic reconstruction of the Earth around 440 Ma (early Silurian: Rhuddanian). Names of the palaeocontinents and oceans are shown in figure 5. From Torsvik and Cocks (2013).

At the beginning of the Silurian, Siberia started moving from low southerly latitudes, across the Equator towards intermediate northerly latitudes (Figs. 3 and 4; Cocks and Torsvik, 2002).

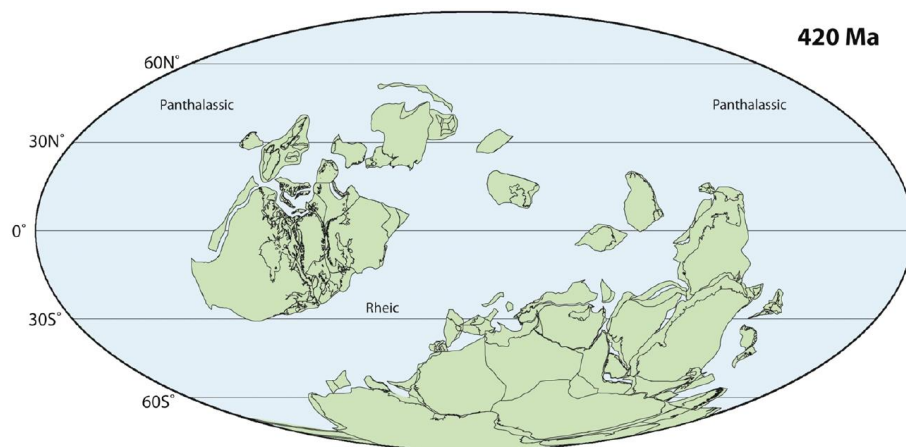


Figure 4: Palaeogeographic reconstruction of the Earth at the end of the Silurian around 420 Ma (Ludfordian). Names of the palaeocontinents and oceans are shown in figure 5. From Torsvik and Cocks (2013).

Towards the end of the Silurian period, rifting occurred at the northern margin of Gondwana, followed by the opening of the Palaeotethys Ocean which was located between North Africa and the terranes of Armorica and Iberia (Fig. 5). Also around this time, South China moved away from Australia (Torsvik and Cocks, 2013).

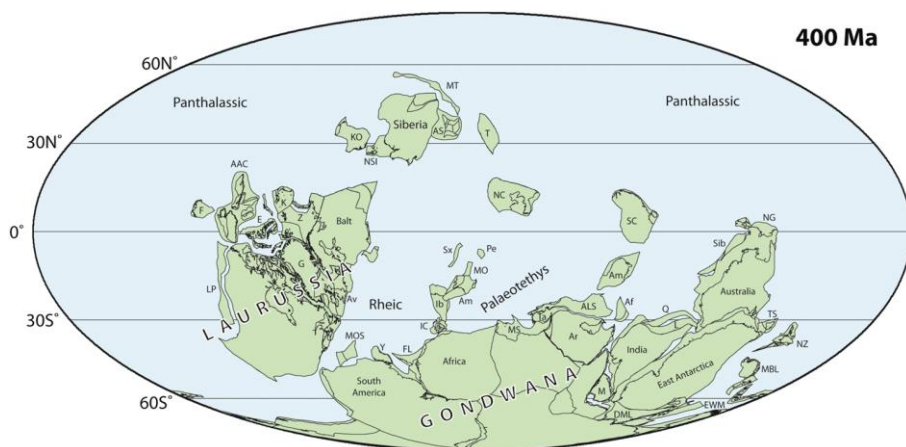


Figure 5: Palaeogeographic reconstruction of the Earth around 400 Ma. From Torsvik and Cocks (2013).

1.5.2. Palaeoclimate and palaeoceanography

The EPI that started in the Ordovician continued into the Silurian. Past work already showed that the Silurian ocean-climate system was highly dynamic (Noble et al., 2005) and within the EPI, glacial maxima were separated by warmer intervals (Fortey and Cocks, 2005). Based on frequent evidence of ice formation and rapid third-order eustatic sea-level variation (Azmy et al. 1998; Caputo, 1998; Loydell et al., 1998; Hamoumi, 1999; Ghienne, 2003; Nielsen, 2003a, b; Johnson, 2006), Page et al. (2007) suggested that ice-sheets may have dynamically expanded and retreated during the EPI. This was confirmed by Trotter et al. (2015) who did a reconstruction of the Silurian climate based on the study of $\delta^{18}\text{O}$ composition of conodonts. Their records show that the Silurian period knew significant climate variability with warm periods that had equatorial temperatures even warmer than today. The EPI ended with the Ireviken event deglacial transgression of the earliest Wenlock (Page et al., 2007), which occurred at a time of climatic amelioration (Cramer and Saltzman, 2005, 2007a). Although the Silurian climate was dynamic, there was an overall warming trend until the end of the Llandovery, reaching maximum temperatures during the middle Llandovery (Trotter et al., 2015). The early and late Wenlock are characterized by two major cooling peaks during which the temperatures decreased up to 8°C. The rest of the Silurian period experienced warmer conditions, except for the middle Ludlow which was subjected to extreme short-lived and rapid warming-cooling events (Trotter et al., 2015).

The Silurian period is characterized by significant eustatic sea-level fluctuations (Johnson, 1987, 1996; Loydell, 1998; Johnson, 2006, 2010; Davies et al., 2016). Sea levels were at its highest during the Katian and from the latest Ordovician into the early Silurian, there was a sharp fall of the sea level. Sea levels rose again just before the end of the Rhuddanian and in the middle and late Aeronian. In between these periods of high sea levels, periods of low sea levels occurred (Davies et al., 2016). Sea levels culminated in the middle Wenlock followed by a decline from Ludlow through the Early Devonian (Haq and Schutter, 2008).

1.6. Upper Ordovician chronostratigraphy

The international chronostratigraphic chart (ICC) divides the Ordovician into 3 series and 7 stages. The Upper Ordovician Serie comprises 3 stages, the Sandbian, the Katian and the Hirnantian (Fig. 6).

GLOBAL			UNITED KINGDOM		NORTH AMERICA		BALTOSCANDIA		Stage Slices (SS)	STAGE SLICE BASE
SYSTEM	SERIES	STAGE	SERIES	STAGE	SERIES	STAGE	SERIES	STAGE		
ORDOVICIAN	UPPER ORDOVICIAN	HIRNANTIAN	ASHGILL	HIRNANTIAN	CINCINNATIAN	GAMACHIAN	HARJU	PORKUNI	Hi2	end of HICE
				RAWTHEYAN CAUTLEYAN PUSGILLIAN		RICHMONDIAN		PIRGU	Hi1	<i>N. extraordinarius</i> Zone (g)
				STREFFORDIAN CHENEYAN		MAYSVILLIAN EDENIAN		VORMSI NABALA	Ka4	<i>D. complanatus</i> Zone (g)
		CHATFIELDIAN	RAKVERE OANDU KEILA			Ka3		<i>A. ordovicicus</i> Zone (c)		
						Ka2		<i>P. linearis</i> Zone (g)		
		SANDBIAN	KATIAN	CARADOC		BURRELLIAN		MOHAWKIAN	TURINIAN	VIRU
	AURELUCIAN				CHAZYAN	KUKRUSE	Sa2		<i>C. bicornis</i> Zone (g)	
							Sa1		<i>N. gracilis</i> Zone (g)	
	WHITE-POUNIAN									

Figure 6: Compilation of the Upper Ordovician global and regional chronostratigraphy for the United Kingdom, North America and Baltoscandia. The stage slices (SS) are given together with the graptolite (g) and conodont (c) biozones that define their bases. Modified from Bergström et al. (2009).

1.6.1. Sandbian Stage ($458.4 \pm 0.9 - 453.0 \pm 0.7$)

This is the lowest stage of the Upper Ordovician. It sits above the Darriwilian of the Middle Ordovician and is overlain by the Katian stage. The GSSP (Global Boundary Stratotype Section and Point) of this stage, and the base of the Upper Ordovician, is placed at Fågelsång in southern Sweden (Bergström et al., 2000). The name of this stage is derived from the Community of South Sandby, where this section is located. The Sandbian Stage is a global stage and the stratigraphic interval runs from the base of the *Nemagraptus gracilis* Graptolite Biozone to the base of the *Diplacanthograptus caudatus* Graptolite Biozone (Fig. 6; Bergström et al., 2006). If we look at the conodont biostratigraphy, the base of the Sandbian Stage has the same age of a level near the middle of the *Pygodus anserinus* Biozone (Bergström et al., 2000).

1.6.2. Katian Stage ($453.0 \pm 0.7 - 445.2 \pm 1.4$)

The Katian Stage is the second stage of the Upper Ordovician (Fig. 6). The GSSP of this stage is defined as the 4.0 m-level above the base of the Bigfork Chert in the Black Knob Ridge section in southeastern Oklahoma, USA (Goldman et al., 2007). This point marks the first appearance datum (FAD) of the globally correlatable graptolite *Diplocanthograptus caudatus*. The Katian Stage comprises the entire *D. caudatus* Biozone and runs to the base of the *Normalograptus extraordinarius* Graptolite Biozone (Fig. 6). The Black Knob Ridge section also contains stratigraphically important conodonts and chitinozoans. In terms of conodont biostratigraphy, the base of the Katian Stage lies just below the top of the *Amorphognathus tvaerensis* Conodont zone of North America. In terms of chitinozoan biostratigraphy, the base of the *Spinachitina cervicornis* Biozone is correlated with the lower-middle part of the *D. caudatus* graptolite Zone (Goldman et al., 2007; Vandenbroucke et al., 2013).

The name of this stage is derived from Lake Katy which was, before it was drained, located near the southern end of Black Knob Ridge (Bergström et al., 2006).

1.6.3. Hirnantian Stage ($445.2 \pm 1.4 - 443.8 \pm 1.5$)

This stage is the highest stage of the Upper Ordovician Series. The GSSP for the base of this stage is defined at a point 0.39 m below the base of the Kuanyinchiao Bed in the Wangjiawan North section near the village of Wangjiawan, Western Hubei, China (Chen et al., 2006). It coincides with the FAD of the graptolite *Normalograptus extraordinarius* (Fig. 6). Secondary markers for the base of the Hirnantian Stage are the FAD of the graptolite *Normalograptus ojsuensis*, 4 cm below the FAD of *N. extraordinarius* (Chen et al., 2006). The Hirnantian Stage and the Upper Ordovician ends with the end of the *N. extraordinarius* graptolite Biozone.

1.6.4. Regional stratigraphic units

Before the Sandbian, Katian and Hirnantian Stages were officially defined, North American strata were locally assigned to regional chronostratigraphic units (Fig. 6). The regional stratigraphy was based on lithological and biostratigraphical characteristics and variations observed in the regional geology.

The Upper Ordovician comprised three regionally defined series: the Witherockian, the Mohawkian and the Cincinnati Series. The Sandbian comprises the Witherockian Series containing the Chazyan Stage and the lower part of the Mohawkian Series with the Turinian Stage. The base of the Chazyan stage is the same as the base of the Sandbian stage and is defined as the FAD of *N. gracillius* graptolite. The base of the Turinian Stage corresponds with the base of the *Climacograptus bicornis* graptolite Biozone of the Pacific Province (Fig. 6; Bergström et al., 2009) and roughly corresponds to the base of the *D. foliaceus* graptolite Biozone of the Atlantic Province. It also coincides with the base of the *Baltoniodus gerdæ* Conodont Subzone (Ross et al., 1982).

The Katian comprises the Chaffeldian Stage, which is the upper part of the Mohawkian Series, and the lower part of the Cincinnati Series containing the Edenian, Maysvillian and Richmondian Stages. The small Chaffeldian Stage has its base located just below the base of the Katian Stage and stretches until the lower Katian (Bergström et al., 2009). The Cincinnati Series has its base located just above the *Belodina confluens* Midcontinent Conodont Zone and the *Amorphognathus superbus* Atlantic Conodont Zone (Bergström and Mitchell, 1986, 1990, 1994) and near the top of the *Diplacanthograptus spiniferus* Graptolite Zone. It corresponds to an early Katian age (Bergström et al., 2009).

The Hirnantian comprises the Gamachian Stage, which is the upper part of the Cincinnati Series. All four stages of the Cincinnati Series are largely based on shelly fossils and although graptolites are present, which makes the correlation to international chronostratigraphy (which is based on standard graptolite zones) possible, these correlations are not precise and their chronostratigraphic boundaries are not yet accurately defined (Bergström et al., 2009).

1.7. lower Silurian chronostratigraphy

The Llandovery Series constitutes the lower half of the Silurian. It comprises all rocks with an age ranging from 443.8 ± 1.5 Ma – 433.4 ± 0.8 Ma (International Commission on Stratigraphy). The Llandovery series is divided into 3 stages: the Rhuddanian Stage, the Aeronian stage and the Telychian Stage (Fig. 7).

A lot of the previously defined GSSP's of Silurian Stages are now being revised for having serious deficiencies (Rong et al., 2008). The International Subcommittee on Silurian Stratigraphy (ISSS) is currently trying to establish new GSSP's for the base of the Telychian and Sheinwoodian Stages. The base of the Aeronian Stage was also under revision of the ISSS, but Štorch et al. (2018) recently proposed a new GSSP for this stage. They proposed the lowest occurrence of the graptolite *Demirtrites triangulates* at the Hlásná Třebaň section in Central Bohemia. *D. triangulates* FAD is 1.38 m above the base of the black-shale succession of the Željkovice Formation in this section. The GSSP of the base of the Rhuddanian Stage (and the Llandovery Series) has also been revised. Although the Stage is named for the Cefn-Rhuddan Farm in the Llandovery area, the GSSP of the Rhuddanian Stage is located 1.6 m above the base of the Birkhill Shale, Dob's Linn in the southern uplands in Scotland. It coincides with the first appearance of graptolite *Akidograptus ascensus*, defining the base of the *A. ascensus* Graptolite Biozone (Williams, 1983: Subcommittee on Silurian stratigraphy).

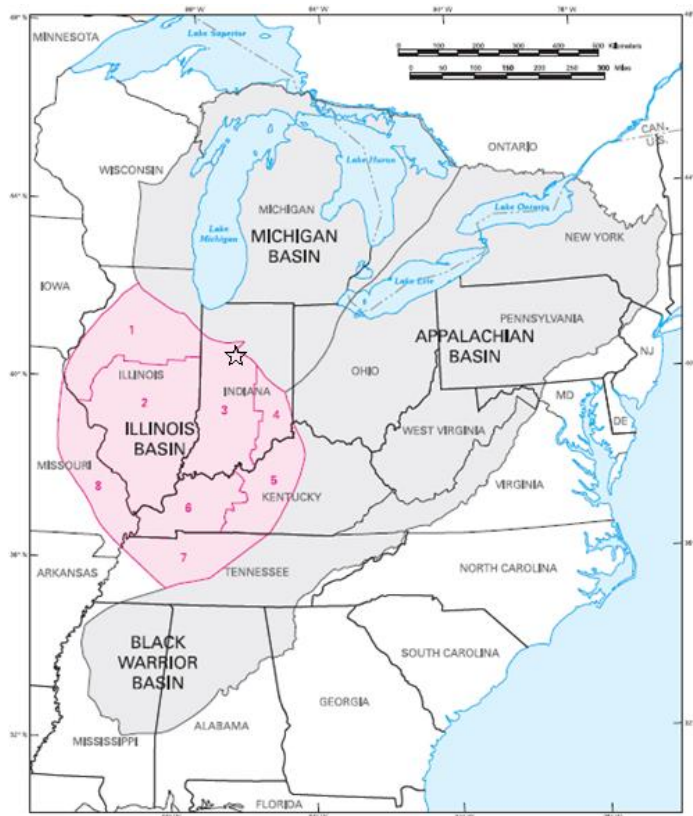


Figure 8: Map of the large structural features of the eastern US midcontinent. The extent of the Illinois Basin is shown in red. The black star indicates the location of core IGS-527. Modified from Swezey (2009).

The formation of the basin was initiated by rifting at the beginning of the Cambrian (ca. 541 Ma) and subsequent rapid mechanical subsidence followed by a period of thermal subsidence (Heidlauf et al., 1986). The thermal subsidence began around 510 Ma and continued until about 360 Ma (Klein and Hsui, 1987). In the beginning, the basin was a rather shallow depression which was structurally only open to the south (west), where the Pascola Arch is situated today (Swann, 1968). So initially, sediments accumulated in a south-facing open-marine embayment that formed by rifting (McGinnis 1970, McGinnis et al., 1976). This caused the deposition of thick Palaeozoic sediment successions in the Illinois Basin, from the Cambrian up to the Pennsylvanian (Buschbach and Kolata, 1990 ; Van der Pluijm and Catacosinos, 1996). The whole region was subjected to uplift towards the end of the Mississippian (Carboniferous). The uplifting continued into the Permian and the basin became structurally closed with the uplift of the Pascola Arch by the end of the Cretaceous. By the end of the Palaeozoic, the whole region has been above sea-level and underwent erosion, forming the present-day structural feature (Klein and Hsui, 1987; Swann, 1969).

Nowadays, this structural feature is surrounded by the Kankakee Arch in the northeast, separating it from the Michigan Basin, by the Cincinnati Arch in the east, separating it from the Appalachian Basin, by the Ozark Dome in the southwest, the Mississippi Embayment in the south and the Forest City Basin in the northwest.

1.8.2. Core location

Core IGS-527 was taken in the US Aggregates Quarry (Delphi Limestone Inc. at the time of drilling) in Delphi, in the northeast of Carroll County, Indiana, USA (40.591092°N, 86.692784°W). This quarry lies in the state of Indiana, about 230 km north of Indianapolis and about 225 km south of Lake Michigan. Carroll County lies in the north-eastern part of the Illinois Basin, at the border with the Kankakee Arch. The quarry floor is in the Silurian, and the core has some 500 ft of unstudied Silurian rocks above the sampled interval.

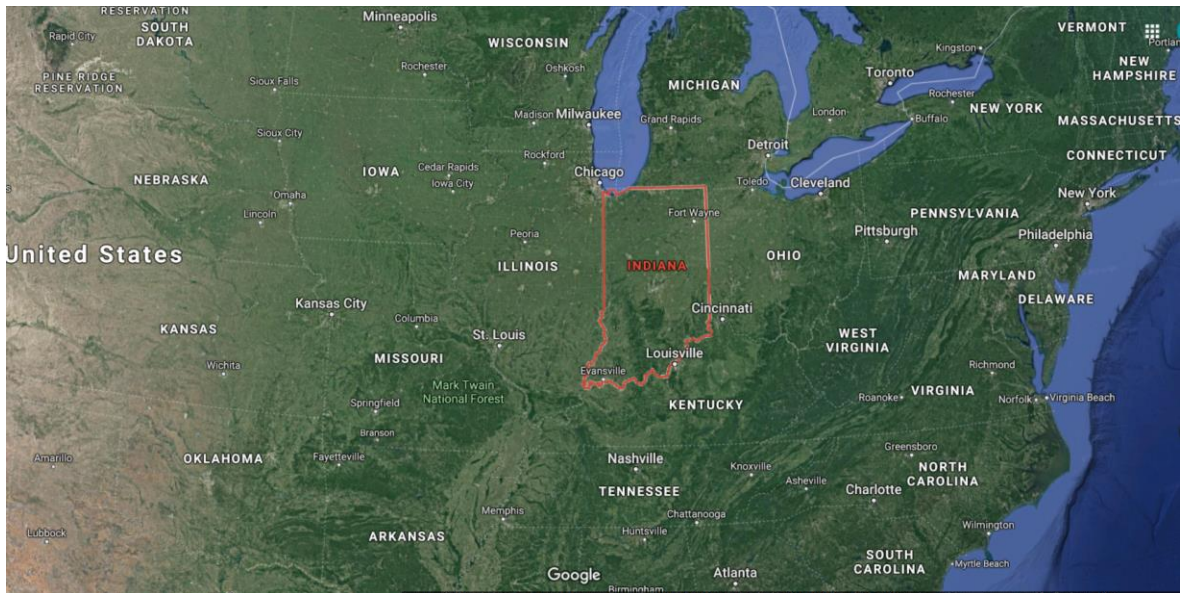


Figure 9: Map with the location of Indiana outlined in red. From <https://www.google.com/maps/> (accessed on 18/06/2019).

The core was taken by the Indiana Geological Survey in October of 1973 and stored in the Indiana Geological Survey core repository, Bloomington, USA. Subsamples were taken between 470 feet and 545 feet on the 21st of June 2017 and shipped to Ghent where they are stored in the Department of Geology of Ghent University.

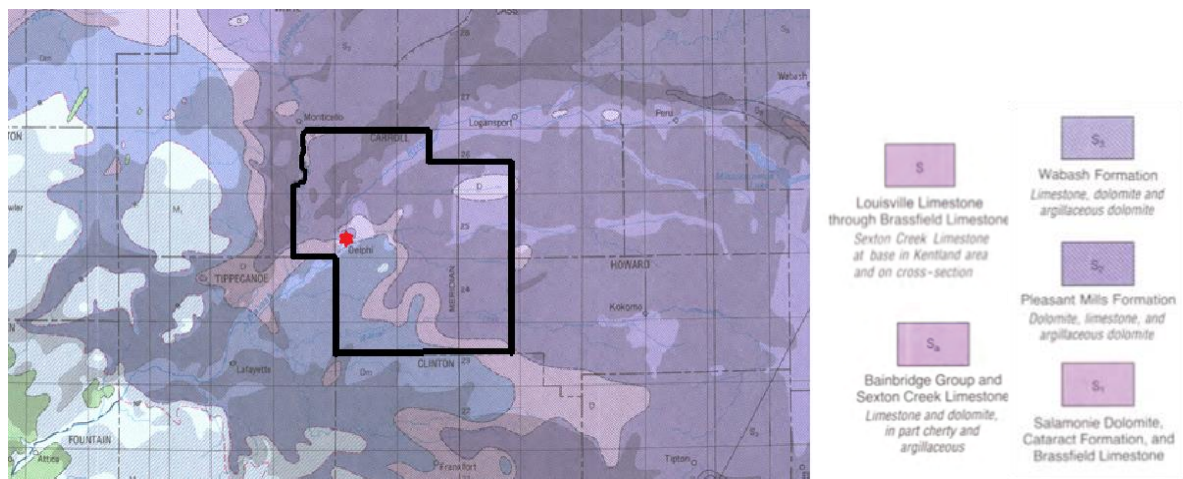


Figure 10: Geologic map of the bedrock of Indiana, USA, zoomed in on the investigated area. Carroll County is outlined in black. The red star indicates the core location. Modified from the Indiana Geological and Water Survey.

1.9. Lithostratigraphy

1.9.1. Upper Ordovician lithostratigraphy

The correlation of different sections across the Midcontinent is not straightforward. Lithostratigraphic units can be diachronous so formations are not always deposited at the same time at different places. Not only the time of deposition can change, but a certain formation or lithostratigraphic unit can also experience lateral facies changes. This can cause misidentification. Fig. 11 shows a compilation by Wicander and Playford (2008) of previous stratigraphic work on the US Midcontinent and represents the current state of the Upper Ordovician stratigraphy of the US Midcontinent.

Stage	Graptolite biozone	Conodont biozone	Midcontinent				Eastern Canada
			Upper Peninsula, Michigan	Arbuckle Mountains, Oklahoma	lowa- Illinois	Cincinnati region	Anticosti island, Quebec
Richmondian	P. ornatus	Amorphognathus ordovicicus					Vauréal
	D. com-planatus		Stontington	Sylvan shale	Maquoketa	Brainard Ft. Atkinson	
	A. manitoulinensis	Bill's Creek shale	Welling/ Fernvale	Scales		Liberty	Waynesville
	A. superbus		Viola Spring			Arnheim	Macasty

Figure 11: Compilation of previous stratigraphic work on the US Midcontinent, focused on the Maquoketa Formation. The upper extent of these formations, relative to each other, is unknown and indicated by dotted lines. The grey bar represents the Waynesville excursion as presented by Bergström et al. (2010) and McLaughlin et al. (2016). Correlations are based on Jacobson and Achab (1985), Bergström and Mitchel (1986), Goldman and Bergström (1997), Bergström (2003), Bergström and Mackenzie (2005), Wicander and Playford (2008), Bergström et al. (2010) and McLaughlin et al. (2016). From De Backer (2017) as modified from Wicander and Playford (2008).

1.9.2. lower Silurian lithostratigraphy

The formation of ice caps at the end of the Ordovician induced a glacio-eustatic sea level drop which resulted in a major regression of the epicontinental sea (Sheehan, 1973a; Berry and Boucot, 1973). This caused a unconformity at the Ordovician-Silurian boundary in the Midcontinent of the USA. Due to the regression, the strata of the Maquoketa Group in northeastern Illinois got exposed and underwent erosion. The erosion removed most of the Neda Formation, much of the Brainard Formation and in some places even parts of the Fort Atkinson Formation (Fig. 12; Mikulic et al., 1985). As a result, the Ordovician Maquoketa Group is unconformably overlain by the Sexton Creek

SYS.	SERIES	GP.	FORMATION	GRAPHIC COLUMN	THICK. (FT)
SILURIAN	LUDLOW (NIAGARAN)		Racine	[Graphic Column: Diagonal lines with triangles]	300+
			Sugar Run	[Graphic Column: Diagonal lines]	0-30
	Joliet		[Graphic Column: Diagonal lines with triangles]	40-80	
	LLAND-OVERY		Kankakee	[Graphic Column: Diagonal lines]	17-50
			Neda	[Graphic Column: Diagonal lines]	0-15
ORDOVICIAN	CINCINNATIAN	Maquoketa	Elwood	[Graphic Column: Diagonal lines]	0-30
			Wilhelmi	[Graphic Column: Diagonal lines]	0-100
			Brainard	[Graphic Column: Diagonal lines]	0-120
			Forr Atkinson	[Graphic Column: Diagonal lines]	5-50
			Scales	[Graphic Column: Horizontal lines]	90-120
			Wise Lake	[Graphic Column: Horizontal lines]	
	CHAMPLAINIAN	Galena	Dunleith	[Graphic Column: Diagonal lines]	170-210
			Guttenberg	[Graphic Column: Diagonal lines]	0-15
			Nachusa	[Graphic Column: Diagonal lines]	0-50
		Platteville	Grand Detour	[Graphic Column: Diagonal lines]	20-40
			Mifflin	[Graphic Column: Diagonal lines]	20-50
			Pecatonica	[Graphic Column: Diagonal lines]	20-50

Figure 12: Ordovician and Silurian strata of northeast Illinois. From Mikulic et al. (1985).

1.9.3. Provisional lithostratigraphy of core IGS-527

1.9.3.1. Sexton Creek Limestone

The Sexton Creek Limestone is present in Indiana, southeastern Missouri, southwestern Illinois and western Kentucky. The lower part of this formation is continuous with the Schweizer Member of the Wilhelmi Formation in Illinois, which in Indiana is called the Schweizer Member of the Sexton Creek Limestone. The main body consists of impure brown dolomite or limestone with high amounts of chert (can be up to 70 percent). The carbonate content is generally light to medium brown, but gray banding and mottling can be present. It is granular, fine to medium grained and can include coarse (bioclastic) lenses and beds. The Schweizer Member contains little to no chert and is more argillaceous. Dolomitic shale is also included in this member (Rexroad and Droste, 1982). The formation has in Indiana a thickness ranging from 1 to 100 feet (Fig. 13). This could even be more in the northwestern corner of Indiana, but the thickness in that area is highly variable due to the relief of the Ordovician erosion surface on which it was deposited (Rexroad and Droste, 1982).

The Sexton Creek Limestone in northwestern Indiana is continuous with the Schweizer Member of the Wilhelmi Formation, the Elwood and the Kankakee formations in northeastern Illinois. The strata recognized as the equivalent Kankakee Formation of Illinois are present as a facies in the upper part of the Sexton Creek Limestone, but no formal name as given to it. The Sexton Creek Limestone is also continuous with the Brassfield Limestone in southeastern Indiana, with the Cataract Formation in northeastern Indiana, more specifically with the Manitoulin Dolomite Member and the Cabot Head

Member, and the Cataract Group in Michigan (Rexroad and Droste, 1982). It is early Llandovery (Rhuddanian to early Aeronian) in age but it also includes late Llandoveryan rocks where it merges with the Brassfield limestone of southwestern Indiana (Butcher et al., 2010; Rexroad and Droste, 1982; Indiana Geological and Water Survey).

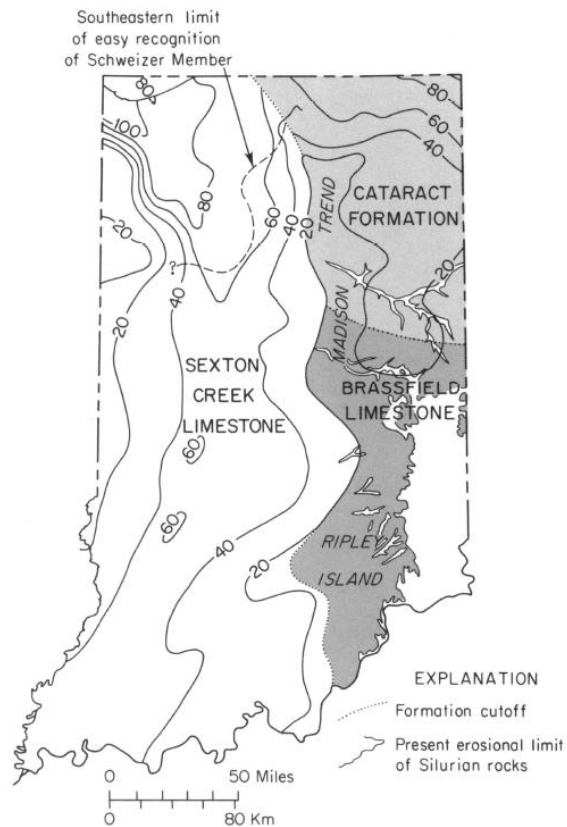


Figure 13: Map of Indiana indicating the thickness of the Sexton Creek Limestone and equivalent Cataract and Brassfield Formation. The geographic limit of the Schweizer Member is indicated. Modified from Rexroad and Droste (1982).

1.9.3.2. Cape La Croix Shale

Consists of dark-greenish-grey to brown, locally silty and moderately calcareous graptolitic shale. The Cape La Croix Shale also contains very minor brown-gray crystalline, argillaceous limestone which occurs as nodules and thin interbeds (Harrison, 1999). The general thickness ranges from 10 to 55 feet and is about 17 feet at the type section in Cape Girardeau County, Missouri (Thompson, 1991). The Cape La Croix Shale belongs to the Maquoketa Group and is mapped undivided with Thebes Sandstone and Orchard Creek Shale, both of Maquoketa Group, in Missouri and Illinois (Harrison, 1999).

1.9.3.3. Fernvale Formation

Also called the Fernvale Limestone, is originally described by Hayes and Ulrich (1903) as soft green and chocolate-coloured shales containing one or more layers of coarse crystalline, occasionally flesh-coloured, limestone, usually containing greenish specks. The lower layer is frequently conglomeratic and highly phosphatic. The lower part of the formation is in some areas composed of 5-6 ft of strongly ferruginous, often vermilion-red limestone. The overall thickness ranges from 0-40 ft (Hayes and Ulrich, 1903).

1.9.3.4. Liberty Formation

This formation was described by Nickles (1903) as even-bedded, dominantly blue-coloured limestones with an average thickness of 3 inches, with generally blue layers of clay and shales intervening. The Liberty Formation belongs to the Dillsboro Formation of the Maquoketa Group (Gray, 1986).

1.10. Carbon Isotope Excursions

1.10.1. General overview

Carbon Isotope Events (CIE's) are excursions in the $\delta^{13}\text{C}$ values recorded in rocks and are the record of perturbations in the carbon cycle. Throughout the Earth's history, many perturbations of the carbon cycle have occurred and the associated CIE's have been identified from the rock record. The major CIE's coincide with severe global environmental perturbations (Cowie and Cohen, 2010). The conditions during which CIE's in the past occurred differed from CIE to CIE, although there are similar features associated with these events. These include acidification and deoxygenation of the oceans and extinction of both marine and terrestrial species (Kaljo et al., 1997; Jeppsson and Aldridge, 2000; Calner, 2008), but also sudden shifts in Earth's climate and hydrological cycle (Cowie and Cohen, 2010; Saltzman and Thomas, 2012).

Clear trends in $\delta^{13}\text{C}$ values from carbonate sediments are very useful data for detailed chronostratigraphic correlations, both at local and global scale (Bergström et al., 2010). This can, however, be complicated by a number of things. An individual $\delta^{13}\text{C}$ excursion rarely has a specific isotopic signature which complicates the separation of such an excursion from other excursions of a similar magnitude and stratigraphic age. This can result in unreliable correlations. So before significant $\delta^{13}\text{C}$ excursions can be correlated, the position of such excursions in a solid biostratigraphic framework must be well established (Kaljo et al., 2007; Cowie and Cohen, 2010). Other complications can be caused by lacking data by erosional hiatuses and unconformities. This can be overcome by assessing the extent of these gaps with biostratigraphy (Kaljo et al., 2007). Another cause of complications is facies substitution and thinning out of beds, which can distort the shape of the carbon isotope curve or range of the measured $\delta^{13}\text{C}$ values. Slow sedimentation and condensed sections cause difficulties in sampling and in that case, very dense is sampling needed for recording high resolution carbon isotope variations (Kaljo et al., 2007).

1.10.2. Upper Ordovician carbon isotope excursions

Two very conspicuous global perturbations of the global carbon cycle are identified in the Upper Ordovician $\delta^{13}\text{C}$ chemostratigraphy (Bergström et al., 2010): the early Katian Guttenberg carbon isotope excursion (GICE) and the HICE (Fig. 14).

The GICE has also been recognized from the Upper Mississippi Valley (Hatch et al., 1987; Ludvigson et al., 2004), in the Arbuckle Mountains in Oklahoma (Gao et al., 1996; Young et al., 2005), in Nevada (Saltzman and Young, 2005) as well as in parts of Asia (Wang et al., 1997) and Estonia (Ainsaar et al., 1999; Kaljo et al., 2001) which confirms the suggestion of its global nature (Bergström et al., 2010). The $\delta^{13}\text{C}$ and peak values of the GICE differ globally and regionally, but the excursion occupies the same biostratigraphic position (Bergström et al., 2010). According to Ainsaar et al. (1999), the GICE reflects an increase in primary production and preservation of organic carbon in particular ocean environments.

The second and most prominent excursion is the HICE and is also globally recognized (Bergström et al., 2010). The Hirnantian glaciation at the end of the Ordovician was caused by a significant drop in the $p\text{CO}_2$ (Brenchley et al., 1994). This is observed by a strong positive $\delta^{13}\text{C}$ excursion in the geological record. Samples from the American Midcontinent show elevated $\delta^{13}\text{C}$ values of +4‰ to +5‰ (Bergström et al., 2006). The HICE extends from a level near the base of the lower Hirnantian *Normalograptus extraordinarius*-*Normalograptus ojsuensis* Biozone to a level within the *N. persculptus* Biozone (upper Hirnantian) (Melchin et al., 2003).

Four other $\delta^{13}\text{C}$ positive excursions above the GICE in the Katian succession of the Cincinnati region have been recognized by Bergström et al. (2007): the Kope, Fairview, Waynesville and the Whitewater excursions (Fig. 14).

The Kope $\delta^{13}\text{C}$ excursion in the Cincinnati region ranges from the uppermost part of the Point Pleasant Formation until just above the middle of the Kope Formation. Here it has a thickness of about 50m. The baseline values below and above are respectively $\pm 0.0\text{‰}$ to -1.5‰ and compared with these, the Kope excursion has peak values of $\pm +0.4\text{‰}$ (in the Cincinnati region). The Kope excursion starts in the upper *Diplacanthograptus spiniferus* Graptolite Zone and ranges into the *Geniculograptus pygmaeus* Graptolite Zone.

The excursion above is the Fairview Excursion (Bergström et al., 2007). Its onset in the Cincinnati region is near the base of the Fairview Formation with background values between -1.5‰ and -1.0‰ . It reaches peak values similar to the Kope excursion in the upper part of the Fairview and lower part of the Grant Lake Formation. The excursion lies in the upper half of the *Oulodus velicuspis* Conodont Zone (Sweet, 1984) and near the base of the *Amplexograptus manitoulinensis* Graptolite Zone, although the interval in which the excursion takes place is biostratigraphically poorly controlled by graptolites (Bergström and Mitchell, 1986).

The Waynesville Excursion has, in the Cincinnati region, peak values of $>+1.3\text{‰}$ which is $\pm 2\text{‰}$ more positive than the baseline values. This makes it probably the most important $\delta^{13}\text{C}$ excursion currently recognized between the GICE and HICE (Bergström et al., 2010). It ranges from the base of the Waynesville into the Liberty Formation, occupying the upper part of the *A. manitoulinensis* Graptolite Zone and in the lower part of the *Amorphognathus ordovicus* Conodont Zone (Atlantic conodont zone scheme).

The Whitewater Excursion ranges from baseline values between -1.8‰ and -1.2‰ , peaks at -0.1‰ in the Whitewater Formation before returning to baseline values of -1.4‰ in the upper Whitewater Formation. In equivalent strata in Illinois, the graptolite *Dicellograptus complatanus* was present, placing it in the *D. complatanus* Graptolite Zone (Bergström et al., 2007; Goldman and Bergström, 1997).

The uppermost excursion is called the Elkhorn excursion by Bergström et al. (2010). A recently studied drill core from St. Marys in western Ohio showed a complete Elkhorn excursion recorded in the top part of the Richmondian Stage (Bergström and Kleffner, 2018). Based on the similarity of this excursion with the Paroveja excursion, recognized in the Katian of Estonia by Ainsaar et al. (2010), these two excursions are regarded as the same (Bergström and Kleffner, 2018). This excursion is pre- *Normalograptus extraordinarius* Graptolite Zone and probably post-*Dicellograptus ornatus* Zone in the standard graptolite zone succession. It occurs in the upper part of the *Aphelognathus divergens* Zone in the North American Midcontinent conodont zonation (Bergström and Kleffner, 2018).

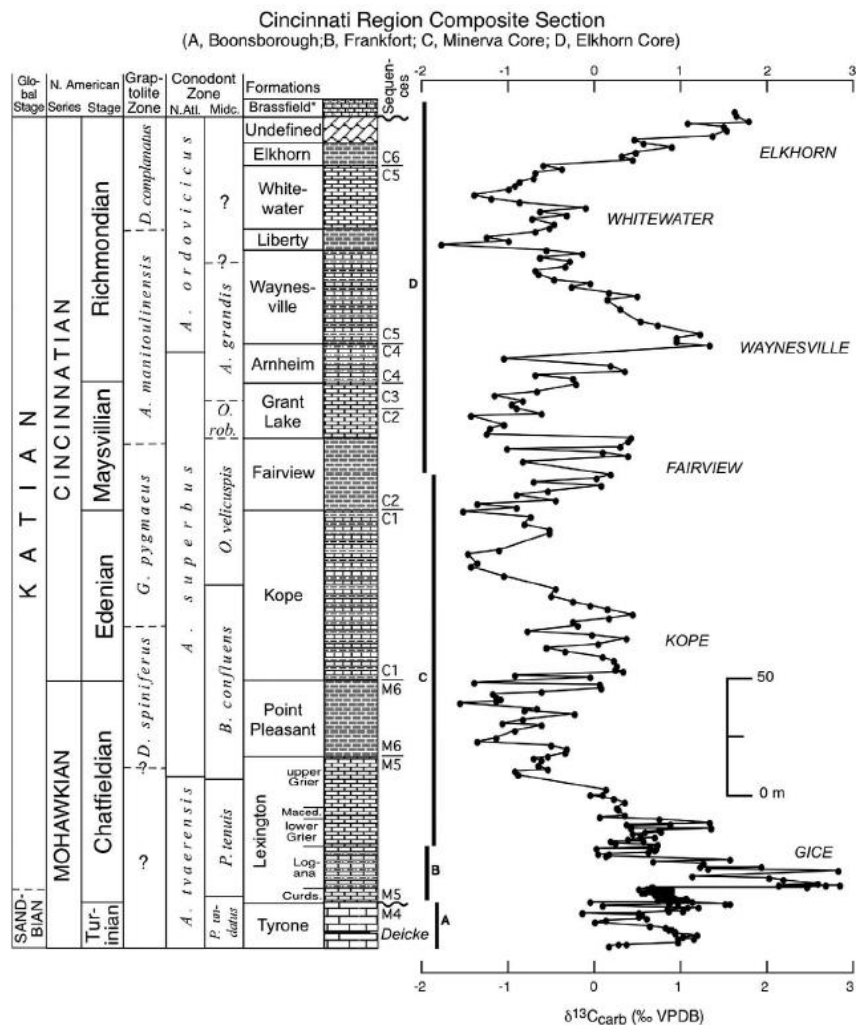


Figure 14: Composite $\delta^{13}\text{C}$ curve through the Cincinnati Series and the underlying upper Mohawkian strata in the Cincinnati region. From Bergström et al. (2010).

1.10.3. lower Silurian carbon isotope excursions

Multiple stable carbon isotopes are found in the geological record of the lower Silurian. The three Silurian $\delta^{13}\text{C}$ positive excursions with the highest amplitude are the Ireviken (early Sheinwoodian), Mulde (mid-Homerian) and Lau (late Ludfordian) Excursion (Fig. 15).

The Ireviken excursion started at the Llandovery-Wenlock boundary and lasted until just before the end of the Sheinwoodian (Fig. 15; Mabillard and Aldridge, 1985; Jeppsson, 1997b; Munnecke et al., 2003). It is named after the extinction interval known as the Ireviken Event (Jeppsson, 1987) and reaches $\delta^{13}\text{C}$ values as high as +5.0‰ (VPDB) (Bickert et al., 1997; Munnecke et al., 2003; Cramer and Saltzman, 2005; Kaljo and Martma, 2006). The driving factor for the Ireviken excursion was an increase in atmospheric $p\text{CO}_2$. This led to elevated $\delta^{13}\text{C}$ values by alteration of the deep-ocean circulation and increase of organic carbon burial (Cramer and Saltzman, 2007b).

The Mulde excursion is associated with the 'Big Crisis' graptolite extinction (Cramer et al., 2006b) and has been well correlated both to graptolite and conodont stratigraphy. It is a dual-peaked excursion, which is something rarely seen in the Palaeozoic (Cramer et al., 2006b). The excursion occurs in the Homerian and the $\delta^{13}\text{C}$ values reach +3.0‰ (+4.0‰ in some localities).

In the lower Silurian, three $\delta^{13}\text{C}$ excursions are present: the Early Aeronian, the Late Aeronian and the Valgu Excursion in the early Telychian (Fig. 15). The Early Aeronian Excursion has been recognized in Arctic Canada (Melchin and Holmden, 2006), Dob's Linn, Scotland (Underwood et al. 1997; Heath 1998), Anticosti Island (Azmy et al. 1998), and Estonia (Kaljo et al. 1998, 2003; Kaljo and Martma 2000). It's a weak positive excursion that coincides with continental glaciation on Gondwana (Melchin and Holmden, 2006). The Late Aeronian Excursion lies in the *S. sedgwickii* Graptolite Biozone and has a slightly greater amplitude than the Early Aeronian one. This excursion

also coincides with continental glaciation on Gondwana (Melchin and Holmden, 2006). The Valgu Excursion begins with a global low stand of the sea. The fall in sea level coincides with an increase in carbon isotope values (McLaughlin et al., 2012). Near the peak of stable carbon isotope values, there was a slight rise in sea level. At the end of the event, when the carbon isotope values decreased again, global temperatures improved, sea levels reached a Silurian high and oxic conditions associated with very low rates of organic carbon burial were established (McLaughlin et al., 2012).

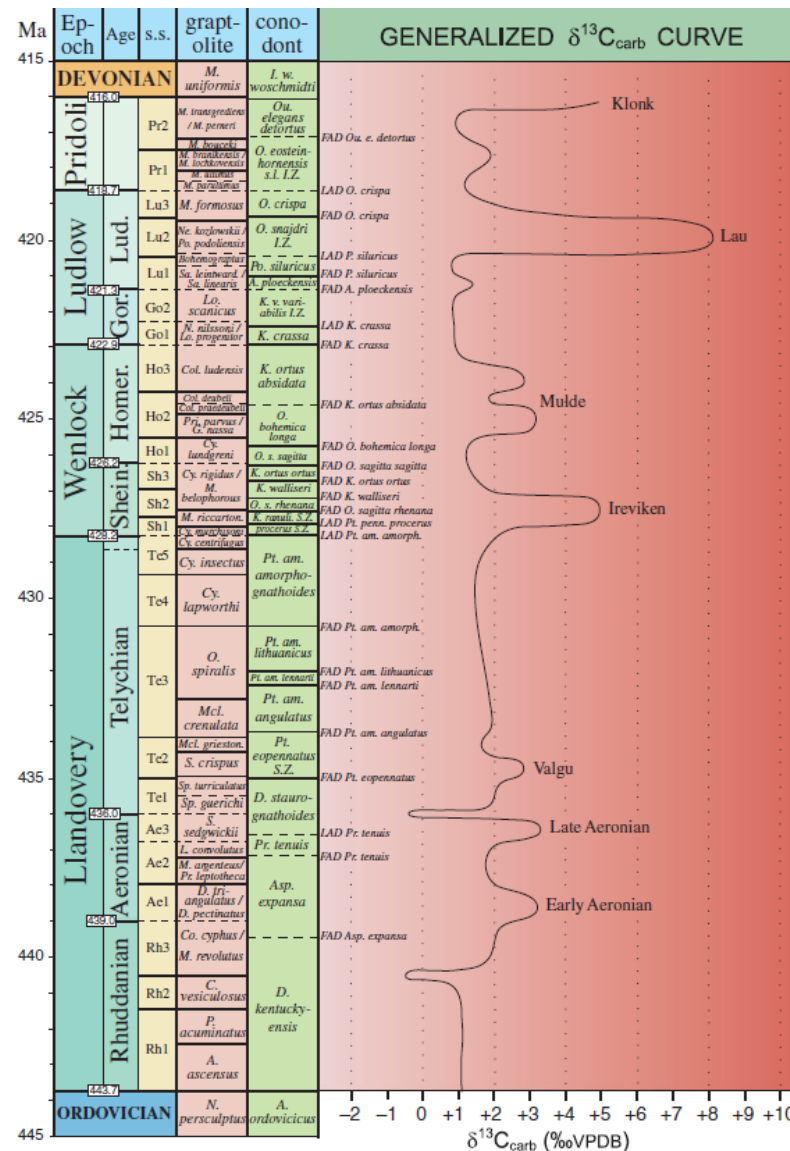


Figure 15: Silurian graptolite and conodont biostratigraphic zonation, shown in relation to global stages and a generalized $\delta^{13}C_{carb}$ curve for the Silurian System. From Cramer et al. (2011a).

1.10.4. Stable carbon isotope curve of core IGS-527

The stable carbon isotope curve was provided by Dr. Patrick McLaughlin (Fig. 16). The interval from ~490 ft to 512 ft represents the tail end of the HICE (Patrick McLaughlin, Pers. Comm.). It is located at the Ordovician-Silurian boundary and has a small amplitude, ranging from $\pm +0.3\text{‰}$ to $\pm -0.7\text{‰}$. The interval from 522 ft to 531 ft represents the Paroveja Excursion as identified by Ainsaar et al. (2010) (Patrick McLaughlin, Pers. Comm.), also known as the Elkhorn Excursion from Bergström et al. (2010). This excursion is located in the Upper Ordovician (uppermost Katian) and ranges from about -0.5‰ to a maximum of $+1.2\text{‰}$ back to about -0.7‰ .

Above these two positive excursions, three negative stable carbon isotope excursions are observed. They are of a larger magnitude compared to the two underlying positive excursions. Between the tail end of the HICE and the Paroveja Excursion, a negative excursion is observed. The interpretation of the excursions of core IGS-527 remains provisional and needs to be confirmed by means of an independent age marker such as biostratigraphy.

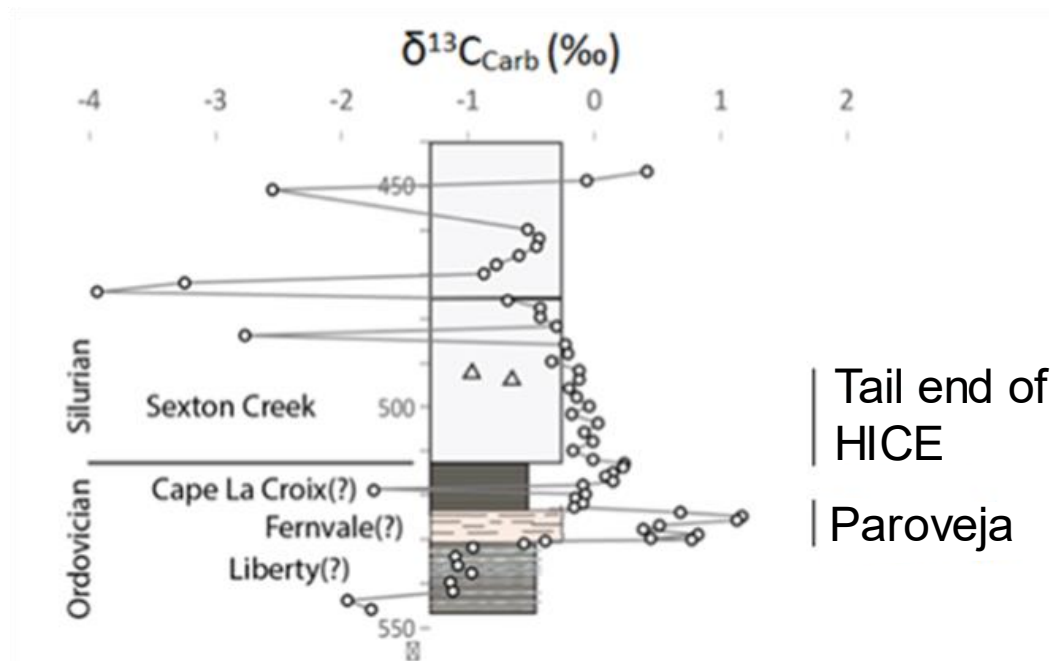


Figure 16: Stable carbon isotope curve for core IGS-527, with the provisional excursions indicated. Modified from McLaughlin (Pers. Comm.)

1.11. Biostratigraphy

1.11.1. Upper Ordovician biostratigraphy

1.11.1.1. Graptolites and conodonts

Most graptolite species dispersed rapidly, are geographically widespread, and are of relatively short stratigraphic duration (0.5-4 myr). This makes them, together with conodonts, extremely valuable fossils for the zonation and correlation of strata (Melchin et al., 2012).

For the Upper Ordovician of North America, a well-established graptolite (Bergström and Mitchell, 1986; Goldman and Bergström, 1997; Webby et al., 2004) and conodont (Bergström, 1970; Sweet, 1984; Richardson and Bergström, 2003; Webby et al., 2004) biostratigraphic framework exists (Fig. 17). The graptolite biostratigraphy is generally continuous for the Upper Ordovician, the conodont biostratigraphy not so much. Some conodont biozonal boundaries are uncertain because key conodont species are missing in some stratigraphic intervals (Richardson and Bergström, 2003). A detailed description of the various biozones falls beyond the scope of this dissertation and the readers are referred to Goldman and Bergström (1997), Štorch et al. (2011) and the references herein.

GSSP 443 Ma	GLOBAL SERIES	GRAPTOLITES		CONODONTS		CHITINOZOANS	TIME SLICE			
		NORTH AMERICA		NORTH AMERICAN MIDCONTINENT	NORTH ATLANTIC	NORTH AMERICA				
GSSP	UPPER ORDOVICIAN	CINCINNATIAN	<i>persculptus</i>	Ga	<i>shatzeri</i>	<i>ellisbaeyensis/tagourdeau</i>	6c			
			<i>extraordinarius</i>					<i>gamachiana</i>		
			<i>pacificus</i>	Ri			<i>divergens</i>	<i>ordovicicus</i>	<i>crickmayi</i>	6b
			<i>ornatus</i>				<i>grandis</i>		<i>anticostiensis</i>	
			<i>complanatus</i>						<i>vaurealensis</i>	6a
		MOHAWKIAN	<i>manitoulinensis</i>	Ma	<i>robustus</i>	<i>superbus</i>	<i>hyalophrys/ C. sp. 2</i>	5d		
			<i>pygmaeus</i>	Ed	<i>velicuspis</i>		<i>pygmaea/cristata</i>			
			<i>spiniferus</i>	Ch	<i>confluens</i>		<i>alobatus</i>	<i>cancellata</i>	5c	
			<i>ruedemanni</i>		<i>tenuis</i>			<i>gracqui</i>		
			<i>americanus</i>		<i>undatus</i>			<i>multispinata/duplicatas</i>		
WITHEROCKIAN	<i>bicornis</i>	Tu	<i>compressa</i>	<i>tvaerensis</i>	<i>primitiva</i>	5b				
	<i>gracilis</i>		<i>quadridactylus</i>		<i>gerdae</i>					
			<i>aculeata</i>		<i>variabilis</i>		<i>S. sp. A</i>			
GSSP 460.5 Ma			<i>sweeti</i>	<i>anserinus</i> <i>inequal.</i>	<i>hirsuta</i>	5a				
					<i>L. sp. A</i>					

Figure 17: Compilation of the Upper Ordovician graptolite, conodont and chitinozoan biozones for North America. Zones are represented by their key species. Modified from Webby et al. (2004).

1.11.1.2. Chitinozoans

The Upper Ordovician chitinozoan biostratigraphy has been established for different palaeocontinents: Canada (Achab, 1989, updated by Soufiane and Achab, 2000a, b; Achab et al., 2011; Achab et al., 2013), Avalonia (Vandenbroucke, 2008a and references therein), Baltoscandia (Nölvak and Paris, 1993; Vandenbroucke et al., 2013), Gondwana (Paris, 1990, 1998). This has also been done for the U.S.A.: Maysville (Vellemen, 2016), Nevada (Soufiane and Achab, 2000a), Oklahoma (Jenkins, 1969; Jenkins, 1970), Indiana (De Boedt, 2018), Illinois (Meyvisch, 2018), Wisconsin (De Backer, 2017), the Upper Mississippi Valley (De Waele, 2017) and Tennessee (Meyvisch, 2018).

The Laurentian chitinozoan biozonations consists of 19 biozones (Fig. 17) and is obtained from sections in North America.

1.11.2. lower Silurian biostratigraphy

1.11.2.1. Graptolites and conodonts

The British graptolite zonation served as the base for the 'standard' zonal scheme for Silurian graptolite biostratigraphy, except for the Pridoli zonation which is based on the succession in Bohemia (Melchin et al., 2012), and was updated by Zalasiewicz et al. (2009). The global graptolite zonation has a high precision and is divided in 36 graptolite zones (Fig. 18). It spans 24.6 myr, an average of 683.000 years each in duration (Melchin et al., 2012). Some parts of the Silurian have exceptionally detailed conodont biozonations: Wenlock and Ludlow (Jeppsson, 1997a; Jeppsson et al., 2006), Telychian (Männik, 1998, 2007b), Ludfordian to Pridoli (Corradini and Serpagli, 1999; Corrigan and Corradini, 2009). The most precise chronostratigraphic resolution of palaeoenvironmental data of the middle-late Llandovery through the Ludfordian is from the Baltic Basin. This is the result of precise conodont biostratigraphic control and widespread application of carbon isotope chemostratigraphy (e.g. Jeppsson 1997a; Kaljo et al. 1997, 1998, 2003, 2012; Männik 1998, 2007a, b; Kaljo and Martma 2006). This is why the Silurian global standard conodont

biozonation and carbon isotope curve for this interval are based primarily on data from the Baltic region (Cramer et al., 2011a; Melchin et al., 2012; Waid and Cramer, 2017b).

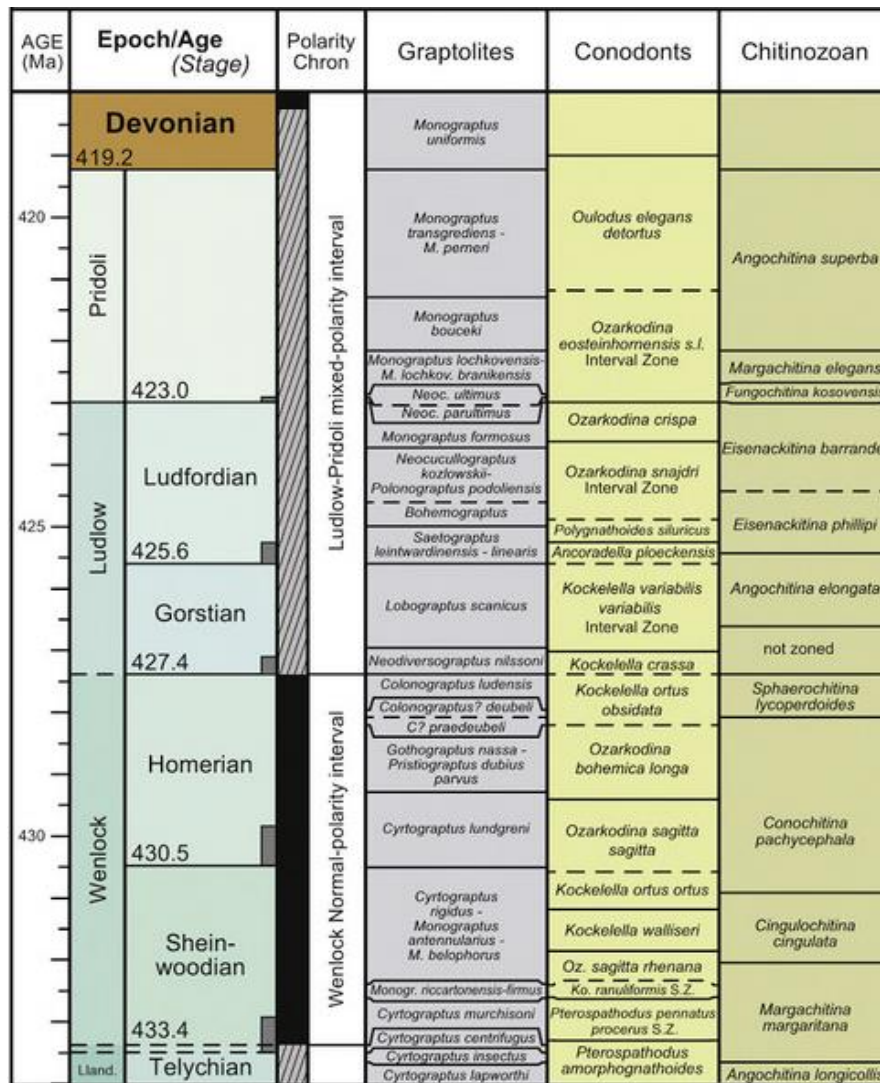


Figure 18: Silurian epochs and ages time scale, geomagnetic polarity scheme, graptolite zonation (based on Cramer et al. (2011a)), conodont zonation (based on Cramer et al. (2011b)) and chitinozoan zonation (slightly modified from Verniers et al. (1995)). Modified from Melchin et al. (2012).

2. Methodology

2.1. Chitinozoans

Chitinozoans are a group of extinct organic-walled microfossils, that are exclusively found in marine sediments. They are mostly found as isolated individuals, but also occur in chains or in aggregates masses (Kozłowski, 1963; Gabbott et al., 1998). Chitinozoans were first described by Eisenack in 1931. They emerge in Stage 5 of the Cambrian (~510 Ma) and are abundant in the fossil record of the Lower Ordovician to Upper Devonian. They gained their maximum species diversity during the Middle Ordovician-Silurian (Shen et al., 2013) and became extinct in the Late Devonian (latest Famennian, ca. 360 Ma) (Paris and Verniers, 2005).

2.1.1. Morphology and structure

Combaz and Poumont (1962) were the first to establish a detailed morphological terminology which Combaz et al. (1967) completed. Major improvements have been made due to routine use of the Scanning Electron Microscope (SEM), which revealed more morphological detail (Paris et al., 1999). Every well-preserved chitinozoan shares three major characteristics: 1) they are made up of an organic membrane delimiting a cavity; 2) they have an aperture sealed with a plug; 3) they generally display radial symmetry (Fig. 19; Paris et al., 1999).

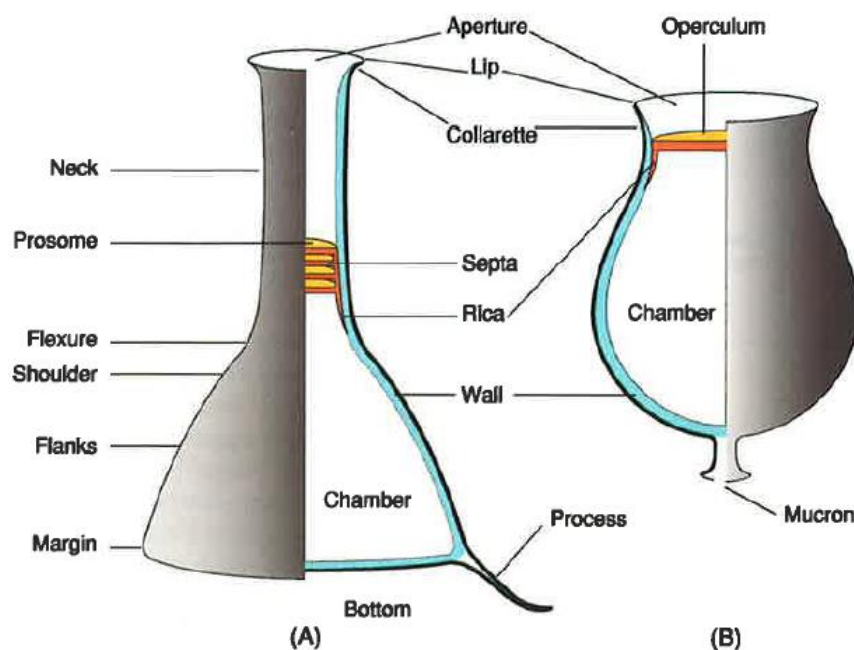


Figure 19: Main morphological features of a chitinozoan. (A) *Lagenochitiniidae*; (B) *Desmochitiniidae*. Black: outer layer. Blue: inner layer. From Paris and Verniers (2005).

The basic element of a chitinozoan is the vesicle with the chamber as the bulging part. Its shape can be quite variable: purse-, vase-, or flask-like. The vesicle is made out of an organic wall, called the test or tegument (Paris and Verniers, 2005). It can range from 50 to 200 μm in length (Paris et al., 1999). Each vesicle has an aperture which is located directly on the chamber or at the distal end of a tube-like neck. A conventional orientation of the vesicle is established in order to avoid discussion: the apertural pole is regarded as presenting the top of the vesicle, the anti-apertural pole is the base of the vesicle (Paris et al., 1999). Around the aperture, a collarette may be present. This is the thinned cylindrical or flaring part of the neck, or of the chamber wall when the neck is absent. The aperture itself is sealed by a plug. The plug is called an operculum (disc-like shape) if it seals the chamber directly (Fig. 19B), when it is situated within the neck it is called a prosome (Fig. 19A). The vesicle wall and the plug are a temporary protection for the inner contents (Paris et al., 1999). The

chamber itself also has a wide variety of forms. It can be spherical, lenticular, ovoid, conical, cylindrical, bell-shaped or claviform (Fig. 20; Paris and Verniers, 2005).

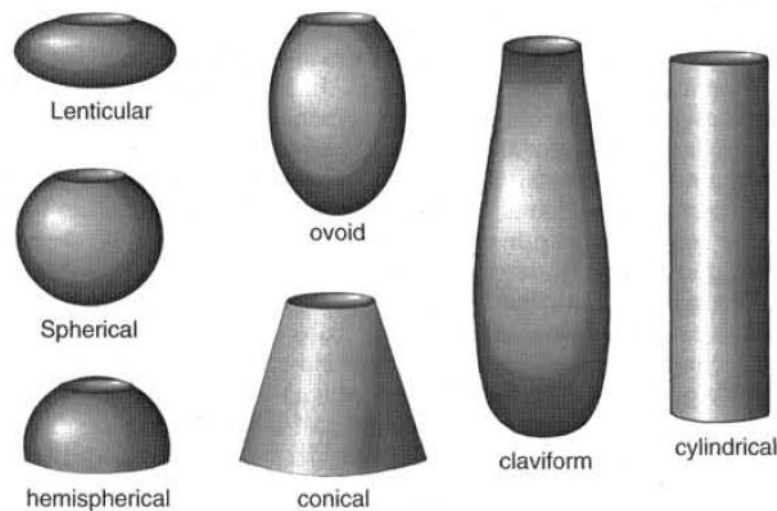


Figure 20: The basic chamber shape of chitinozoans. From Paris et al. (1999).

The margin is the junction between the flanks and the bottom. Its shape and ornamentation, i.e. processes, spines, carina, are of primary importance in generic assignment (Paris and Verniers, 2005). The vesicle wall itself can also display numerous different kinds of ornamentation which can occur randomly or geometrically distributed (as rims, rows or ridges) either on the whole vesicle or on parts of the vesicle. The ornamentation can vary largely in size, structure, shape and place.

The wall of chitinozoans comprises an inner layer and outer layer. The composition and molecular structure of the organic wall were unknown for a long time. Studies investigating the chemistry of chitinozoans with techniques such as micro-FTIR spectroscopy, laser micro-Raman spectroscopy, Curie-point-pyrolysis gas chromatography–mass spectrometry and lasermicropyrolysis gas chromatography–mass spectrometry detected no compounds diagnostic of chitin. This would indicate that chitin has been destroyed during diagenesis or that chitinozoans were not made up of chitin (Dutta et al., 2007; Jacob et al., 2007). A study of Dutta (2013) showed that the biogeomacromolecules of chitinozoans are enriched with aromatic compounds with little amount of aliphatic components (Dutta et al., 2007, 2013; Jacob et al., 2007).

The inner layer is usually thicker than the outer layer and constitutes the frame of the vesicle. It does not display any structures. The same goes for the interior of the chamber (Paris and Verniers, 2005). The outer layer on the other hand displays ornamentations through outgrowth (e.g. verrucae, cones, granules, spines), evagination (e.g. hollow spines or processes) or folding (e.g. carina, crests, wrinkles). The shape, size, density, location and organization of the ornamentation on the vesicle are used as taxonomic criteria (Paris et al., 1999; Paris and Verniers, 2005).

2.1.2. Biological interpretation and systematic position

What chitinozoans really were remained unclear for a long time. Their systematic position has been a topic of debate for many years. The group has been assigned to protozoans, protists and even fungi. But based on the similarities between chitinozoans and eggs or egg capsules of different metazoans, there is now a general agreement that they are in fact eggs of soft-bodied metazoans. This theory was first proposed by Kozłowski in 1963 and is backed up by the discovery of a complete coiled catenary (chain-like) structure preserved in three dimensions. Due to the arrangement of the vesicles into catenary structures and the presence of a tightly sealed operculum, the larvae could not escape from the chamber. This is why these structures are interpreted as an immature stage in the development of the eggs, i.e. an intra-oviduct stage, instead of the final laying of eggs. They represent the release of immature eggs after death and decay of the producing organism (Paris and Nolvak, 1999; Paris and Verniers, 2005).

Even though there is now somewhat of a consensus about what chitinozoans are, the organisms that produce them have never been found in the sedimentary rock record. None of the body fossil groups usually recorded in the Palaeozoic fossil record matches the chitinozoans in range (Paris, 1981), environmental control or palaeogeographic distribution (Paris and Nolvak, 1999). So it is likely that the 'chitinozoan animals' or chitinozoophorans, as they are named by Grahn (1981), are an extinct group of soft-bodied organisms which are not preserved in the fossil record. Based on the dimensions of chitinozoans, the chitinozoophorans probably range from a few millimeters up to a few centimeters in length (Paris and Verniers, 2005). They had a worm-like appearance (based on the elongate chains) and a nectic or pelagic mode of life (Paris, 1981; Paris and Nolvak, 1999; Paris and Verniers, 2005). The chitinozoophorans were most likely part of the zooplankton. This is based on the fact that chitinozoans occur in all types of sedimentary rocks (except for reefs and coarse, well-sorted sandstones), including black shales and cherts devoid of any bioturbation or evidence of benthic fauna (Vandenbroucke et al., 2010b)

2.1.3. Classification

The first classification for chitinozoans was created by Eisenack in 1931 and was based on parataxonomy. Other classifications were created over the years until Paris et al. (1999) revised all of them and proposed the suprageneric classification that is still used today. Because of the uncertainty of their biological affinity, it is based purely on the morphology of the chitinozoans (Paris and Verniers, 2005). The highest subdivision is the order level and is based on the presence of an operculum (Order Operculatifera) or a prosome (Order Prosomatifera). Differentiation in families is based on the presence/absence of a neck and its flexure. Sub-family and genera levels are defined by the surface, shape and arrangement of the ornamentation of the chamber (Paris et al., 1999).

2.1.4. Biostratigraphic value

Chitinozoans are considered amongst the most useful biostratigraphical fossil groups for early-mid Palaeozoic time. Their spatial and temporal occurrences are used for biostratigraphic applications (Webby et al., 2004) and for the assessment of palaeoenvironments and palaeoclimates (Vandenbroucke et al., 2010b; Pohl et al., 2016). This is because of their rapid morphological changes through time, their records in a large variety of marine sedimentary rocks, their wide palaeogeographical distribution and a fairly simple technical preparation and straightforward taxonomy (Paris and Verniers, 2005). Their biostratigraphical value has been improved over the last couple of years thanks to: 1) closely spaced sampling and studies around GSSP's; 2) better investigation techniques; 3) routine SEM observations; 4) more complete stratigraphical and geographical coverage of the samples sequences and areas; 5) independent palaeontological controls, provided by graptolites and/or conodonts; 6) an improved taxonomy (Paris and Verniers, 2005).

2.2. Core sampling

The samples for this master dissertation were collected from one core, IGS-527, which was taken in Carrol County, Indiana, USA. The core was sampled for chitinozoan study by Julie De Weirdt in July 2017. A total of 37 samples were taken. Although both shales and limestone were sampled, shales are the preferred target. They have a higher organic matter content compared to limestone and they provide the most optimal yield in organic microfossils, such as chitinozoans. Subsamples, residues and picked microfossils are stored at the Department of Geology of Ghent University. Each sample is named after the core and the top of the sample depth (in feet): e.g. sample IGS-527-500 was taken from core IGS-527 and its top lies at a depth of 500 feet.

2.3. Sample selection

In total, 22 samples were selected for analyses and processing. Initially, every other sample was selected for analysis. Additional samples were taken around the lithostratigraphic boundary levels in order to have a better resolution at these crucial horizons.

Sample Depth Top		Sample Depth Base		Sample Name	Lithostratigraphy
ft(')	inches (")	ft (')	inches (")		
470	4,5	471	2	IGS-527-470	
472	8,5	473	3	IGS-527-472	
475	0	476	9	IGS-527-475	
477	9	478	8	IGS-527-477	
479	11,5	480	6	IGS-527-479	
482	2	482	10	IGS-527-482	
484	8	485	1	IGS-527-484	
487	3	487	11	IGS-527-487	
489	4	490	0	IGS-527-489	
490	8	491	3	IGS-527-490	Sexton Creek (?)
492	8	493	3	IGS-527-492	
495	2	495	9	IGS-527-495	
497	0	497	8	IGS-527-497	
500	9	501	4	IGS-527-500	
501	8	502	4	IGS-527-501	
504	4	505	1	IGS-527-504	
506	7	507	3	IGS-527-506	
508	6	509	1	IGS-527-508	
510	8	511	6	IGS-527-510	
512	6	512	10	IGS-527-512	
514	4	514	8	IGS-527-514	
517	3	517	9	IGS-527-517	
519	2	519	8	IGS-527-519	Cape La Croix (?)
521	6	522	0	IGS-527-521	
523	2	523	3	IGS-527-523	
523	3	523	5	IGS-527-523LH	
524	6	524	0	IGS-527-524	
526	8	527	1	IGS-527-526	Fernvale Limestone (?)
528	0	528	4	IGS-527-528	
530	8	531	1	IGS-527-530	
532	7	533	0	IGS-527-532	
535	4	535	8	IGS-527-535	
536	3	536	7	IGS-527-536	
539	8	540	0	IGS-527-539	Liberty (?)
541	9	542	0	IGS-527-541	
544	0	544	3	IGS-527-544	
545	4	545	7	IGS-527-545	

Table 1: The 37 samples taken from core IGS-527. The 22 analyzed samples are indicated in green. The (provisional) lithostratigraphy of the samples is given in the right column.

2.4. Sample preparation

The standard palynological preparation technique was used as described by Paris (1981). Prior to chemical treatment, the rock samples were cleaned to avoid contamination and dried in an oven at 60°C. Subsequently, they were fragmented into smaller pieces with the aid of a geological hammer into pieces of about 1 cm. These smaller fragments were sieved with a 1 mm sieve in order to avoid the fine rock powder that formed during the fragmenting process. For limestone samples, about 55-65 g was used, while for the shale samples about 30-35 g was used.

The first step in the chemical procedure comprised decarbonatization. This is accomplished by putting the adding a 2N hydrochloric acid solution (HCl) for 24 hours. It is important that all the carbonates are removed before we add hydrofluoric acid (HF) in our next step to prevent the formation of CaF₂. To make sure that all the calcium is removed from the samples, the samples are rinsed with demineralized water 2-6 times.

In the next step, 200 ml of HF (40%) was added to the samples and they were placed in a warm water bath (60°C) for 2 days. This was done in order to remove all the silicates present. Subsequently, the samples were rinsed with demineralized water. The following step comprised the removal of HF and a second HCl treatment in order to dissolve possibly newly formed fluorsilicates. 2N HCl was added to the samples and they were kept at 65°C for 24 hours. This step was repeated if the samples were not completely dissolved, until only the organic fraction remained. The samples were then made neutral by successive addition and removal of demineralized water.

After this process of chemical treatment, the residue is washed through a 53 µm sieve and both residues are collected in glass vials with a plastic cap. The smaller fraction is not of interest for this study but stored for later as it contains other palynomorphs (e.g. acritarchs). The larger fraction will be hand-picked as they contain the chitinozoans. Some samples were not completely dissolved after receiving this chemical treatment. These were then washed through a 125 µm sieve. The large fraction was dried, weighted and stored in a small bag for future research.

2.5. Picking and light microscopy

The chitinozoans are hand-picked from the larger fraction (> 53 µm) residue. This was performed with the aid of a WILD Heerbrugg binocular stereomicroscope at magnification x25 to x50. The residue was brought in suspension in the glass vial. With the use of a micropipette, about 100 µL was taken out of the vial and put on a watch glass, which was then placed under the stereomicroscope. The individual chitinozoans were transferred to a second watch glass with the use of glass pipette. The pipette was modified so that it had an aperture of ca. 100 µm, so the uptake of unwanted organic material would be limited. This made it easier and more efficient to place droplets containing multiple individual chitinozoans onto a glass slide. This glass slide had a diameter of 1 cm and was pre-mounted on a metal stub. About 100 chitinozoans were then aligned on each stub with a single haired brush. This organization made it easier to systematically photograph the specimens using the SEM (see below). Three stubs for each sample were filled so we had 300 individual chitinozoans per sample.

2.6. Scanning Electron Microscopy (SEM) imaging

The stubs were treated with a gold (Au) coating prior to Scanning Electron Microscopy (SEM) imaging, to avoid electron charging of the specimen, and in order to obtain a better image quality. The SEM used in this master dissertation is a JEOL JSM-5310LV and the software for photomicrography LINK ISIS by Oxford Instruments. The working distance (WD) was set at 20 mm and an electron beam of 15 keV was used. A scale bar was added to each image. Original resolution of the SEM images is 1024x800 pixels and all pictures were saved as TIFF files.

2.7. Palynological identification

First, the individual chitinozoan specimens were classified into general groups based on their overall morphology. With the aid of the classification scheme of Paris et al. (1999), the specimens were further identified on a genus and species level based on the shape of the chamber and the arrangement of the ornamentation. This was done by using the chitinozoan catalogue, and references therein, which were available in micropalaeontology lab at the Department of Geology of Ghent University. Not all chitinozoans could be identified with certainty and Bengtson's (1988) rules for open nomenclature were applied for these specimens:

- **?** indicates that the determination is uncertain. This is mostly due to poor preservation of the material.
- **cf.** (= conferator) indicates that the identification is provisional. The specimen looks similar to a previously defined species, but there is a difference in diagnostic characteristic(s).
- **sp.** indicates that a species cannot be related to any formally defined species or that specific identification has not (yet) been attempted.

- **spp.** is used for specimens that could only be determined down to genus level. This notation indicates that there are multiple species from the same genus grouped together.

For some specimens, measurements of their vesicles were performed using the measurement tool of the image processing software Fiji (= ImageJ). This was done in order to aid the classification. Mostly the length (L), maximum vesicle diameter (Dp) and minimum vesicle diameter (Dc) were measured. Sometimes the minimum vesicle diameter and structures such as spines and appendices were measured as well. The L/Dp-ratio is used as diagnostic measures as well. The systematic section including descriptions and discussions can be found in annex II.

3. Results

3.1 Overview

In this master dissertation, 22 samples were analyzed for chitinozoans. Two samples, IGS-527-526 and IGS-527-528, did not contain any chitinozoans. The remaining 20 samples yielded 4151 specimens of which 2339 were identified down to species level. Some of the analyzed samples contained a small amount of conodonts and acritarchs, but they were not further studied in this dissertation. Not all of the samples contained well preserved specimens, especially sample IGS-527-514, for which no specimens could be identified with certainty down to species level. Other elements that complicated the determination were pyritized specimens and the presence of sticky amorphous organic material that obscured the chitinozoans. The identified chitinozoan species and their absolute abundances can be found in table 2.

At the base of the core, long ranging specimens of the *Cyathochitina* genus are present and occur throughout the whole core. *Angochitina capillata* is very abundant at the base of the core and drastically decreases in numbers until a depth of 530 ft, where they disappear. Only two more specimens of *A. capillata* higher in the core are found at a depth of 495 and 492 ft. *Tanuchitina ontariensis* occurs together with *A. capillata*. It is abundant, but less abundant than *A. capillata*, in the last two samples (541 ft and 545 ft depth). It does not occur higher in the core except for four questionable specimens at a depth of 530-532 ft. *Cyathochitina latipatagium* is also present from the base of the core and ranges until 524 ft depth (except for thin interval between 528 ft and 526 ft depth). When *A. capillata* and *T. ontariensis* are at their highest numbers, *Kalochitina multispinata* appears. This species has the same range *Hercochitina* sp.2 sensu De Backer (2017), although the latter one emerges just above *K. multispinata*, and they both have their last appearance at 519 ft depth.

Ancyrochitina merga, *Hercochitina longi* sensu De Backer (2017) and *Hercochitina pinguis* all three occur in just in one sample at a depth of 536 ft. *Nevadachitina* cf. *praevininica* and *Cyathochitina hunderumensis* both have their first appearance at this depth. The former ranges until a depth of 350 ft, the latter until a depth of 524 ft and questionably until 512 ft depth. *Ancyrochitina spongiosa* ranges from 532 ft to 512 ft depth. *Belonechitina* sp. 2 sensu Meyvisch (2018) and *Belonechitina* sp. 3 both have their first appearance at a depth of 530 ft. The former has its highest numbers at 530 ft depth and ranges until 524 ft depth, the latter has its highest numbers more towards the end of its range and occurs until 519 ft depth. *Cyathochitina patagiata* ranges from 524 ft to 512 ft depth. The last appearance of *Belonechitina* sp. 2 sensu Meyvisch (2018) marks the first appearance of *Angochitina* sp.3, *Belonechitina micracantha*, *Conochitia elegans* and *Tanuchitina bergstroemi*, which coincides with the base of the provisional Cape La Croix Formation. These four species all range from 523 ft to 519 ft depth. *Belonechitina* sp. 3 occurs in the same interval, but 2 specimens have also been found at 530 ft and 524 ft depth. *Belonechitina* cf. *cactacea*, *Hercochitina turnbulli* and *Belonechitina* sp. 1 are only present in 1 sample, respectively at 524 ft depth, 521 ft depth and 512 ft depth.

A clear distinction between the base of the core until 512 ft depth and the upper part between 512 ft and 472 ft depth can be seen. The upper part is dominated by specimens of the *Ancyrochitina*, *Angochitina* and *Cyathochitina* genus. Most of the *Ancyrochitina* specimens were too damaged and not sufficiently well preserved to identify them to species level. *Ancyrochitina nodifera* is with certainty identified and occurs from 510 ft to 490 ft depth, two uncertain specimens are found at 482 ft depth. *Ancyrochitina* sp. 1 is present at 506 ft, 490 ft and 482 ft depth. The specimens of the *Angochitina* genus are identified as *Angochitina hansonica*, *Angochitina* sp. 1 and *Angochitina* sp. 2. *Angochitina hansonica* ranges with certainty from 506 ft to 490 ft depth and questionably until 477 ft depth. *Angochitina* sp. 1 occurs throughout this whole interval and does not occur lower than a depth of 510 ft. *Angochitina* sp. 2 occurs at 495 ft depth and is abundant at 487 ft and 472 ft depth. *Fugochitina illinoisensis* is associated with that assemblage in the upper part of the core. *Cyathochitina calix* is present at 500 ft and 506 ft depth.

Sample IGS-527-521 contained two strange looking specimens that could not be identified and need further investigation. They can be found on plate 5, fig. 10-11.

3.2. Stratigraphic ranges of selected species

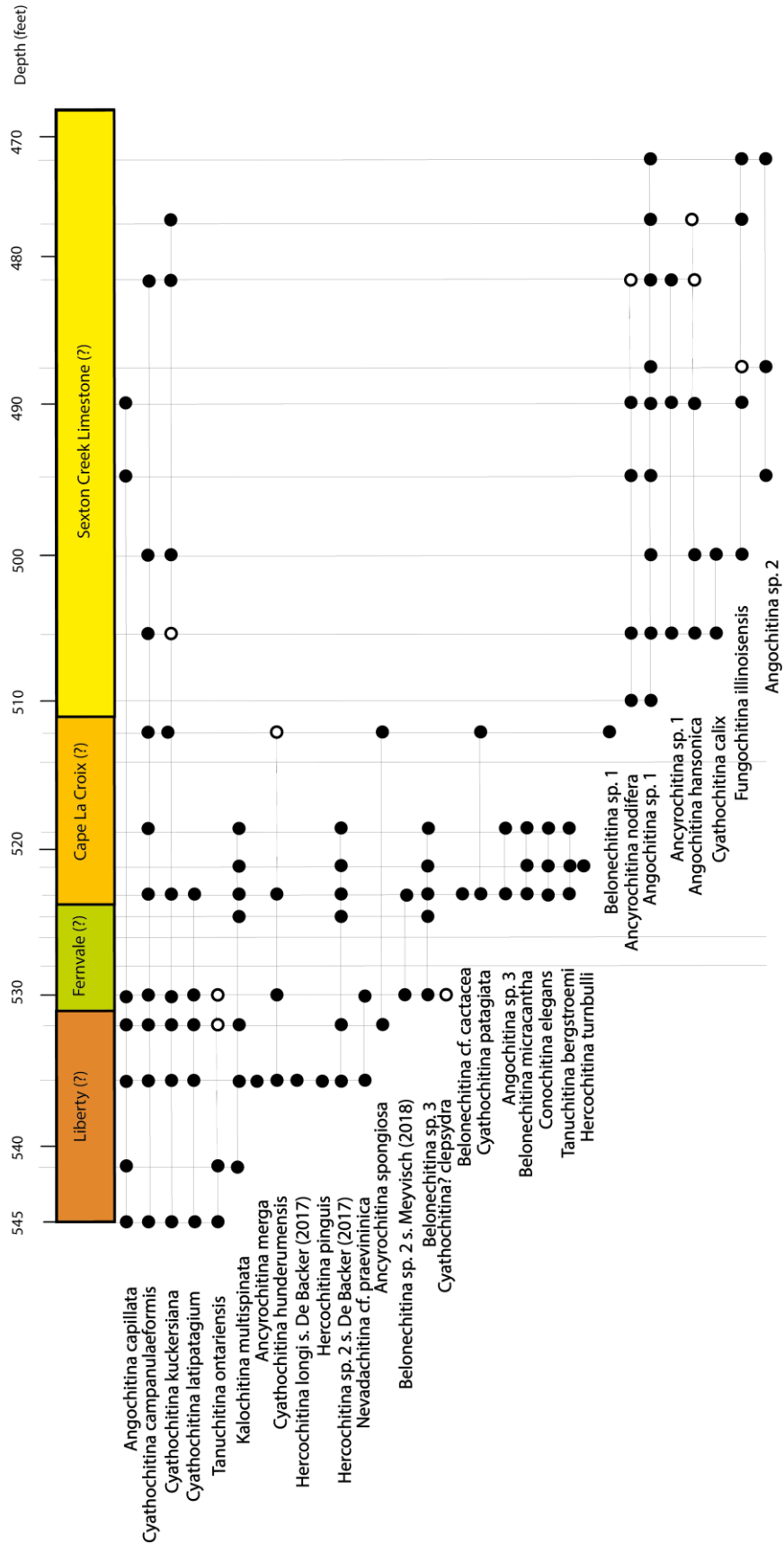


Figure 21: Stratigraphic ranges of the recovered chitinozoan species from this study. A filled dot represents a certain identification, an open dot represents an uncertain identification. The ranges of the species are indicated with full continuous lines, the dashed lines extend the ranges through uncertain identifications.

3.3. Systematic palaeontology

3.3.1. Alphabetical list

The alphabetical list of all the chitinozoan species observed in this master dissertation can be found in Annex I.

3.3.2. Systematics

The systematic description of all the chitinozoan species observed in this master dissertation can be found in Annex II.

4. Discussion

4.1. Assemblages

From bottom to top, the core contains the following assemblages. The first assemblage is characterized by *Angochitina capillata*, *Tanuchitina ontariensis*, *Kalochitina multispinata*, *Nevadachitina* cf. *praevininica*, *Hercochitina longi* sensu De Backer (2017) and *Hercochitina pinguis*. Associated species are *Hercochitina turnbulli*, *Ancyrochitina spongiosa*, *Ancyrochitina merga* and species of the *Cyathochitina* genus, some of which are long ranging. *A. capillata* and *T. ontariensis* dominate the lower part of this assemblage while the *Cyathochitina* genus is more prevalent in the upper part. This assemblage contains a lot of species with pronounced ornamentation. They characterize the lowest lithostratigraphic units in the core, more in particular the provisional Fernvale and Liberty formations, and can be correlated into the Maquoketa Group. This assemblage has been given a late Katian age based on the co-occurrence of a few species such as *Nevadachitina praevininica*, *Ancyrochitina spongiosa*, *Angochitina capillata*, *Kalochitina multispinata* and *Hercochitina* sp. 2 sensu De Backer (2017).

A second delimited assemblage is characterized by *Tanuchitina bergstroemi*, *Conochitina elegans* and a suite of species belonging to the *Belonechitina* genus, such as *Belonechitina* sp. 2 sensu Meyvisch (2018), *Belonechitina* sp. 3, *Belonechitina* cf. *cactacea*, *Belonechitina micracantha* and *Belonechitina* sp. 1. This assemblage is present in the provisional Cape La Croix and Fernvale formations and is dominated by *C. elegans* and *B. micracantha*. It is the first time a long *Tanuchitina* species is found in these rocks and in this region. *T. bergstroemi* is an indicator of Ashgill in the UK (Vandenbroucke, 2008b) and Baltoscandia (Laufeld, 1967), but also identical to *Tanuchitina elongata*, which is the index species for the Hirnantian in Gondwana. A sample from the Maquoketa Group strata of core Principia #4, western Illinois, yielded a monospecific assemblage of *C. elegans*, which is suggestive of a Late Ordovician age. This assemblage has a late Katian-early Hirnantian age.

The third assemblage is characterized by *Ancyrochitina nodifera* and *Angochitina hansonica*. Associated species are *Angochitina* sp. 1, *Ancyrochitina* sp. 1, *Fungochitina illinoisensis*, *Cyathochitina calix* and *Angochitina* sp. 2. Specimens of the genus *Ancyrochitina*, *Angochitina* and *Cyathochitina* dominate this assemblage. This is characteristic for levels immediately below and above the Ordovician-Silurian boundary (Vandenbroucke et al., 2008a; Verniers and Vandenbroucke, 2006). Almost all of the specimens of the genus *Cyathochitina* present in this assemblage belong to the long ranging species of *campanulaeformis* and *kuckersiana*. The few other specimens are *Cyathochitina calix*, which is found in specific stratigraphic intervals of the East Baltic Llandovery. They are restricted to the upper part of the core and occur at a depth of 500 ft to 506 ft. *Angochitina hansonica* and *Fungochitina illinoisensis* indicate a latest Ordovician to early Silurian age. *Ancyrochitina nodifera* and the *Cyathochitina* assemblage found in the upper part of the core, however, indicate an early Silurian age (early Rhuddanian) for the assemblage in the interval between 510 ft to 472 ft depth, given the fact that the *Cyathochitina* genus disappears from the record in the early Rhuddanian (Verniers et al., 1995).

4.2. Correlations

4.2.1. Correlation with the Maquoketa Group of Indiana (De Boodt, 2018)

The Elgin, Clermont, Fort Atkinson and 'Brainard' formations of the Maquoketa Group from core IGWS-440 have 11 species in common with core IGS-527: *Angochitina capillata*, *Cyathochitina campanulaeformis*, *Cyathochitina kuckersiana*, *Cyathochitina hunderumensis*, *Ancyrochitina spongiosa*, *Tanuchitina ontariensis*, *Kalochitina multispinata*, *Hercochitina turnbulli*, *Ancyrochitina merga*, *Conochitina elegans* and *Belonechitina micracantha* (Fig. 22). These species range from the Elgin Formation into the 'Brainard' Formation, except for *Ancyrochitina spongiosa* and *Tanuchitina ontariensis* whose last appearances are in the Fort Atkinson Formation. The 11 species above, co-occur in core IGS-527 in the interval between 512 ft and 545 ft depth. The large number of species these two cores have in common is not remarkable given their proximity. The upper part of the

Brainard Formation of core IGWS-440 is completely barren of chitinozoans. This does not coincide with the barren samples at 526 ft and 528 ft depth in core IGS-527, because *K. multispinata*, *H. sp. 2* sensu De Backer (2017), species of the *Cyathochitina* genus and *Ancyrochitina spongiosa* are observed above the barren interval, which is not the case for core IGWS-440.

If we look at the $\delta^{13}\text{C}$ curve of core IGWS-440, we see that the Elgin Formation and the lower part of the Clermont Formation coincide with the Waynesville Excursion. It has not been observed in core IGS-527, but appears to occur lower in the stratigraphy (Patrick McLaughlin, Pers. Comm.). The species these two cores have in common, however, also occur above the Waynesville Excursion. The interval between 512 ft and 545 ft depth in core IGS-527 can be correlated with the upper part of the Clermont Formation, the Fort Atkinson Formation and the 'Brainard' Formation of core IGWS-440.

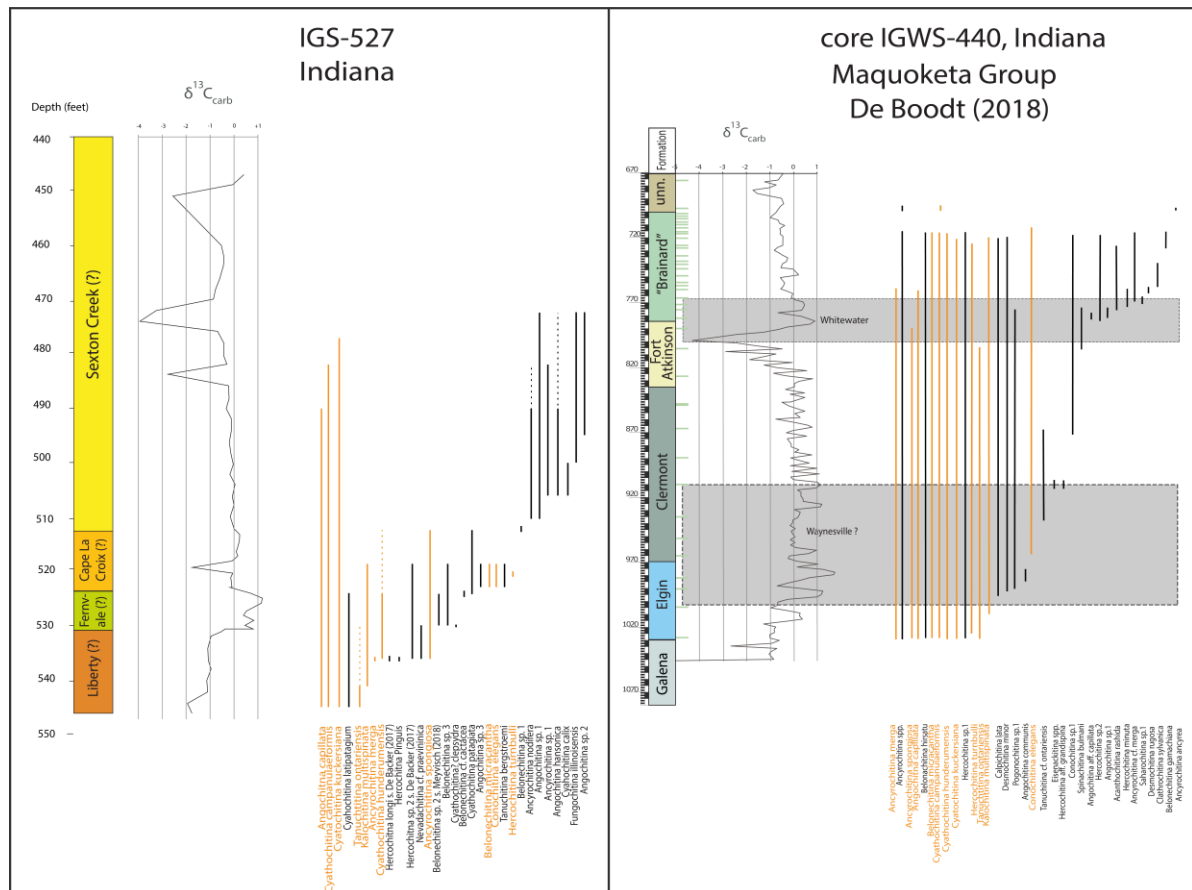


Figure 22: Chitinozoan bio- and chemostratigraphy of core IGS-527 and the Maquoketa Group in Indiana (De Boodt, 2018). Species found in both locations are indicated in orange, species only found in their respective locations are indicated in black. Correlations, as suggested in the text, are based on overlap of chitinozoan assemblages and chemostratigraphy.

4.2.2. Correlation with the Maquoketa Group of Wisconsin (De Backer, 2017)

The study of the Maquoketa Group from the Gardner Kiln core in Wisconsin (De Backer, 2017) showed a steady decrease in the palaeobiodiversity of the chitinozoans between the lower part of the Elgin Formation and the Brainard Formation (Fig. 23). The Elgin Formation contains an assemblage dominated by *Belonechitina hirsuta*, *Conochitina elegans*, species of the *Cyathochitina* genus, *Hercochitina turnbulli*, *Kalochitina multispinata* and *Tanuchitina ontariensis*. Associated species are *Ancyrochitina merga*, *Angochitina capillata*, *Belonechitina micracantha* and *Calpichitina lata*. Some species such as the *Calpichitina lata* and the *Cyathochitina* genus, range into the Clermont formation above. *Hercochitina sp. 2* (*Hercochitina sp. 2* sensu De Backer (2017) in this study) and *Hercochitina longi* (*Hercochitina longi* sensu De Backer (2017) in this study) occur just above this assemblage, respectively in the Upper Elgin and Clermont formations and in the Clermont Formation. The diversity of chitinozoans drops from the Elgin Formation until the Brainard

formation where there is a void of chitinozoans, except for the one sample containing *Eisenackitina ripae*.

The Elgin and Clermont formations from the Gardner Kiln core have 14 species in common with core IGS-527, belonging to both assemblage 1 and 2 (*Conochitina elegans* and *Belonechitina micracantha*). These shared species range from 512 ft to 545 ft depth in the core. *Hercoclitina* sp. 2 and *Hercoclitina longi* co-occur in this interval, as opposed to the Elgin and Clermont formations from the Maquoketa Group in Wisconsin, where they occur later than the rest of the assemblage.

Based on these biostratigraphical observations, a correlation between the interval from 512 ft to 545 ft depth with the Elgin and Clermont formations of the Maquoketa Group in Wisconsin can be made.

However, if we look at the $\delta^{13}\text{C}$ curve of the Gardner Kiln core, we see that the Elgin and Clermont formations co-occur with the Waynesville Excursion, as was the case for core IGWS-440, but only a few species range just above the excursion. This forms a discrepancy between the biostratigraphical and chemostratigraphical observations, as this excursion appears to occur stratigraphically lower in core IGS-527 (Patrick McLaughlin, Pers. Comm.).

A reason for this could be that the Maquoketa group in Wisconsin was heavily affected by the Waynesville excursion which only a few species survived. The discrepancy could also be explained by an underestimation of the stratigraphical ranges of the species in Wisconsin meaning that their ranges would be longer than is observed from the Gardner Kiln core. The local palaeo-environment would have also played a role in the distribution of these species.

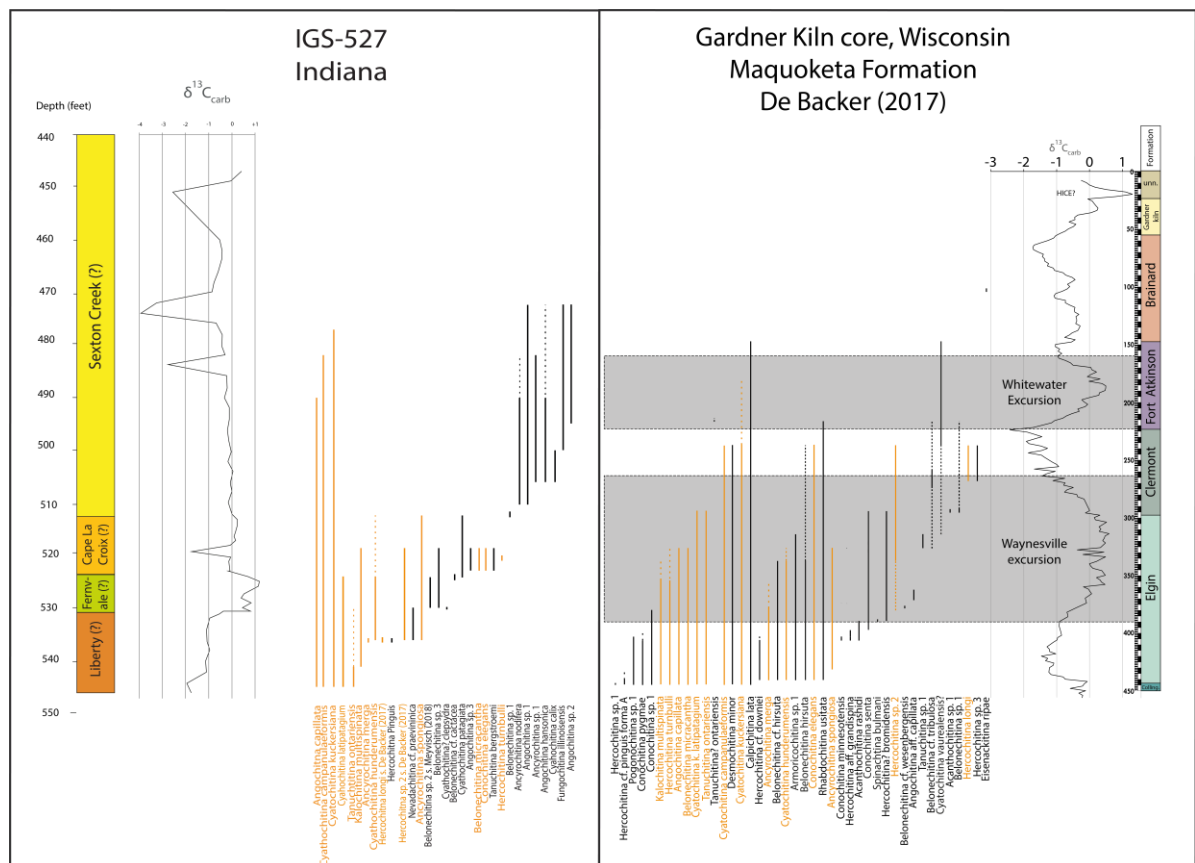


Figure 23: Chitinozoan bio- and chemostratigraphy of core IGS-527 and the Maquoketa Group in Wisconsin (De Backer, 2017). Species found in both locations are indicated in orange, species only found in their respective location are indicated in black. Correlations, as suggested in the text, are based on overlap of chitinozoan assemblages and chemostratigraphy.

4.2.3. Correlation with the Arbuckle Mountains, Oklahoma

Chitinozoans from the Viola Spring Formation, Fernvale Formation (now called the Welling Formation) and the Sylvan Shale in the Arbuckle Mountains in Oklahoma are described by Jenkins (1969, 1970). He noticed a difference in chitinozoan assemblage between the former two formations and the latter one and assumed a stratigraphic gap between these two sections. Only one species

was found in all three formations in the Arbuckle Mountains: *Desmochitina minor*. This is a very long-ranging species spanning almost the entire Ordovician (Eisenack, 1965). The Fernvale-Viola Spring succession is characterized by relatively long-ranging species such as *Desmochitina minor*, *Conochitina minnesotensis*, *Desmochitina lata* (now *Calpichitina lata*) and *Angochitina capillata*. Other species such as *Belonechitina micracantha*, *Belonechitina tribulosa*, *Belonechitina hirsuta*, *Hercochitina turnbulli*, *Cyathochitina patagiata* and *Cyathochitina latipatagium* are also present. The Sylvan Shale on the other hand is characterized by *Conochitina elegans*, *Conochitina cactacea* (now *Belonechitina cactacea*), *Kalochitina multispinata*, *Ancyrochitina merga* and *Cyathochitina ontariensis* (now *Tanuchitina ontariensis*). Typical species from the lower part of the Sylvan Shale are *Clathrochitina Sylvanica* and *Acanthochitina rashidi*.

Core IGS-527 has 6 species in common with the Fernvale-Viola Spring succession: *A. capillata*, *B. micracantha*, *H. turnbulli*, *C. patagiata*, *C. latipatagium* and *C. kuckersiana*; and 4 with the Sylvan Shale: *C. elegans*, *K. multispinata*, *A. merga* and *T. ontariensis*. These 10 species are not separated by a stratigraphic gap, but co-occur in the lower half of core IGS-527 from 545 ft up to 512 ft depth (Fig. 24). The absence of such a stratigraphic gap between the two successions and the co-occurrence of species of the two successions has also been observed by De Backer (2017) for the Elgin-Clermont formations in Wisconsin, by De Boodt (2018) for the Elgin, Clermont, Fort Atkinson and "Brainard" (temporary name) formations in Indiana and by Meyvisch (2018) in the Fernvale and Mannie formations in his Green Gap core from Tennessee. De Backer (2017) suggested that the Sylvan-specific taxa (from Oklahoma) had an earlier FAD in Wisconsin (and in this case the lower half of core IGS-527) or a later FAD in Oklahoma.

Another hypothesis is that the lower half of core IGS-527 was deposited during the transition from the Fernvale-Viola Spring succession to the Sylvan shale, characterized by a hiatus in the Arbuckle Mountains, and represents the missing interval with the transition between both assemblages. This would explain why species of both the Fernvale-Viola Spring succession and the Sylvan Shale co-occur in core IGS-527.

If we combine this biostratigraphical information with the $\delta^{13}\text{C}$ curve, a tentative correlation can be made between the lower part of core IGS-527 (545 ft to 512 ft depth), the Sylvan Shale and the underlying stratigraphic gap between the Sylvan Shale and the Fernvale-Viola Spring succession.

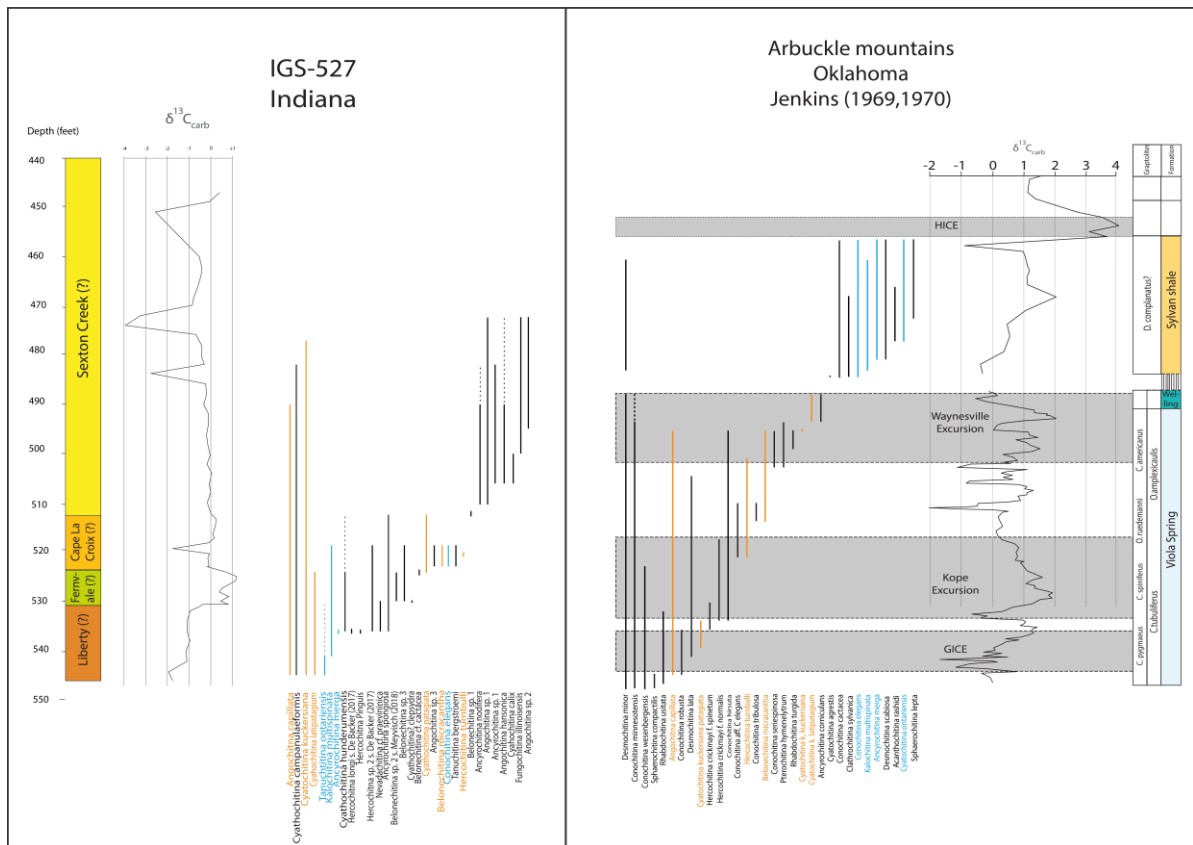


Figure 24: Chitinozoan biostratigraphy of core IGS-527 and the formations from the Arbuckle Mountains, Oklahoma (Jenkins, 1969, 1970). Species only found in their respective location are indicated in black, species occurring in the Viola Spring-Welling formations and core IGS-527 are indicated in orange, those occurring in the Sylvan Shale and core IGS-527 are indicated in blue. The $\delta^{13}C$ curve for the Viola Spring-Welling succession is taken from Bergström et al. (2010) and provided by Patrick McLaughlin for the Sylvan Shale. Graptolite zones are derived from Finney (1986) and Finney et al. (1999). Correlations, as suggested in the text, are based on overlap of chitinozoan species and chemostratigraphy.

4.2.4. Correlation with the Fernvale of Tennessee (Meyvisch, 2018)

Core IGS-527 has 7 species in common with the Green Gap core in Tennessee from Meyvisch (2018). Two of them occur both in the provisional Fernvale Formation of core IGS-527 and the Fernvale Formation of the Green Gap core, of which only the uppermost part has been sampled: *Angochitina capillata* and *Conochitina elegans* (Fig. 25). Core IGS-527 has 8 species in common with the Thompson's Station location in Tennessee of Meyvisch (2018) of which 4 occur in both Fernvale formations: *Hercochitina* sp. 2 sensu De Backer (2017), *Cyathochitina kuckersiana*, *Cyathochitina latipatagium* and *Cyathochitina campanulaeformis* (Fig. 26). The assemblage in the provisional Fernvale Formation of core IGS-527 not clearly delimited and is characterized species ranging in the Cape La Croix and Liberty formations and the overlying Mannie Shale. Based on biostratigraphy and the age of the assemblages found in the cores, a very tentative correlation can be made between the provisional Fernvale Formation of core IGS-527 and the Fernvale formation of the Green Gap and Thompson's Station locations in Tennessee.

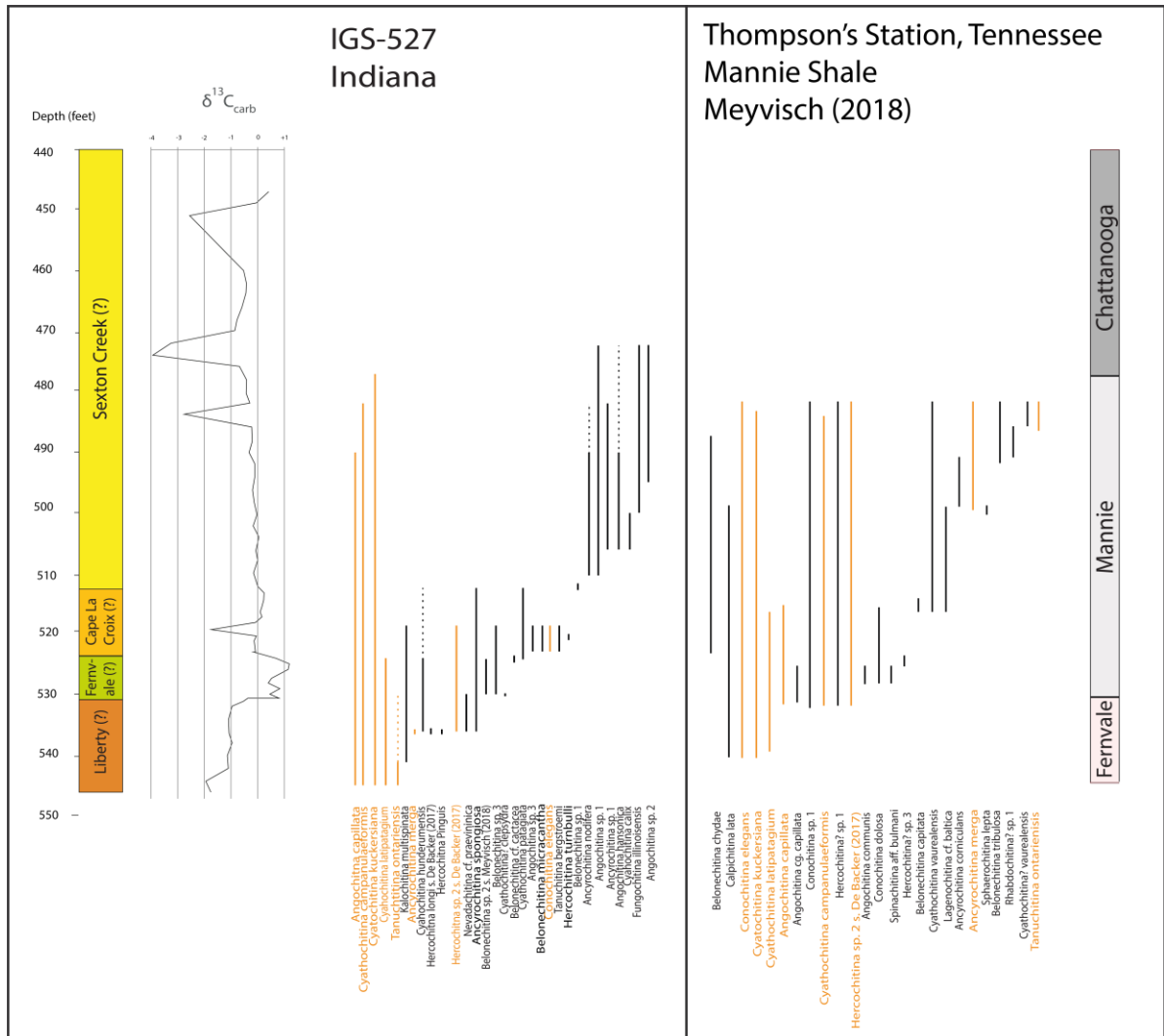


Figure 26: Chitinozoan biostratigraphy of core IGS-527 and the Mannie Shale of the Thompson's Station location in Tennessee (Meyvisch, 2018). Species found in both locations are indicated in orange, species only found in their respective location are indicated in black. Correlations, as suggested in the text, are based on overlap of chitinozoan assemblages.

4.2.5. Correlation with the Cincinnati Arch, Ohio

Velleman (2016) constructed a biostratigraphical framework for the Cincinnati region (Fig. 27) by combining a lithostratigraphic framework established for the Maysville area with his own biostratigraphical findings and data from Miller (1976), who studied a section a few miles away from where Velleman (2016) did his research. Velleman (2016) found several faunal turnovers in his chitinozoan assemblage. 9 species found in core MY-14 from Maysville, Kentucky, are also present in core IGS-527. These include *Angochitina capillata*, species of the *Cyathochitina* genus and *Kalochitina multispinata* and species with a shorter range such as *Hercoclitina turnbulli*, *Ancyrochitina spongiosa*, *Ancyrochitina merga* and *Belonechitina micracantha*. These species are found in the provisional Cape La Croix, Fernvale and Liberty formations (545 ft to 512 ft depth). Based on biostratigraphy, these provisional formations can be correlated with the Fairview, Grand Lake Limestone and Arnheim formations of core MY-14.

The $\delta^{13}\text{C}$ curve, however, shows a discrepancy in stratigraphic occurrences as the mutual species occur stratigraphically together or below with the Waynesville Excursion in core MY-14. This mismatch in stratigraphic occurrences has also been observed by De Backer (2017) and by De Boodt (2018) in their effort to correlate the Maquoketa Group of Wisconsin and Indiana with the Cincinnati Arch in Ohio.

This discrepancy could be explained in the same way as the mismatch between core IGS-527 and the Gardner Kiln core of De Backer (2017): underestimation of the stratigraphic ranges in core MY-14 and the role of the local palaeo-environment on the distribution of the species.

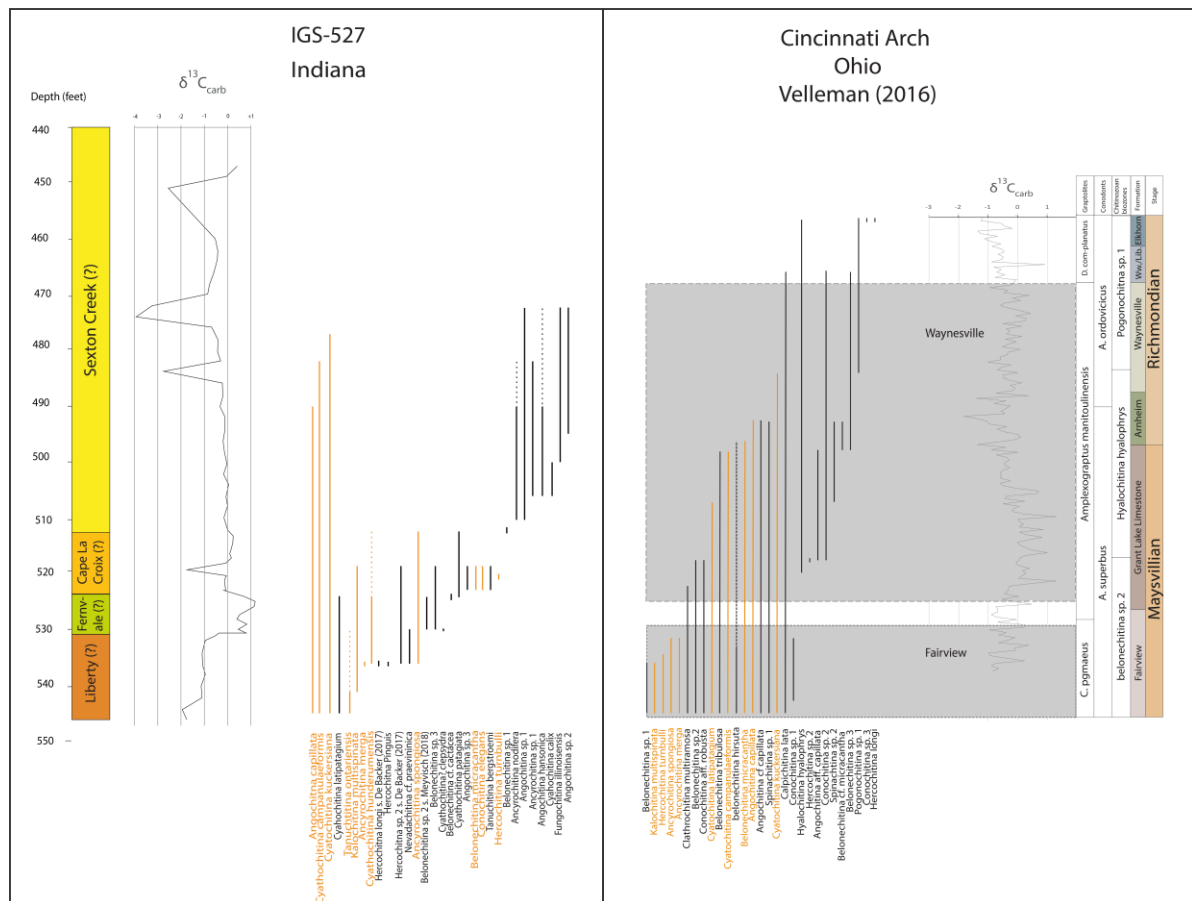


Figure 27: Chitinozoan bio- and chemostratigraphy of core IGS-527 and the Cincinnati Arch region (Velleman, 2016). Species found in both locations are indicated in orange, species only found in their respective location are indicated in black. The $\delta^{13}\text{C}$ curve was provided by Patrick McLaughlin. Correlations, as suggested in the text, are based on overlap of chitinozoan assemblages and chemostratigraphy.

4.2.6. Correlation with Anticosti Island

Anticosti Island in the Gulf of St. Lawrence, Canada, is known to host one of the best preserved Upper Ordovician-lower Silurian successions known today, making this a key section to correlate with core IGS-527. Anticosti Island contains thick, carbonate-dominated succession containing extremely well preserved shelly fauna (Ghienne et al., 2014; Melchin, 2008). However, building a high-resolution chronostratigraphic framework has proven to be difficult due to the low number of graptolites recovered from the Vauréal and Ellis Bay formations (McLaughlin et al., 2016), although the base of the Hirnantian Stage is defined by graptolites (base of the *N. extraordinarius* Biozone, Chen et al., 2006). A summarizing study by Melchin (2008) and recent chemostratigraphic research by McLaughlin et al. (2016) reconfirm that the Vauréal Formation represents a small part of the upper Katian and that the Ellis Bay Formation has a Hirnantian age.

The Vauréal and Ellis Bay formations on Anticosti Island have 6 species in common with core IGS-527: *C. latipatagium*, *K. multispinata*, *A. spongiosa*, *A. merga*, *C. kuckersiana* and *B. micracantha* (Fig. 28). The former three species characterize the Waynesville Excursion on Anticosti Island. *B. micracantha* occurs in the Ellis Bay Formation (Hirnantian), just below the stable carbon isotope peak at the end of the Hirnantian. There it is associated with key species *Belonechitina gamachiana*, which has not been found in core IGS-527. These 6 mutual species co-occur in core IGS-527 in the interval between 512 ft and 545 ft depth, while this is not the case in the Vauréal and Ellis Bay formations. Some of these are long ranging so it is possible that their occurrence differ from section to section. So the provisional Cape La Croix, Fernvale and Liberty formations of core IGS-527 could

be correlated with the Vauréal and Ellis Bay formations on Anticosti Island based on chitinozoan biostratigraphy. The $\delta^{13}\text{C}$ curve however tells us that the species associated with the Waynesville Excursion on Anticosti Island occur stratigraphically below core IGS-527, causing a mismatch in biostratigraphy and chemostratigraphy. This could be explained by the fact that the mutual species are long ranging, but not continuous, so their occurrence can differ from section to section.

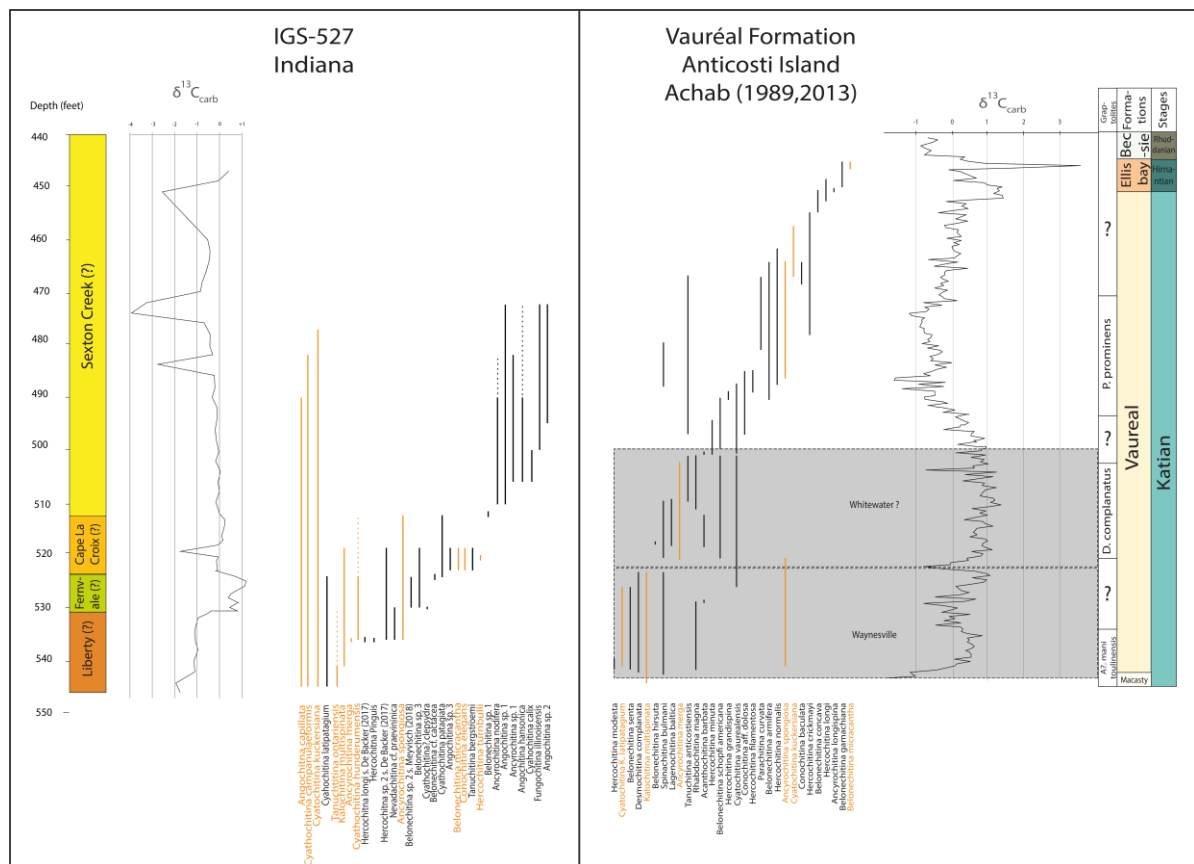


Figure 28: Chitinozoan biostratigraphy of core IGS-527 and the Vauréal and Ellis Bay formations on Anticosti Island, Quebec. Species found in both locations are indicated in orange, species only found in their respective location are indicated in black. The chitinozoan ranges are taken from Achab (1977a, b; 1978a, b; 1989), Achab et al. (2013) and McLaughlin et al. (2016). The $\delta^{13}\text{C}$ curve was taken from McLaughlin et al. (2016). Correlations, as suggested in the text, are based on overlap of chitinozoan species and chemostratigraphy.

The Becscie Formation on Anticosti Island, early Rhuddanian in age (McLaughlin et al. (2016)), has 3 species in common with core IGS-527: *Ancyrochitina nodifera* (identified as *Plectochitina nodifera* on this location), *Ancyrochitina spongiosa* (identified as *Plectochitina spongiosa* on this location) and *Cyathochitina kuckersiana*. They co-occur at the base of the Becscie Formation (Fig. 29). In core IGS-527, *C. kuckersiana* is long-ranging and occurs throughout almost the entire core. *A. spongiosa* is not found above 510 ft, while *A. nodifera* is not found below 512 ft depth. The reason that *A. spongiosa* does not co-occur with the other two species could be that it ranges from the middle Katian into the lowermost Silurian, but it is seldom observed continuous for the entire interval. *P. nodifera* and *C. kuckersiana* are associated with *Angochitina hansonica* and *Fungochitina illinoisensis* in core IGS-527, but these last two species are not observed on Anticosti Island. Based on biostratigraphy, the upper part of core IGS-527, the provisional Sexton Creek Formation, between 510 ft and 490 ft (and questionably until 482 ft) can be correlated to the lower part (Member 1) of the Becscie Formation on Anticosti Island.

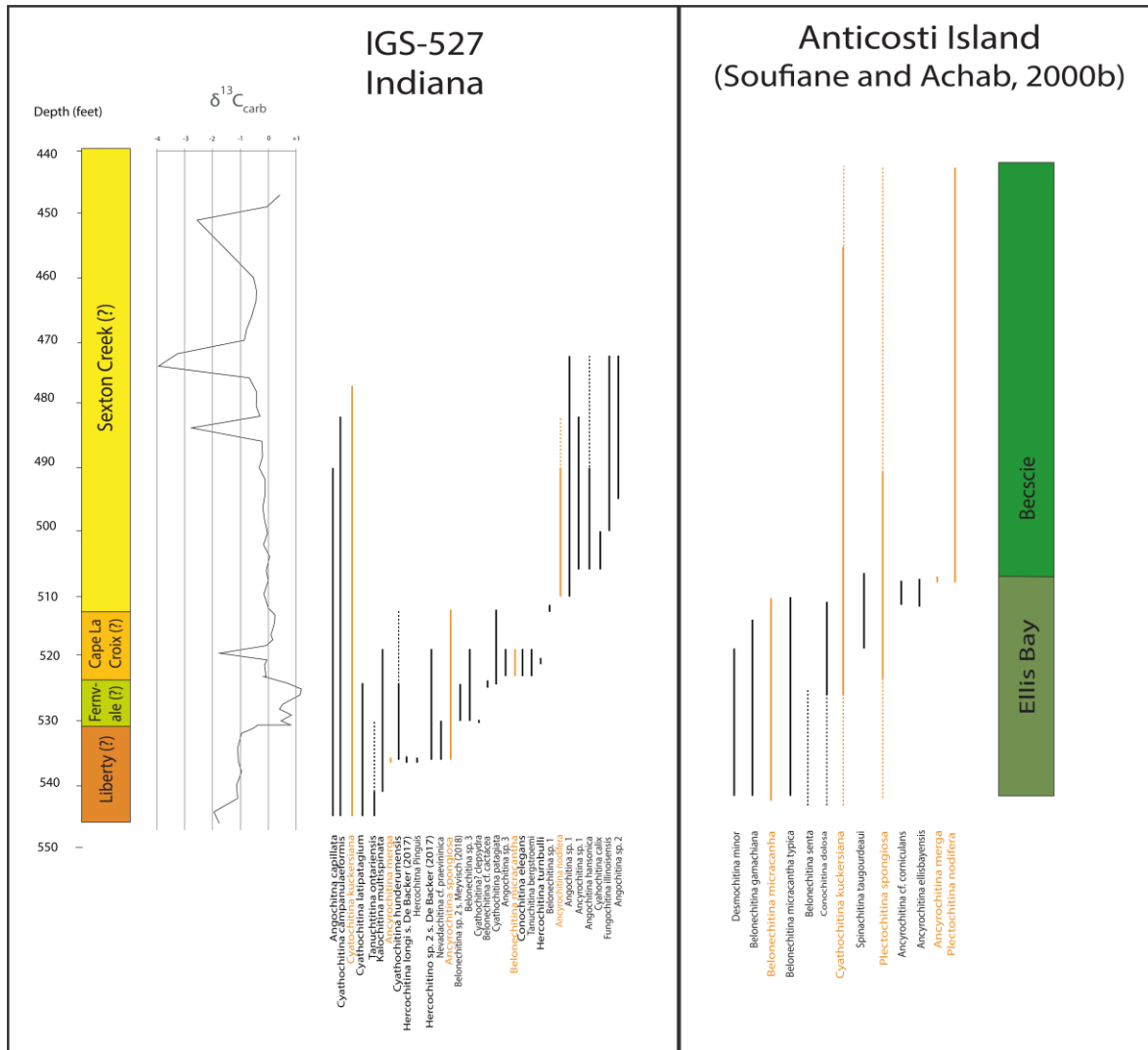


Figure 29: Chitinozoan biostratigraphy of core IGS-527 and the Ellis Bay and Becscie formations on Anticosti Island, Quebec. Species found in both locations are indicated in orange, species only found in their respective location are indicated in black. The chitinozoan ranges are taken from Soufiane and Achab (2000b). Correlations, as suggested in the text, are based on overlap of chitinozoan species.

Species of the Silurian assemblage of core IGS-527 have also been found in Baltoscandia. In the Ohne and Staciunai formations of the lowermost Juuru Regional Stage of Estonia and Latvia, *Ancyrochitina nodifera* (identified as *Plectochitina nodifera* on this location) co-occurs with abundant *Cyathochitina campanulaeformis*, *Ancyrochitina spongiosa* (identified as *Plectochitina spongiosa* on this location) and *Ancyrochitina laevaensis* in the *A. laevaensis* Biozone (early Rhuddanian). Following the same line of thinking as for the Becscie Formation, we can correlate the interval of core IGS-527 between 510 ft and 490 ft (and questionably until 482 ft) with the Ohne and Staciunai formations of the lowermost Juuru Regional Stage of Estonia and Latvia.

4.2.7. Correlation with western Illinois (core Principia #4)

Core Principia #4 from western Illinois only yielded two samples that contained chitinozoans (Fig. 30). The sample from the upper part of the Bowling Green Dolomite contained *A. hansonica*, *C. campanulaeformis* and *F. illinoisensis* and is Rhuddanian to Aeronian in age (early Silurian). These three species co-occur in core IGS-527 at a depth from 472 ft to 506 ft. The upper part of core IGS-527, the Sexton Creek Formation, between 472 ft and 506 ft depth could be correlated with the sample from the upper part of the Bowling Green Dolomite from core Principia #4. The fact that these species are found in one sample only hampers this correlation.

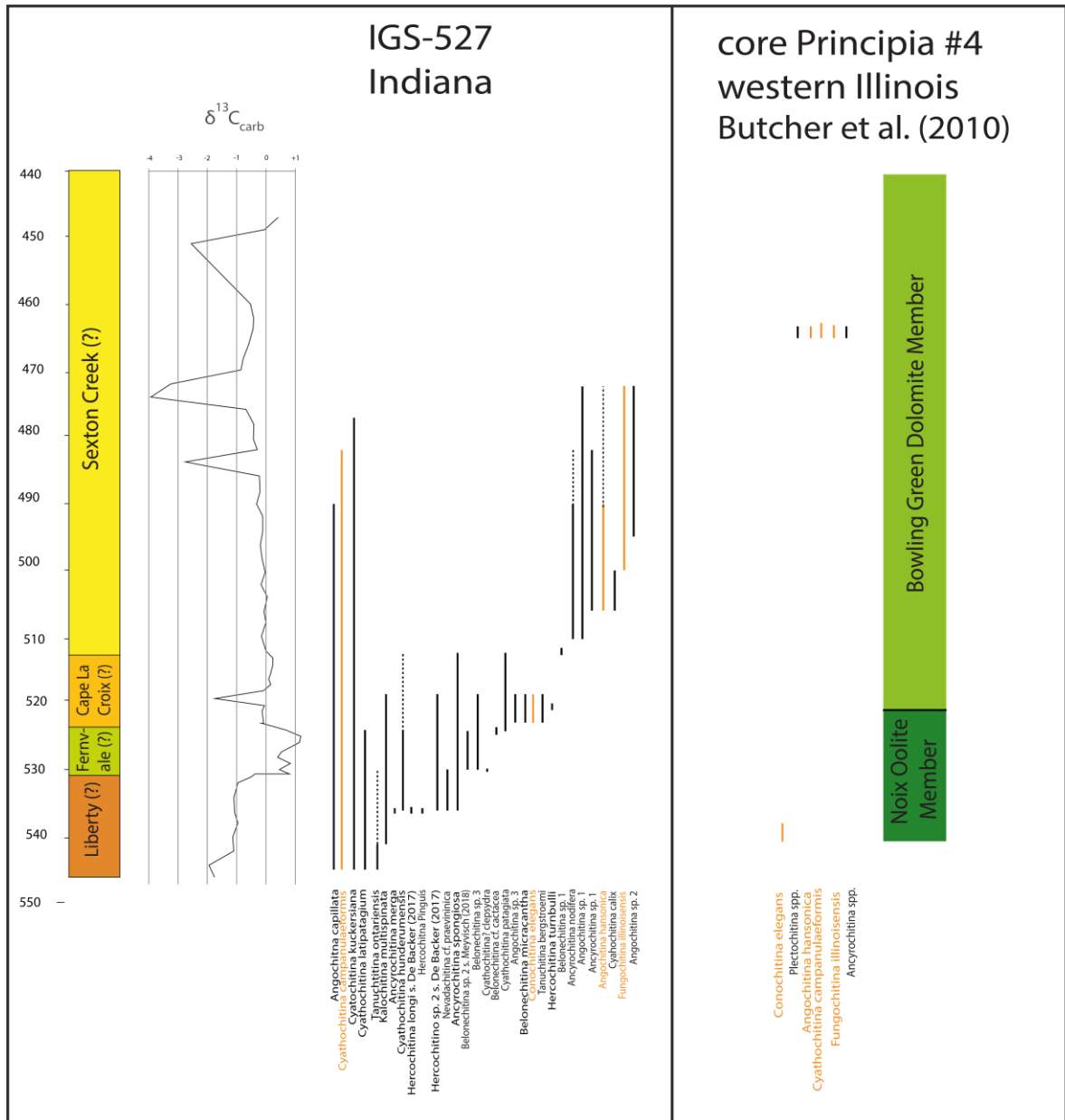


Figure 30: Chitinozoan biostratigraphy of core IGS-527 and the Noix Oolite and Bowling Green Dolomite members in western Illinois. Species found in both locations are indicated in orange, species only found in their respective location are indicated in black. The chitinozoan ranges are taken from Butcher et al. (2010). Correlations, as suggested in the text, are based on overlap of chitinozoan species.

4.2.8. Correlation with Nevada

The Hanson Creek Formation in Nevada has 3 species in common with core IGS-527: *Kalochitina multispinata*, *Angochitina hansonica* and *Cyathochitina campanulaeformis* (Fig. 31). *Angochitina hansonica* co-occurs with *Cyathochitina campanulaeformis* in the uppermost part of the Hanson Creek Formation: the *A. hansonica* Biozone (latest Ordovician to early Silurian). These two species co-occur in core IGS-527 in the interval between 490 ft and 506 ft depth, making a correlation between this depth interval and the uppermost strata of the Hanson Creek Formation possible.

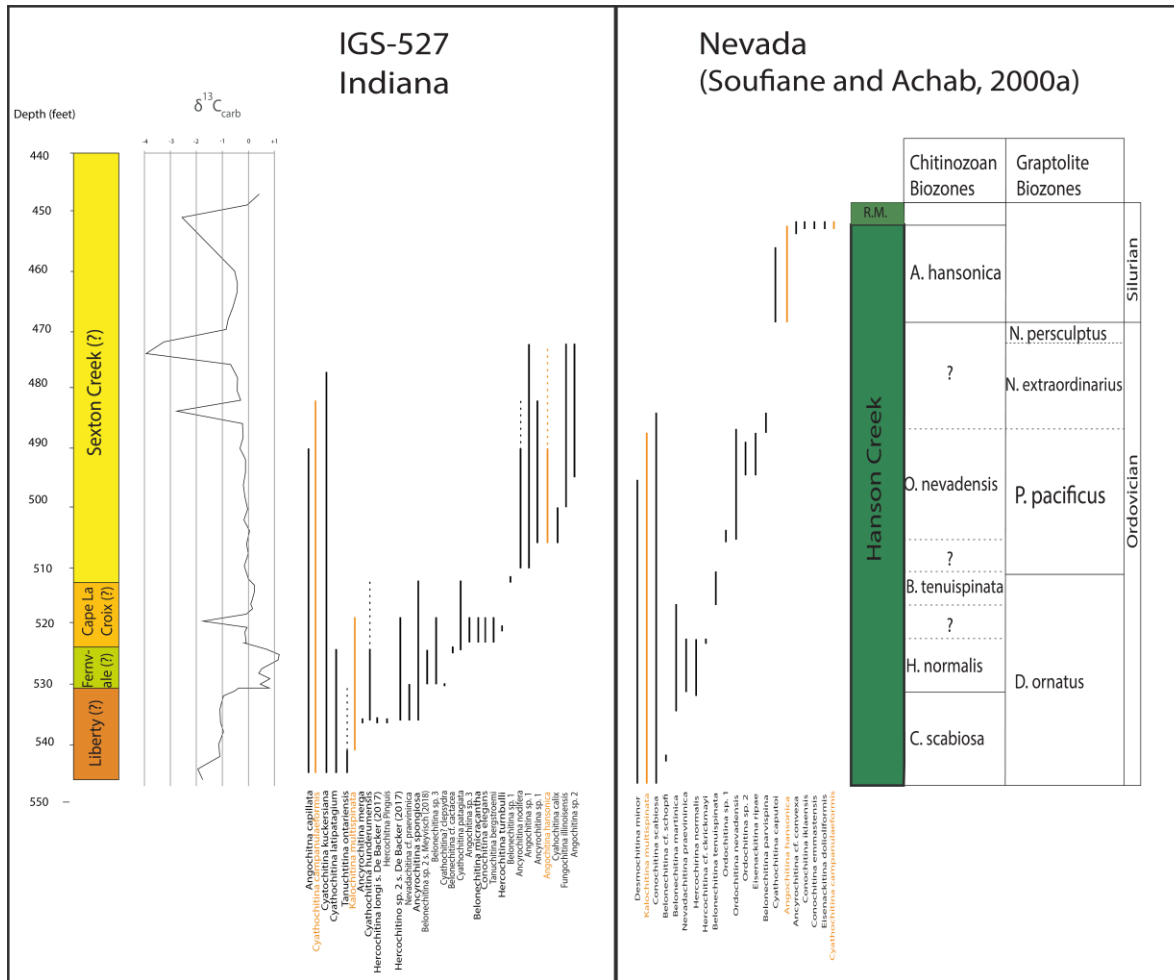


Figure 31: Chitinozoan biostratigraphy of core IGS-527 and the Hanson Creek Formation in Nevada. Species found in both locations are indicated in orange, species only found in their respective location are indicated in black. The chitinozoan ranges and chitinozoan biozones are taken from Soufiane and Achab (2000a), as modified from Soufiane and Achab (1999). The graptolite biozones are taken from Finney et al. (1999). Correlations, as suggested in the text, are based on overlap of chitinozoan species.

5. Conclusions

The chitinozoan content of core IGS-527 in Carrol County, Indiana, was investigated in the context of a collaborative project aiming to provide the age of the strata and to enhance the Upper Ordovician and especially the lower Silurian biostratigraphy of the Indiana region of the US Midcontinent. The 22 analyzed samples yielded 4151 chitinozoan specimens of which 2339 could be identified down to species level. These were classified in 31 different species for which the stratigraphic ranges were established.

3 distinct assemblages were observed in the chitinozoan biostratigraphy of the core. The first one is characterized by species with pronounced ornamentation and include *Angochitina capillata*, species of the *Cyathochitina* genus, *Tanuchitina ontariensis*, *Kalochitina multispinata*, *Nevadachitina* cf. *praevininica*, *Ancyrochitina spongiosa* and *Ancyrochitina merga*. *A. capillata* and *T. ontariensis* dominate the lower part of this assemblage while the *Cyathochitina* genus is more prevalent in the upper part. They characterize the lowest lithostratigraphic units in the core, the provisional Fernvale and Liberty formations, and can be correlated into the Maquoketa Group. This assemblage has a late Katian age. A second delimited assemblage, present in the provisional Cape La Croix and Fernvale formations, is characterized by *Tanuchitina bergstroemi*, *Conochitina elegans* and a suite of species belonging to the *Belonechitina* genus. *Belonechitina micracantha* and *Belonechitina* sp. 1., *C. elegans* and *B. micracantha* dominate this assemblage. This assemblage has a late Katian-early Hirnantian age. The third assemblage is characterized by *Ancyrochitina nodifera*, *Angochitina hansonica* and associated *Fungochitina illinoisensis* and is present in the interval between 510 ft to 472 ft depth, the provisional Sexton Creek Formation. Specimens of the genus *Ancyrochitina*, *Angochitina* and *Cyathochitina* dominate this assemblage, which is characteristic for levels immediately below and above the Ordovician-Silurian boundary. This assemblage indicates an early Rhuddanian (early Silurian) age.

The bio- and chemostratigraphy was used to tentatively correlate core IGS-527 with the Maquoketa Group in Indiana and Wisconsin, the Fernvale Formation in Tennessee, the Arbuckle Mountains in Oklahoma, the Cincinnati Arch Region, the Vauréal Ellis Bay and Becscie formations on Anticosti Island, western Illinois and Nevada. Correlation with the Maquoketa Group in Wisconsin, the Cincinnati Arch Region and the Vauréal and Ellis Bay formations on Anticosti Island show a discrepancy between the biostratigraphical and chemostratigraphical observations and requires further research. The scarcity of retrieved chitinozoan specimens in western Illinois and Nevada makes a correlation with the Sexton Creek Formation possible, but a better biostratigraphical framework of these areas is needed to confirm this.

The proposed Fernvale Limestone Formation in core IGS-527 contains some species of the Fernvale assemblage. However, these are long ranging so further research is required. The age of the assemblages and the correlation with other locations suggest that the gap between the Upper Ordovician and lower Silurian (see section 2.6) is hardly present in core IGS-527 and the core covers the Upper Ordovician-lower Silurian interval. The ages of the retrieved samples, with a late Katian-early Hirnantian age for the laminated facies at the base of the provisional Sexton Creek Formation, largely correspond with the age of the provisional lithostratigraphic units and with the provisional chemostratigraphy.

References

- Achab, A. (1977a). Les chitinozoaires de la zone a *Climacograptus prominens elongatus*, de la Formation de Vauréal (Ordovicien supérieur), Ile d'Anticosti, Quebec. *Canadian Journal of Earth Sciences*, 14, 2193–2212.
- Achab, A. (1977b). Les chitinozoaires de la zone a *Dicellograptus complanatus* Formation de Vauréal, Ordovicien supérieur, Ile d'Anticosti, Quebec. *Canadian Journal of Earth Sciences*, 14(3), 413-425.
- Achab, A. (1978a). Sur quelques chitinozoaires de la formation de Vauréal et de la formation de Macasty (Ordovicien supérieur), ile d'anticosti, Quebec, Canada. *Review of Palaeobotany and Palynology*, 25(3-4), 295-314.
- Achab, A. (1978b). Les Chitinozoaires de l'Ordovicien supérieur, Formations de Vauréal et d'Ellis Bay, de l'Ile d'Anticosti, Quebec. *Palinologia número extraordinario*, 1, 1–19.
- Achab, A. (1989). Ordovician chitinozoan zonation of Quebec and Western Newfoundland. *Journal of Paleontology*, 63(1), 14–24.
- Achab, A. Paris, F. (2007) The Ordovician chitinozoan biodiversification and its leading factors. *Palaeogeography, Palaeoclimatology, Palaeoecology*, 245, 5–19.
- Achab, A., Asselin, E., Desrochers, A., Riva, J. F. (2013). The end-Ordovician chitinozoan zones of Anticosti Island, Québec: Definition and stratigraphic position, *Review of Palaeobotany and Palynology*, 198, 92–109.
- Achab, A., Asselin, E., Desrochers, A., Riva, J. F., Farley, C. (2011). Chitinozoan biostratigraphy of a new Upper Ordovician stratigraphic framework for Anticosti Island, Canada. *Bulletin of the Geological Society of America*, 123(1–2), 186–205.
- Ainsaar, L., Kaljo, D., Martma, T., Meidla, T., Männik, P., Nõlvak, J., Tinn, O. (2010). Middle and Upper Ordovician carbon isotope chemostratigraphy in Baltoscandia: A correlation standard and clues to environmental history. *Palaeogeography, Palaeoclimatology, Palaeoecology* 294, 189–201.
- Ainsaar, L., Meidla, T., Martma, T. (1999). Evidence for a widespread carbon isotopic event associated with late Middle Ordovician sedimentological and faunal changes in Estonia. *Geological Magazine* 136 (1), 49–62.
- Atherton, E. (1971). Tectonic development of the Eastern Interior region of the United States, in Background materials for symposium on future petroleum potential of NPC region 9 (Illinois basin, Cincinnati arch, and northern part of Mississippi Embayment): Illinois State Geological Survey, *Illinois Petroleum* 96, p. 29-43.
- Azmy, K., Veizer, J., Bassett, M.G., Copper, P. (1998). Oxygen and carbon isotopic composition of Silurian brachiopods: Implications for coeval seawater and glaciations. *Geological Society of America Bulletin*, 110, 1499–1512.
- Bas, J. (2017). *Changes in Chitinozoan Assemblages Through Ordovician And Devonian Stable Carbon Isotope Excursions*. (Master's thesis) Ghent University.
- Bengtson, P. (1988). Open nomenclature, *Palaeontology* 31, 223–227.
- Bennett, C.E., Williams, M., Leng, M.J., Lee, M.R., Bonifacie, M., Calmels, D., Fortey, R.A., Laurie, J.R., Owen, A.W., Page, A.A., Munnecke, A., Vandenbroucke, T.R.A. (2018). Oxygen isotope analysis of the eyes of pelagic trilobites: testing the application of sea temperature proxies for the Ordovician. *Gondwana Research*, 57, 157-169.
- Bergström, S., Finney, S.C., Xu, C., Goldman, D. Leslie, S.A. (2006). Three new Ordovician global stage names. *Lethaia*, 39(4), 287-288.
- Bergström, S.M. (1970). Conodont biostratigraphy of the Middle and Upper Ordovician of Europe and eastern North America. *Geological Society of America Memoir* 127, 83–161.
- Bergstrom, S.M. (2003). The Red River problem revisited: stratigraphic relationships in the Upper Ordovician of central and western United States. 47–52. In: Albanesi, G.L., Beresi, M.S., Peralta, S.H. (eds). INSUGIO, serie Correlacion Geologica, Ordovician from the Andes, *Registro Nacional de la Propiedad Intelectual*, San Juan, 549.
- Bergström, S.M., Chen, X.U., Gutierrez-Marco, J.C., Dronov, A., (2009). The new chronostratigraphic classification of the Ordovician System and its relations to major regional series and stages and to $\delta^{13}\text{C}$ chemostratigraphy. *Lethaia*, 42, 97-107.
- Bergström, S.M., Finney, S.C., Chen Xu, Pålsson, C., Wang Zhi-hao, Grahn, Y. (2000). A proposed global boundary stratotype for the base of the Upper Series of the Ordovician System: The Fågelsång section, Scania, southern Sweden. *Episodes* 23, 102-109.
- Bergström, S.M., Kleffner, M.A. (2018). Katian (Upper Ordovician) global $\delta^{13}\text{C}$ chemostratigraphy: implications of the discovery of a complete Elkhorn Excursion in its type area in western Ohio. In *52nd Annual North-Central GSA Section Meeting Abstracts with Programs*, Ames, Iowa.

- Bergstrom, S.M., MacKenzie, P. (2005). Biostratigraphic and paleoceanographic relations between the type Richmondian (Upper Ordovician) in the Cincinnati region and the Upper Mississippi Valley succession, *Iowa Geological Survey Guidebook Series*, 24, 35–37.
- Bergström, S.M., Mitchell, C.E. (1986). The graptolite correlation of the North American Upper Ordovician Standard. *Lethaia* 19, 247–266.
- Bergström, S.M., Mitchell, C.E. (1990). Trans-Pacific graptolite faunal relations: the biostratigraphic position of the base of the Cincinnati Series (Upper Ordovician) in the standard Australian graptolite zone succession. *Journal of Paleontology*, 64, 992–997.
- Bergström, S.M., Mitchell, C.E. (1994). Regional relationships between late Middle and early Late Ordovician standard successions in New York and Quebec and the Cincinnati region in Ohio, Indiana, and Kentucky. *New York State Museum Bulletin*, 481, 5–20.
- Bergström, S.M., Saltzman, M.R., Schmitz, B. (2006). First record of the Hirnantian (Upper Ordovician) $\delta^{13}\text{C}$ excursion in the North American Midcontinent and its regional implications. *Geological Magazine* 143, 657–678.
- Bergström, S.M., Young, S., Schmitz, B. (2010). Katian (Upper Ordovician) $\delta^{13}\text{C}$ chemostratigraphy and sequence stratigraphy in the United States and Baltoscandia: A regional comparison. *Palaeogeography, Palaeoclimatology, Palaeoecology*, 296(3–4), 217–234.
- Bergström, S.M., Young, S., Schmitz, B., Saltzman, M.R. (2007). Upper Ordovician (Katian) $\delta^{13}\text{C}$ chemostratigraphy: a trans-Atlantic comparison. *Acta Palaeontologica Sinica* 46, 37–39.
- Berry, W.B.N., Boucot, A.J. (1973). Glacio-eustatic control of Late Ordovician-Early Silurian platform sedimentation and faunal changes. *Geol. Soc. Am. Bull.* 84:275–84
- Bickert, T., Pätzold, J., Samtleben, C., Munnecke, A. (1997). Paleoenvironmental changes in the Silurian indicated by stable isotopes in brachiopod shells from Gotland, Sweden. *Geochimica et Cosmochimica Acta* 61, 2717–2730.
- Brenchley, P.J., Marshall, J.D., Carden, G.A.F., Robertson, D.B.R., Anderson, T.F. (1994). Bathymetric and isotopic evidence for a short-lived Late Ordovician glaciation in a greenhouse period. *Geology*, 22 (April), 295–298.
- Buschback, T.C., Kolata, D.R. (1990). Chapter 1: Regional Setting of Illinois Basin, 29–58. In: Leighton, M.W., Kolata, D.R., Oltz, D.F., Eidel, J.J. (Eds.). Interior Cratonic Basins, *American Association of Petroleum Geologists*.
- Butcher, A., Mikulic, D., Kluessendorf, J. (2010). Late Ordovician-Early Silurian chitinozoans from northeastern and western Illinois, USA, *Review of Palaeobotany and Palynology* 159(1-2): 81–93.
- Calner, M. (2008). Silurian global events - at the tipping point of climate change, in: Mass Extinction. Springer Berlin Heidelberg, Berlin, *Heidelberg*, pp. 21–57.
- Caputo, M.V. (1998). Ordovician–Silurian glaciations and global sea-level changes. In: Landing, E., Johnson, M.E. (eds) *Silurian Cycles, Linkages of Dynamic Stratigraphy with Atmospheric, Oceanic, and Tectonic Changes*. *New York State Museum Bulletin*, 491, 15–25.
- Chen, X., Rong, J., Fan, J., Zhan, R., Mitchell, C.E., Harper, D.A.T., Melchin, M.J., Peng, P., Finney, S.C., Wang, X. (2006). The Global Boundary Stratotype Section and Point (GSSP) for the base of the Hirnantian Stage (the uppermost of the Ordovician System). *Episodes*. 29 (3): 183–96.
- Cocks, L.R.M., Torsvik, T.H. (2002) Earth geography from 500 to 400 million years ago: a faunal and paleomagnetic review. *Journal of the Geological Society*, 159 (February), 631–644.
- Cocks, L.R.M., Torsvik, T.H. (2011) The Palaeozoic geography of Laurentia and western Laurussia: A stable craton with mobile margins. *Earth Science Review*, 106, 1–51.
- Combaz, A., Lange, F.W., Pansart, J. (1967). Les "Leiofusidae" Eisenack, 1938. *Review of Palaeobotany and Palynology* 1, 291–307.
- Combaz, A., Poumont, C. (1962). Observations sur la structure des Chitinozoaires. *Revue de Micropaléontologie* 5, 147–160.
- Corradini, C., Serpagli, E. (1999). A Silurian conodont biozonation from late Llandovery to end Pridoli in Sardinia (Italy). *Bollettino della Società Paleontologica Italiana* 37, 255–273.
- Corriga, M.G., Corradini, C. (2009). Upper Silurian and Lower Devonian conodonts from the Monte Cocco II section (Carnic Alps, Italy). *Bulletin of Geosciences* 84, 155–168.
- Cowie, J., Cohen, A. (2010). Past Carbon Isotopic Events and Future Ecologies. Abstract Book for the symposium 2nd – 3rd November. *Geological Society*, London.
- Cramer, B.D., Brett, C.E., Melchin, M.J., Männik, P., Kleffner, M.A., McLaughlin, P.I., Loydell, D.K., Munnecke, A., Jeppsson, L., Corradini, C., Brunton, F.R., Saltzman, M.R. (2011a). Revised correlation of Silurian Provincial Series of North America with global and regional chronostratigraphic units and $\delta^{13}\text{C}_{\text{carb}}$ chemostratigraphy. *Lethaia* 44, 185–202.
- Cramer, B.D., Davies, J.R., Ray, D.C., Thomas, A.T., Cherns, L. (2011b). Siluria Revisited: An introduction. In: Ray, D.C. (Ed.), *Siluria Revisited, a Field Guide*, International Subcommission on Silurian Stratigraphy Field Meeting 2011, pp. 6–27.

- Cramer, B.D., Kleffner, M.A., Saltzman, M.R. (2006b). The Late Wenlock Mulde positive carbon isotope excursion in North America. *GFF* 128, 85–90.
- Cramer, B.D., Saltzman, M.R. (2005). Sequestration of ^{12}C in the deep ocean during the early Wenlock (Silurian) positive carbon isotope excursion. *Palaeogeography, Palaeoclimatology, Palaeoecology* 219, 333–349.
- Cramer, B.D., Saltzman, M.R. (2007a). Early Silurian paired $\delta^{13}\text{C}_{\text{carb}}$ and $\delta^{13}\text{C}_{\text{org}}$ analyses from the Midcontinent of North America: implications for paleoceanography and paleoclimate. *Palaeogeography, Palaeoclimatology, Palaeoecology* 256, 195–203.
- Cramer, B.D., Saltzman, M.R. (2007b). Fluctuations in epeiric sea carbonate production during Silurian positive carbon isotope excursions: A review of proposed paleoceanographic models. *Palaeogeography, Palaeoclimatology, Palaeoecology* 245, 37–45
- Dabard, M.P., Loi, A., Paris, F., Ghienne, J.F., Pistis, M., Vidal, M. (2015). Sea-level curve for the Middle to early Late Ordovician in the Armorican Massif (western France): Icehouse third-order glacio-eustatic cycles. *Palaeogeography, Palaeoclimatology, Palaeoecology*, 436, 96–111.
- Davies, J.R., Waters, R.A., Molyneux, S.G., Williams, M., Zalasiewicz, J.A., Vandenbroucke, T.R.A. (2016). Gauging the impact of glacioeustasy on a mid-latitude early Silurian basin margin, mid Wales, UK. *Earth-Science Reviews* 156, 82–107.
- De Backer, T. (2017). *Chitinozoan contributions to Maquoketa Formation holostratigraphy (Upper Katian, Wisconsin, USA)*. (Master's thesis) Ghent University.
- De Boedt (2018). *Towards putting order to the events leading up to the Late Ordovician mass extinction: Integrated biochemostratigraphy of the Maquoketa Group in IGWS core 440 from NW Indiana, USA*. (Master's thesis) Ghent University, University of Brussels, University of Antwerp.
- De Waele (2017). *Chitinozoan palynology of a Katian (Late Ordovician) carbon cycle perturbation along a palaeo-environmental gradient in the Upper Mississippi Valley, USA*. (Master's Thesis). Ghent University.
- De Weirtdt, J., Vandenbroucke, T.R.A., Emsbo, P., McLaughlin, P.I., Delabroye, A., Munnecke, A., Desrochers, A. (2016). Testing global anoxia as an alternative cause for Hirnantian mass extinction: New evidence from Western Anticosti Island, Canada. [Abstract], In: GSA Annual meeting; 2016, September 27, Denver, Colorado: Article # 240-8
- De Weirtdt, J., Vandenbroucke, T.R.A., Emsbo, P., McLaughlin, P.I., Delabroye, A., Munnecke, A., Desrochers, A. (2017). Is Global Anoxia an Alternative Cause for the Hirnantian Mass Extinction? [Abstract], In: EGU general assembly; 2017, April 23-28, Vienna, Austria: Article #14885
- Dutta, S., Brocke, R., Hartkopf-Fröder, C., Littke, R., Wilkes, H., Mann, U. (2007). Highly aromatic character of biogeomacromolecules in Chitinozoa: a spectroscopic and pyrolytic study. *Organic Geochemistry* 38, 1625–1642.
- Dutta, S., Hartkopf-Fröder, C., Witte, K., Brocke, R., Mann, U. (2013). Molecular characterization of fossil palynomorphs by transmission micro-FTIR spectroscopy: implications for hydrocarbon source evaluation. *International Journal of Coal Geology* 115, 13-23.
- Eisenack, A. (1931). Neue Mikrofossilien des baltischen Silurs. I. *Palaeontologische Zeitschrift*, 13, 74-118.
- Eisenack, A. (1965). Die Mikrofauna der Ostseekalke. Chitinozoen, Hystrichosphären. *Neueus Jb. Geol. Palaont. Abh.* 123: 115-148.
- Emsbo, P., McLaughlin, P.I., Munnecke, A., Breit, G.N., Koenig, A.E., Jeppsson, L., Verplanck, P. (2010). The Ireviken event: A Silurian OAE. *Geol. Soc. Am.*, 42, 561.
- Finney, S.C. (1986). Graptolite biofacies and correlation of eustatic, subsidence, and tectonic events in the Middle to Upper Ordovician of North America. *Palaios*, 435-461.
- Finney, S.C., Berry, W.B., Cooper, J.D., Ripperdan, R.L., Sweet, W.C., Jacobson, S.R., Soufiana, A., Achab, A., Noble, P.J. (1999). Late Ordovician mass extinction: A new perspective from stratigraphic sections in central Nevada. *Geology*, 27(3), 215-218.
- Fortey, R.A., Cocks, L.R.M. (2005). Late Ordovician global warming – The Boda Event. *Geology*, 33, 405–408.
- Gabbott, S.E., Aldridge, R.J., Theron, J.N. (1998). Chitinozoan chains and cocoons from the Upper Ordovician Soom Shale Lagerstätte, South Africa: Implications for affinity: *Geological Society of London Journal* 155, 447–452.
- Gao, G., Dworkin, S.I., Land, L.S., Elmore, R.D. (1996). Geochemistry of Late Ordovician Viola Limestone, Oklahoma: implications for marine carbonate mineralogy and isotopic compositions. *The Journal of Geology* 104, 359–367.
- Ghienne, J.F. (2003). Late Ordovician sedimentary environments, glacial cycles, and post-glacial transgression in the Taoudeni Basin, West Africa. *Palaeogeography, Palaeoclimatology, Palaeoecology*, 189, 117–145.

- Ghienne, J.F., Desrochers, A., Vandenbroucke, T.R.A., Achab, A., Asselin, E., Dabard, M.P., Farley, C., Loi, A., Paris F., Wickson, S., Veizer, J. (2014). A Cenozoic-style scenario for the end-Ordovician glaciation. *Nature Communications*, 5, 4485.
- Goldman, D., Bergström, S. M. (1997). Late Ordovician graptolites from the North American Midcontinent, *Palaeontology*, 40(4), 965–1010.
- Goldman, D., Leslie, S.A., Nölvak, J., Young, S., Bergström, S.M., Huff, W.D. (2007). The Global Stratotype Section and Point (GSSP) for the base of the Katian Stage of the Upper Ordovician Series at Black Knob Ridge, Southeastern Oklahoma, USA. *Geology Faculty Publications*, 6, 258- 270.
- Grahn, Y. (1981). Ordovician Chitinozoa from the Stora Asbotorp boring in Västergötland, south-central Sweden, *Sveriges Geologiska Undersökning*, C. NR 787, p. 40.
- Gray, H.H. (1986). In: Compendium of Paleozoic Rock-Unit Stratigraphy in Indiana – a Revision. Indiana Geological Survey, Bulletin 59, p. 37.
- Hammarlund, E.U., Dahl, T.W., Harper, D.A.T., Bond, D.P.G., Nielsen, A.T., Bjerrum, C.J., Schovsbo, N.H., Schönlaub, H.P., Zalasiewicz, J.A., Canfield, D.E. (2012). A sulfidic driver for the end-Ordovician mass extinction. *Earth and Planetary Science Letters*, 331–332, 128–139.
- Hamoumi, N. (1999). Upper Ordovician glaciation spreading and its sedimentary record in Moroccan North Gondwana margin. In: Kraft, P., Fjäckä, O. (eds) Quo Vadis Ordovician? Acta Universitatis Carolinae, *Geologica*, 43, 111–114.
- Haq, B. U., Schutter, S. R. (2008). A Chronology of Palaeozoic sea level changes. *Science*, 322 (October), 64–69.
- Harrison, R.W. (1999). Geological map of the Thebes quadrangle, Missouri and Illinois: U.S. Geological Survey Geologic Quadrangle Map, GQ-1779, Scale 1:24,000.
- Hatch, J.R., Jacobson, S.R., Witzke, B.J., Risatti, J.B., Anders, D.E., Wattney, W.L., Newell, K.D., Hayes, C.W., Ulrich, E.O. (1903). Columbia folio, Tennessee: U.S. Geological Survey Geologic Atlas of the United States Folio, GF-95, 6 p., scale 1: 125,000.
- Heath, R.J. (1998). *Palaeoceanographic and Faunal Changes in the Early Silurian*. (Ph.D. Thesis) University of Liverpool, Liverpool, U.K. 239 pp.
- Heidlauf, D.T., Hsui, A.T., Klein, G.D. (1986). Tectonic subsidence analysis of the Illinois Basin. *J. Geol.* 94, 779-794.
- Jacob, J., Paris, F., Monod, O., Miller, M.A., Tang, P., George, S.C., Bény, J.M. (2007). New insights into the chemical composition of chitinozoans. *Organic Geochemistry* 38, 1782–1788.
- Jacobson, S.R., Achab, A. (1985). Acritarch biostratigraphy of the *Dicellograptus complanatus* graptolite zone from the Vaureal Formation (Ashgillian), Anticosti Island, Quebec, Canada, *Palynology*, 9, 165- 198.
- Jenkins, W.A.M., (1969). Chitinozoa from the Ordovician Viola and Fernvale Limestones of the Arbuckle Mountains Oklahoma. *Special Papers in Palaeontology*, 5, 1–43.
- Jenkins, W.A.M., (1970). Chitinozoa from the Ordovician Shale of the Arbuckle Mountains, Oklahoma. *Palaeontology*, 13, 261–288.
- Jenkyns, H.C. (2010) Geochemistry of oceanic anoxic events. *Geochemistry Geophysics Geosystems*, 11 (3), 1-30.
- Jeppsson, L. (1987). Lithological and conodont distributional evidence for episodes of anomalous oceanic conditions during the Silurian. In: Aldridge, R.J. (Ed.), *Palaeobiology of Conodonts*. Ellis Horwood Ltd., Chichester, pp. 129–145.
- Jeppsson, L. (1997a). A new latest Telychian, Sheinwoodian and early Homerian (early Silurian) standard conodont zonation. *Transactions of the Royal Society of Edinburgh, Earth Sciences* 88, 91-114.
- Jeppsson, L. (1997b). Recognition of a probable secundo-primo event in the Early Silurian. *Lethaia* 29, 311-315.
- Jeppsson, L., Aldridge, R.J. (2000). Ludlow (late Silurian) oceanic episodes and events, *Journal of the Geological Society* 157, 1137–1148.
- Jeppsson, L., Eriksson, M.E., Calner, M. (2006). A latest Llandovery to latest Ludlow high-resolution biostratigraphy based on the Silurian of Gotland – a summary. *GFF* 128, 109-114.
- Johnson, M.E. (1987). Extent and bathymetry of North American platform seas in the early Silurian. *Paleoceanography* 2, 185–211.
- Johnson, M.E. (1996). Stable cratonic sequences and a standard for Silurian eustasy. In: Witzke, B.J., Ludvigson, G.A., Day, J. (Eds.): *Paleozoic Sequence Stratigraphy: View from the North American Craton. Geological Society of America Special Paper* 306, 203–211.
- Johnson, M.E. (2006). Relationship of Silurian sea-level fluctuations to oceanic episodes and events. *GFF* 128, 115–121.
- Johnson, M.E. (2010). Tracking Silurian eustasy: alignment of empirical evidence or pursuit of deductive reasoning? *Palaeogeography, Palaeoclimatology, Palaeoecology* 296, 276–284.

- Kaljo, D., Hints, L., Hints, O., Martma, T., Nõlvak, J. (2001). Carbon isotope stratigraphy in the latest Ordovician of Estonia. *Chemical Geology* 175, 49–59.
- Kaljo, D., Kiipli, T., Martma, T. (1997). Carbon isotope event markers through the Wenlock-Pridoli sequence at Ohesaare (Estonia) and Priekule (Latvia). *Palaeogeography, Palaeoclimatology, Palaeoecology* 132, 211–223.
- Kaljo, D., Kiipli, T., Matma, T. (1998). Correlation of carbon isotope events and environmental cyclicity in the East Baltic Silurian, 297–312. In Landing, E., Johnson, M. (eds) *Silurian Cycles: Linking Dynamic Stratigraphy with Atmospheric, Oceanic, and Tectonic Changes*. *New York State Museum Bulletin* 491.
- Kaljo, D., Martma, T. (2000). Carbon isotopic composition of Llandovery rocks (East Baltic Silurian) with environmental interpretation. *Proceedings of the Estonian Academy of Sciences, Geology* 49, 267–283.
- Kaljo, D., Martma, T. (2006). Application of carbon isotope stratigraphy to dating the Baltic Silurian rocks. *GFF* 128, 123–129.
- Kaljo, D., Martma, T., Grytsenko, V., Brazauskas, A., Kaminskas, D. (2012). Pridolí carbon isotope trend and upper Silurian to lowermost Devonian chemostratigraphy based on sections in Podolia (Ukraine) and the East Baltic area. *Estonian Journal of Earth Sciences* 61, 162–180.
- Kaljo, D., Martma, T., Männik, P., Viira, V. (2003). Implications of Gondwana glaciations in the Baltic Late Ordovician and Silurian and a carbon isotopic test of environmental cyclicity. *Bulletin de la Societe Geologique de France* 174, 59–66.
- Kaljo, D., Martma, T., Saadre, T. (2007). Post-Hunnebergian Ordovician carbon isotope trend in Baltoscandia, its environmental implications and some similarities with that of Nevada. *Palaeogeography, Palaeoclimatology, Palaeoecology*, 245 (1–2), 138–155.
- Klein, G. deV., Hsui, A.T., 1987. Origin of cratonic basins. *Geology* 15: 1094-1098.
- Kozłowski, R. (1963). Sur la nature des chitinozoaires. *Acta Palaeont. Pol.*, 8: 425–449.
- Laufeld, S. (1967). Caradocian Chitinozoa from Dalarna, Sweden. *Geologiska Föereningen ii Stockholm. Föerhandlingar*, 89, 275–349.
- Loydell, D.K. (1998). Early Silurian sea-level changes. *Geological Magazine* 135, 447–471.
- Loydell, D.K., Kaljo, D., Männik, P. (1998). Integrated biostratigraphy of the lower Silurian of the Ohesaare core, Saaremaa, Estonia. *Geological Magazine*, 135, 769–783.
- Ludvigson, G.A., Witzke, B.J., Schneider, C.L., Smith, E.A., Emerson, N.R., Carpenter, S.J., González, L.A. (2004). Late Ordovician (Turonian–Chatfieldian) carbon isotope excursions and their stratigraphic and paleoceanic significance. *Palaeogeography, Palaeoclimatology, Palaeoecology* 210, 187–214.
- Mabillard, J.E., Aldridge, R.J. (1985). Microfossil distribution across the base of the Wenlock Series in the type area. *Palaeontology* 28, 89–100.
- Männik, P. (1998). Evolution and taxonomy of the Silurian conodont Pterospathodus. *Paleontology* 41, 1001–1050.
- Männik, P. (2007a). An updated Telychian (Late Llandovery, Silurian) conodont zonation based on Baltic faunas. *Lethaia* 40, 45–60.
- Männik, P. (2007b). Recent developments in the Upper Ordovician and lower Silurian conodont biostratigraphy in Estonia. *Estonian Journal of Earth Sciences* 56, 35–46.
- McGinnis, L.D. (1970). Tectonics and the gravity field in the continental interior: *Journal of Geophysical Research* 75, p. 317-331.
- McGinnis, L.D., Heigold, C.P., Ervin, C.P., Heidi, M. (1976). The gravity field and tectonics of Illinois. *Illinois State Geological Survey Circular* 494, p. 24.
- McLaughlin, P.I., Emsbo, P., Brett, C.E. (2012). Beyond black shales: The sedimentary and stable isotope records of oceanic anoxic events in a dominantly oxic basin (Silurian; Appalachian Basin, USA). *Palaeogeography, Palaeoclimatology, Palaeoecology*, 367–368, 153–177.
- McLaughlin, P.I., Emsbo, P., Desrochers, A., Bancroft, A. M., Brett, C., Premo, W., Neynard, L., Riva, J., Achab, A., Asselin, E., Emmons, M.M. (2016). Refining 2 km of Ordovician chronostratigraphy beneath Anticosti Island utilizing integrated chemostratigraphy, *Canadian Journal of Earth Sciences*, 53(8), 865-874.
- Melchin, M. J. (2008). Restudy of some Ordovician–Silurian boundary graptolites from Anticosti Island, Canada, and their biostratigraphic significance. *Lethaia*, 41(2), 155- 162.
- Melchin, M.J., Holmden, C. (2006). Carbon isotope chemostratigraphy of the Llandovery in Arctic Canada: implications for global correlation and sea-level change. *GFF* 128, 173–180.
- Melchin, M.J., Holmden, C., Williams, S.H. (2003). Correlation of graptolite biozones, chitinozoan biozones and carbon isotope curves through the Hirnantian. In: Albanesi, G.L., Beresi, S., Peralta, S.H. (Eds.), *Ordovician from the Andes: INSUGEO, Serie Correlación Geológica* 17, p. 101-104.

- Melchin, M.J., Sadler, P.M., Cramer, B.D. (2012). Chapter 21: The Silurian Period, 525–588. In Gradstein, F., Ogg, J., Schmitz, M., Ogg, G. (eds) *The Geologic Time Scale 2012*. Elsevier, New York.
- Meyvisch, P. (2018). *Comparative chitinozoan palynology of the Upper Ordovician Mannie and Cape La Croix Shales: refining age relations between the Appalachian and Illinois Basins*. (Master's thesis) Ghent University.
- Mikulic, D.G., Sargent, M.L., Norby, R.D., Kolata, D.R. (1985). Silurian geology of the Des Plaines River valley, northeastern Illinois. *Illinois State Geological Survey Guidebook 17*, p. 56.
- Miller, M.A. (1976). *Maysvillian (Upper Ordovician) chitinozoans from the Cincinnati region of Ohio, Indiana and Kentucky* (Master's thesis). Ohio State Survey.
- Munnecke, A., Samtleben, C., Bickert, T. (2003). The Ireviken Event in the lower Silurian of Gotland, Sweden — relation to similar Palaeozoic and Proterozoic events. *Palaeogeography, Palaeoclimatology, Palaeoecology* 195, 99–124.
- Nardin, E., Godd ris, Y., Donnadiou, Y., Le Hir, G., Blakey, R.C., Puc at, E., Aretz, M. (2011). Modelling the early Palaeozoic long-term climatic trend, *Geol. Soc. Am. Bull.*, 123(5–6), 1181–1192.
- Nickles, J.M. (1903). The Richmond group in Ohio and Indiana and its subdivisions, with a note on the genus *Strophomena* and its type: *American Geologist*, v. 32, p. 202–218.
- Nielsen, A.T. (2003a). Ordovician sea level changes: a Baltoscandinavian perspective. In: Webby, B.D., Paris, F., Droser, M., Percival, I.G. (eds) *The Great Ordovician Biodiversification Event*. *Columbia University Press*, New York, 84–93.
- Nielsen, A.T. (2003b). Late Ordovician sea level changes: evidence of Caradoc glaciations? *Geophysical Research Abstracts, European Geosciences Union*, 5.
- Nielsen, A.T. (2004). Ordovician sea level changes: a Baltoscandinavian perspective. In: Webby, B.D., Paris, F., Droser, M., Percival, I. (Eds.), *The Great Ordovician Diversification Event*. *Columbia University Press*, New York, pp. 84–93.
- Noble, P.J., Zimmerman, M.K., Holmden, C., Lenz, A.C. (2005). Early Silurian (Wenlock) $\delta^{13}\text{C}$ and elemental geochemistry from the Cape Phillips Formation, Arctic Canada and its relation to biotic events. *Canadian Journal of Earth Sciences* 42, 1419–1430.
- N lvak, J., Grahn, Y. (1993). Ordovician chitinozoan zones from Baltoscandia. *Review of Palaeobotany and Palynology*, 79, 245–269.
- Page, A.A., Zalasiewicz, J.A., Williams, M., Popov, L.E. (2007). Were transgressive black shales a negative feedback modulating glacioeustasy in the Early Palaeozoic Icehouse? In: Williams, M., Haywood, A.M., Gregory, F.J., Schmidt, D.N. (Eds), *Deep-Time Perspectives on Climate Change: Marrying the Signal from Computer Models and Biological Proxies*, p. 123–156. The Micropalaeontological Society, Special Publications; London.
- Pancost, R.D., Freeman, K.H., Herrmann, A.D., Patzkowsky, M.E., Ainsaar, L., Martma, T. (2013). Reconstruction Late Ordovician carbon cycle variations. *Geochim. Cosmochim. Acta*, 105, 433–454.
- Paris, F. (1981) Les Chitinozoaires dans le Pal ozoique du sud-ouest de l'Europe (cadre g ologique -  tude syst matique – biostratigraphie). *M moire de la Soci t  g ologique et min ralogique de Bretagne*, 26, 492.
- Paris, F. (1990). The Ordovician chitinozoan biozones of the Northern Gondwana Domain, *Review of Palaeobotany and Palynology* 66, 181–209.
- Paris, F. (1998). Early Palaeozoic palaeobiogeography of northern Gondwana regions, *Acta Universitatis Carolinae, Geologica* 42(2/4): 473–483.
- Paris, F., Grahn, Y., Nestor, V., Lakova, I. (1999). A revised chitinozoan classification, *Journal of Paleontology*, 73, 549–570.
- Paris, F., N lvak, J. (1999). Biological interpretation and paleobiodiversity of a cryptic fossil group : The “chitinozoan animal”. *GEOBIOS*, 32(2), 315–324.
- Paris, F., Verniers, J. (2005). Chitinozoa, in: Selley, R.C., Cocks, L.R.M., Plimer, I.R. (Eds.), *Encyclopaedia of Geology: Volume Three*, Elsevier Ltd., Amsterdam, 428–440.
- Pohl, A., Donnadiou, Y., Le Hir, G., Ladant, J., Dumas, C., Alvarez-Solas, J., Vandenbroucke, T.R.A. (2016). Glacial onset predated Late Ordovician climate cooling. *Paleoceanography*, 31, 1–22.
- Pope, M., Read, J.F. (1998). Ordovician metre-scale cycles: implications for climate and eustatic fluctuations in the central Appalachians during a global greenhouse, non-glacial to glacial transition. *Palaeogeography, Palaeoclimatology, Palaeoecology*, 138, 27–42.
- Prigmore, J.K., Butler, A.J., Woodcock, N.H. (1997). Rifting during separation of Eastern Avalonia from Gondwana: Evidence from subsidence analysis. *Geology*, 25 (3): 203–206.

- Rasmussen, C.M.Ø., Ullmann, C.V., Jakobsen, K.G., Lindskog, A., Hansen, J., Hansen, T., Eriksson M.E., Dronov, A., Frei, R., Korte, C., Nielsen, A.T., Harper, D.A.T. (2016). Onset of main Phanerozoic marine radiation sparked by emerging Mid Ordovician icehouse. *Scientific reports*, 6, 18884.
- Rexroad, C.B., Droste, J.B. (1982). Stratigraphy and conodont paleontology of the Sexton Creek Limestone and Salamonie Dolomite (Silurian) in northwestern Indiana. Indiana Geological Survey Special Report 25, 29 pp.
- Richardson, J.G., Bergström, S.M. (2003) Regional stratigraphic relations of the Trenton Limestone (Chatfieldian, Ordovician) in the Eastern North American midcontinent, *Northeast Geol. Environ. Sci.* 18, 93-115.
- Rong, J.Y., Melchin, M.J., Williams, S.H., Koren, T.N., Verniers, J. (2008). Report of the restudy of the defined global stratotype of the base of the Silurian System. *Episodes* 31, 315–318.
- Ross, R.J., Jr, Adler, F.J., Amsden, T.W., ..., Webers, G.F. (1982). The Ordovician System in the United States. Correlation chart and explanatory notes. *International Union of Geological Sciences Publication* 12, 1-73.
- Rothman, D.H. (2002). Atmospheric carbon dioxide levels for the last 500 million years. *PNAS*, 99 (7) 4167-4171.
- Saltzman, M.R., Thomas, E. (2012). Carbon isotope stratigraphy, In: *The Geologic Time Scale*, 20-224.
- Saltzman, M.R., Young, S.A. (2005). Long-lived glaciation in the Late Ordovician? Isotopic and sequence-stratigraphic evidence from western Laurentia, *Geology*, 33(2), 109–112.
- Sheehan, P.M. (1973a). The relation of Late Ordovician glaciation to the Ordovician- Silurian changeover in North American brachiopod faunas. *Lethaia* 6:147–54
- Shen, C., Aldridge, R.J., Williams, M., Vandenbroucke, T.R.A., Zhang, X. (2013). Earliest chitinozoans discovered in the Cambrian Duyun fauna of China. *GEOLOGY*, 41(2), 191–194.
- Soufiane, A., Achab, A. (2000a). Upper Ordovician and Lower Silurian chitinozoans from central Nevada and Arctic Canada, *Review of Palaeobotany and Palynology*, 113, 165–187.
- Soufiane, A., Achab, A. (2000b). Chitinozoan zonation of the Late Ordovician and the Early Silurian of the island of Anticosti, Quebec, Canada, *Review of Palaeobotany and Palynology*, 109, 85–111.
- Soufiane, A., Achab, A., (1999). Chitinozoan biostratigraphy of the uppermost Vinini and the Hanson Creek formations, Late Ordovician, central Nevada. *Acta Univ. Carol., Geologica* 43, 303–306.
- Štorch, P., Manda, Š., Tasáryová, Z., Frýda, J., Chadimová, L., Melchin, M.J. (2018). A proposed new global stratotype for Aeronian Stage of the Silurian System: Hlásná Třebaň section, Czech Republic. *Lethaia* 51, p. 357–388.
- Štorch, P., Mitchell, C.E., Finney, S.C., Melchin, M.J. (2011). Uppermost Ordovician (upper Katian-Hirnantian) graptolites of north-central Nevada, U.S.A., *Bulletin of Geosciences*, 86(2), 301-386.
- Swann, D.H. (1968). A summary geologic history of the Illinois Basin Geology and Petroleum Production of the Illinois Basin, *Illinois Geologic Society*, pp. 3-21
- Sweet, W.C. (1984). Graphic correlation of upper Middle and Upper Ordovician rocks, North American Midcontinent Province, U.S.A., 23-35. In: Bruton, D.L. (ed.). Aspects of the Ordovician System. *Palaeontological Contributions from the University of Oslo*, 295, 1-228.
- Swezey, C.S. (2009). Regional stratigraphy and petroleum systems of the Illinois Basin, U.S.A.: U.S. Geological Survey Scientific Investigations Series Map SIM-3068, 1 sheet.
- Thompson, T.L. (1991). Paleozoic succession in Missouri; Part 2, Ordovician System: Missouri Division of Geology and Land Survey Report of Investigations, no. 70, pt. 2, 282 p.
- Torsvik, T.H., Cocks, L.R.M. (2013). Gondwana from top to base in space and time: Gondwana Research, v. 24, p.999–1030.
- Torsvik, T.H., Cocks, L.R.M. (2016) Chapter 6: Ordovician. In: *Earth History and Palaeogeography* (101-123).
- Torsvik, T.H., Rehnström, E.F. (2003). The Tornquist Sea and Baltica – Avalonia docking. *Tectonophysics*, 362, 67–82.
- Torsvik, T.H., Smethurst, M.A., Van der Voo, R., Trench, A., Abrahamsen, N., Halvorsen, E. (1992). BALTICA - A synopsis of Vendian-Permian palaeomagnetic data and their palaeotectonic implications. *Earth Science Reviews*, 33, 133-152.
- Torsvik, T.H., van der Voo, R., Preeden, U., Mac Niocail, C., Steinberger, B., Doubrovine, P.V., van Hinsbergen, D.J.J., Domeier, M., Gaina, C., Tohver, E., Meert, J.G., McCausland, P.J.A., Cocks, L.R.M. (2012). Phanerozoic polar wander, paleogeography and dynamics, *Earth-Science Reviews* 114, 325-368.

- Trotter, J.A., Williams, I.S., Barnes, C.R., Lecuyer, C., Nicoll, R. (2008). Did cooling oceans trigger Ordovician Biodiversification? Evidence from conodont Thermometry. *Science magazine*, 321, 550- 554.
- Trotter, J.A., Williams, I.S., Barnes, C.S., Männik, P., Simpson, A. (2015). New conodont $\delta^{18}\text{O}$ records of Silurian climate change: Implications for environmental and biological events. *Palaeogeography, Palaeoclimatology, Palaeoecology*.
- Underwood, C.J., Crowley, S.F., Marshall, J.D., Brenchley, P.J. (1997). High-resolution carbon isotope stratigraphy of the basal Silurian stratotype (Dob's Linn, Scotland) and its global correlation. *Journal of the Geological Society*, London 154, 709–718.
- Van der Pluijm, B.A., Catocinos, P.A. (1996). Basement and basins of eastern North America. *Geological Society of America Special Paper* 308, pp. 205.
- Vandenbroucke, T.R.A., (2008a). Upper Ordovician chitinozoans from the British historical type areas and adjacent key sections, *Monograph of the Palaeontological Society*, 1–113.
- Vandenbroucke, T.R.A., (2008b). An Upper Ordovician Chitinozoan Biozonation in British Avalonia (England & Wales). *Lethaia*, 41: 275–294.
- Vandenbroucke, T.R.A., Armstrong, H.A., Williams, M., Paris, F., Zalasiewicz, J.A. (2010a). Polar front shift and atmospheric CO_2 during the glacial maximum of the Early Paleozoic Icehouse. *PNAS*, 107(34), 14983–14986.
- Vandenbroucke, T.R.A., Armstrong, H.A., Williams, M., Paris, F., Sabbe, K., Zalasiewicz, J.A., Nolvak, J., Verniers, J. (2010b). Epipelagic chitinozoan biotopes map a steep latitudinal temperature gradient for earliest Late Ordovician seas: Implications for a cooling Late Ordovician climate. *Palaeogeography, Palaeoclimatology, Palaeoecology*, 294(3–4), 202–219.
- Vandenbroucke, T.R.A., Emsbo, P., Munnecke, A., Nuns, N., Duponchel, L., Lepot, K., Quijada, M., Paris, F., Servais, T., Kiessling, W. (2015). Metal-induced malformations in early Palaeozoic plankton are harbingers of mass extinction. *Nature Communications*, 6, 7966.
- Vandenbroucke, T.R.A., Hennissen, J., Zalasiewicz, J.A., Verniers, J. (2008b). New chitinozoans from the historical type area of the Hirnantian Stage and additional key sections in the Wye Valley, Wales, UK. *Geological Journal*, 43(4), 397-414.
- Vandenbroucke, T.R.A., Recourt, P., Nolvak, J., Nielsen, A.T. (2013). Chitinozoan biostratigraphy of the Upper Ordovician *D. clingani* and *P. linearis* graptolite biozones on the Island of Bornholm, Denmark. *Stratigraphy*, 10, 281–301.
- Velleman, J. (2016). *Building a chitinozoan biostratigraphy to anchor Upper Ordovician chemostratigraphy in the Cincinnati Arch (USA)*. (Master's thesis) Ghent University.
- Verniers, J., Nestor, V., Paris, F., Dufka, P., Sutherland, S., Van Grootel, G. (1995). A global Chitinozoa biozonation for the Silurian. *Geological Magazine* 132 (6), 651-666
- Verniers, J., Vandenbroucke, T.R.A. (2006). Chitinozoan biostratigraphy in the Dob's Linn Ordovician-Silurian GSSP, Southern Uplands, Scotland. *GFF*, 128, 195-202
- Vuletich, A.K. (1987). Possible late Middle Ordovician organic carbon isotope excursion: evidence from Ordovician oils and hydrocarbon source rocks, mid-continent and east-central United States. *American Association of Petroleum Geologists Bulletin* 71, 1342–1354.
- Waid, C.B., Cramer, B.D. (2017b). Global chronostratigraphic correlation of the Llandovery Series (Silurian System) in Iowa, USA, using high-resolution carbon isotope ($\delta^{13}\text{C}_{\text{carb}}$) chemostratigraphy and brachiopod and conodont biostratigraphy. *Bulletin of Geosciences* 92(3), 373–390.
- Wang, K., Chatterton, B.D.E., Wang, Y. (1997). An organic carbon isotope record of Late Ordovician to Early Silurian marine sedimentary rocks, Yangtze Sea, South China: implications for CO_2 changes during the Hirnantian glaciation. *Palaeogeography, Palaeoclimatology, Palaeoecology* 104, 61–79.
- Webby, B.D., Droser, M.L., Paris, F., Percival, I. (2004). The Great Ordovician Biodiversification Event. *New York: Columbia University Press*.
- Wicander, R., Playford, G. (2008). Upper Ordovician microphytoplankton of the Bill's Creek Shale and Stonington Formation, Upper Peninsula of Michigan, U.S.A.: Biostratigraphy and paleogeographic significance, *Revue de Micropaleontologie*, 51(1), 39–66.
- Williams, S. H. (1983). The Ordovician-Silurian boundary graptolite fauna of Dob's Linn, southern Scotland. *Palaeontology*, 26, 605-639.
- Young, S.A., Saltzman, M.R., Bergström, S.M. (2005). Upper Ordovician (Mohawkian) carbon isotope ($\delta^{13}\text{C}$) stratigraphy in eastern and central North America: regional expression of a perturbation of the global carbon cycle. *Palaeogeography, Palaeoclimatology, Palaeoecology* 222, 53–76.
- Zalasiewicz, J.A., Taylor, L., Rushton, A.W.A., Loydell, D.K., Rickards, R.B., Williams, M. (2009). Graptolites in British stratigraphy. *Geological Magazine* 146, 785–850.

Annex I

The alphabetical list of all the chitinozoan species observed in this master dissertation:

Ancyrochitina merga
Ancyrochitina nodifera
Ancyrochitina spongiosa
Ancyrochitina sp. 1
Angochitina capillata
Angochitina hansonica
Angochitina sp. 1
Angochitina sp. 2
Angochitina sp. 3
Belonechitina cf. *cactacea*
Belonechitina micracantha
Belonechitina sp. 1
Belonechitina sp. 2 sensu Meyvisch (2018)
Belonechitina sp. 3
Conochitina elegans
Cyathochitina calix
Cyathochitina campanulaeformis
Cyathochitina? *clepsydra*
Cyathochitina hunderumensis
Cyathochitina kuckersiana
Cyathochitina latipatagium
Cyathochitina patagiata
Fungochitina illinoisensis
Hercochitina longi sensu De Backer (2017)
Hercochitina pinguis
Hercochitina sp. 2 sensu De Backer (2017)
Hercochitina turnbulli
Kalochitina multispinata
Nevadachitina cf. *praevininica*
Tanuchitina bergstroemi
Tanuchitina ontariensis

Annex II

The systematic description of all the chitinozoan species observed in this master dissertation:

Group CHITINOZOA Eisenack, 1931
Order OPERCULATIFERA Eisenack, 1931
Family DESMOCHITINIDAE Eisenack, 1931
Subfamily EISENACKITININAE Paris, 1981

Genus KALOCHITINA Jansonius, 1964
Kalochitina multispinata Jansonius, 1964
Pl. 9, fig. 9-11; Pl. 11, fig. 1-2.

Holotype: *Kalochitina multispinata* Jansonius, 1964, p. 909, pl. 2, fig. 21.

Material: 41 specimens + 8 questionable identifications.

Dimensions: (25 specimens measured): L, mean: 125 μm , range: 105-154 μm ; Dp, mean: 84 μm , range: 38-104 μm ; L/Dp, mean: 1.54, range: 1.16-3.45.

Description: Pear-shaped vesicle with a conical chamber. The neck is reduced and can be flaring. It is not always well differentiated from the chamber. The flanks are straight to convex. The basal margin is rounded and the base is convex or flat. The whole vesicle is covered with spines, usually aligned in longitudinal rows.

Discussion: The pear-shape is characteristic for this species. The ornamentation can vary. The spines are usually arranged in longitudinal rows, but these rows are not always well developed. Simple, lambda-shaped spines and spines with connecting tips also occur. *K. multispinata* resembles *Hercochitina turnbulli*, especially when the neck is reduced. The latter one has not the typical pear-shaped body of *K. multispinata*. However, transitional forms can exist as described by De Backer (2017). *K. multispinata* resembles *Acanthochitina rashidi*. Jenkins (1970) described the latter species as a very densely ornamented *K. multispinata* up to the point where a reticulum is formed. *A. rashidi* however is not observed in this core. *K. multispinata* resembles *Hercochitina pinguis*. The difference between these two species is based on the shape, although it is possible that some transitional forms are present.

Occurrence: *Kalochitina multispinata* occurs in the interval between 519 ft and 524 ft depth and the interval between 532 ft and 541 ft depth.

Genus NEVADACHITINA Soufiane & Achab, 2000
Nevadachitina cf. praevininica
Pl. 10, fig. 1-11.

Material: 16 specimens.

Dimensions: (15 specimens measured): L, mean: 161 μm , range: 132-217 μm ; Dp, mean: 89 μm , range: 64-110 μm ; L/Dp, mean: 1.84, range: 1.46-2.86.

Description: Conical chamber with a short cylindrical to flaring neck. The flanks are straight to slightly convex and the base is flat. The whole vesicle is covered with simple and bifurcating spines. These spines are aligned in crowns and longitudinal rows.

Discussion: This species differs from *Nevadachitina praevininica* in being longer than the holotype and having bifurcating spines (specimens at 530 ft depth). All of the specimens are with spines over the whole vesicle, while the spines for the holotype are absent on the upper third to fourth of the vesicle. *N. cf. praevininica* differs from *Nevadachitina vininica*. The latter has a clear ovoid chamber, while the chamber of *N. cf. praevininica* is conical. *N. cf. praevininica* resembles *Belonchitina* sp. 2 sensu Meyvisch (2018), but the difference is the more dense ornamentation of the latter species.

Occurrence: *Nevadachitina cf. praevininica* occurs at a depth of 530 ft and 536 ft.

Order PROSOMATIFERA Eisenack, 1972
Family CONOCHITINIDAE Eisenack, 1931 emend. Paris, 1981
Subfamily BELONECHITININAE Paris, 1981

Genus BELONECHITINA Jansonius, 1964

Belonechitina cf. *cactacea* Eisenack, 1937

Pl. 12, fig. 7-8.

Material: 3 specimens.

Dimensions: (3 specimens measured): L, mean: 107 μm , range: 95-114 μm ; Dp, mean: 65 μm , range: 60-74 μm ; L/Dp, mean: 1.68, range: 1.28-1.88.

Description: Conical chamber with a short cylindrical or flaring neck. The flanks are slightly convex, the basal margin is rounded and the base is flat. The whole vesicle is covered with short, simple and occasionally bifurcating spines.

Discussion: *Belonechitina* cf. *cactacea* differs from *Belonechitina cactacea* in having short and occasionally bifurcating spines. *B.* cf. *cactacea* differs from *Belonechitina tribulosa* because the latter has a greater size. *B.* cf. *cactacea* differs from *A. capillata* in having a more dense ornamentation.

Occurrence: *Belonechitina* cf. *cactacea* occurs at a depth of 524 ft.

Belonechitina micracantha Eisenack, 1931

Pl. 12, fig. 1-6.

Holotype: *Conochitina micracantha* Eisenack 1931, p. 84, pl. 1, fig. 19.

Material: 220 specimens + 20 questionable identifications.

Dimensions: (72 specimens measured): L, mean: 245 μm , range: 157-367 μm ; Dp, mean: 79 μm , range: 60-107 μm ; L/Dp, mean: 3.09, range: 2.04-4.38.

Description: Elongated species with a conical to cylindrical chamber and a cylindrical neck. The walls of the chamber are generally straight, but can also be slightly convex or concave. The flexure can be both conspicuous as inconspicuous. The chamber walls are smooth except for the region around the basal margin. This region contains ornamentation in the form of small granules.

Discussion: *B. micracantha* resembles *Conochitina elegans* in shape. The difference is that *C. elegans* does not bear ornamentation in the region around the basal margin. It can also be bigger in size compared to *B. micracantha*.

Occurrence: *B. micracantha* occurs in the interval between 519 ft and 523 ft depth.

Belonechitina sp. 1

Pl. 8, fig. 10-12; Pl. 9, fig. 1-1.

Material: 68 specimens.

Dimensions: (10 specimens measured): L, mean: 223 μm , range: 170-273 μm ; Dp, mean: 114 μm , range: 61-225 μm ; L/Dp, mean: 2.35, range: 1.19-3.51.

Description: Conical to cylindrical chamber with a short reduced neck. The chamber can be granulate or ornamented with short simple spines. The ornamentation increases in density and size towards the region around the basal margin.

Discussion: Some specimens of *Belonechitina* sp. 1 resemble *Belonechitina* sp. 3. The bad preservation of these specimens makes it hard to identify them with certainty.

Occurrence: *Belonechitina* sp. 1 occurs at a depth of 512 ft.

Belonechitina sp. 2 sensu Meyvisch (2018)

Pl. 13, fig. 1-11.

Material: 35 specimens.

Dimensions: (22 specimens measured): L, mean: 162 µm, range: 111-208 µm; Dp, mean: 87 µm, range: 64-110 µm; L/Dp, mean: 1.88, range: 1.36-2.60.

Description: Conical to cylindrical vesicle with a short neck. The flanks are straight to slightly convex and the flexure is inconspicuous. The base is bluntly rounded and the base is flat to slightly convex. The whole vesicle is covered with simple spines and occasionally bifurcating spines. The spines are organized in a well-developed pattern of longitudinal and lateral rows.

Discussion: *Belonechitina* sp. 2 sensu Meyvisch (2018) differs from *N. praevininica* and *N. cf. praevininica* by having much denser ornamentation.

Occurrence: *Belonechitina* sp. 2 sensu Meyvisch (2018) occurs at 524 ft and 530 ft depth.

Belonechitina sp. 3

Pl. 11, fig. 8-13.

Material: 34 specimens.

Dimensions: (30 specimens measured): L, mean: 178 µm, range: 133-242 µm; Dp, mean: 91 µm, range: 63-114 µm; L/Dp, mean: 1.98, range: 1.17-2.63.

Description: Conical chamber with a cylindrical neck. The flanks are straight to convex and the flexure is usually well-developed. The basal margin is rounded and the base is flat to slightly convex. The whole vesicle is covered by simple and thorn-like spines. The length of the spines decreases towards the neck. The basal margin carries a crown of longer spines, of which some can bifurcate.

Discussion: *Belonechitina* sp. 3 resembles some specimens from *B. sp. 1*, although the general morphology of the latter is more elongated. The bad preservation of these specimens makes it hard to identify them with certainty. For some specimens of *B. sp. 3*, the spines have a pseudo-alignment. This makes them resemble *Hercochitina minuta*. They differ however by the fact that *H. minuta* has clear developed crests, which is absent for *B. sp. 3*. *B. sp. 3* resembles *A. capillata*, but the longer spines on the basal margin are not present on the latter. *B. sp. 3* resembles *Spinachitina bulmani*, but the latter carries no ornamentation on the neck and chamber.

Occurrence: *Belonechitina* sp. 3 occurs in the interval between 519 ft and 524 ft depth and at a depth of 530 ft.

Genus HERCOCHITINA Jansonius, 1964

Hercochitina longi sensu De Backer (2017)

Pl. 8, fig. 7-9.

Material: 4 specimens.

Dimensions: (3 specimens measured): L, mean: 248 µm, range: 228-269 µm; Dp, mean: 99 µm, range: 89-108 µm; L/Dp, mean: 2.53, range: 2.28-3.02.

Description: Cylindrical to slightly conical chamber. The flanks are straight. The basal margin is bluntly rounded and the base is flat. The chamber and especially the region around the basal margin is covered with very discrete longitudinal crests. The crests are not dense and maximum five crests are observed. The basal margin carries spines which can be interpreted as the ornamentation that extends beyond the basal margin.

Discussion: This species differs from *B. sp. 3* by having a chamber which is not covered with spines which is clearly the case for *B. sp. 3*. *Hercochitina longi* described by Achab et al. (2013) has an ornamented aperture, which is not the case for the specimens found in this core. De Backer (2017) described *H. longi* specimens from the Maquoketa Formation in Wisconsin without an ornamented aperture.

Occurrence: *Hercochitina longi* sensu De Backer (2017) occurs at a depth of 536 ft.

Hercochitina pinguis Melchin and Legault, 1985
Pl. 11, fig. 3-7.

Holotype: *Hercochitina pinguis* Melchin and Legault, 1985, p. 199-210, pl. 2, fig. 2.

Material: 47 specimens.

Dimensions: (38 specimens measured): L, mean: 130 μm , range: 107-178 μm ; Dp, mean: 81 μm , range: 61-95 μm ; L/Dp, mean: 1.62, range: 1.31-5.51.

Description: Conical to ovoid chamber with a short neck that can be flaring. The flanks are convex. The flexure is usually well-developed, the shoulder not always. The basal margin is rounded and the base is flat to convex. The ornamentation consists of longitudinal bars which are connected to the wall by spines. These spines can be both simple and multi-rooted and are also present on the neck. The longitudinal bars are usually not continuous.

Discussion: The specimens recovered in this core are somewhat stouter than the ones Melchin and Legault (1985) described, however, they are considered the same species. Their stouter morphology makes them resemble *K. multispinata*. The difference between these two species is based on the shape, although it is possible that some transitional forms are present. *H. pinguis* resembles *Hercochitina turnbulli*. The difference is made based on the denser ornamentation and the lack of low longitudinal ridges of the latter one. *H. pinguis* resembles *Hercochitina* sp. 2 sensu De Backer (2017). The difference is made based on the clear presence of low longitudinal ridges for *H. pinguis*. Although it is possible that transitional forms exist.

Occurrence: *Hercochitina pinguis* occurs at a depth of 536 ft.

Hercochitina sp. 2 sensu De Backer (2017)
Pl. 9, fig. 3-8.

Material: 42 specimens + 9 questionable identifications.

Dimensions: (19 specimens measured): L, mean: 132 μm , range: 114-188 μm ; Dp, mean: 84 μm , range: 71-100 μm ; L/Dp, mean: 1.57, range: 1.24-1.88.

Description: Conical to ovoid chamber with a small cylindrical to flaring neck. The flanks are straight to slightly convex. The basal margin is rounded and the base is flat to slightly convex. The ornamentation consist of spines that form discontinuous longitudinal ridges on the upper part. The lower part of the vesicle is ornamented with multirooted spines. The transition between these two styles of ornamentation is variable. It can be both located close to the neck or at the base.

Discussion: *Hercochitina* sp. 2 sensu De Backer (2017) resembles *H. pinguis*. The difference is made based on the fact that the latter has less dense ornamentation. *H. sp. 2* sensu De Backer (2017) resembles *K. multispinata*. The difference is made based on the typical pear-shaped morphology of *K. multispinata*, although it is possible that transitional forms between these species exist, especially since they occur in the same range. *H. sp. 2* sensu De Backer (2017) resembles *Hercochitina turnbulli*. The latter one however does not really form longitudinal ridges.

Occurrence: *Hercochitina* sp. 2 sensu De Backer (2017) occurs in the interval between 519 ft and 524 ft depth and in the interval between 532 ft and 536 ft depth.

Hercochitina turnbulli Jenkins, 1969
Pl. 7, fig. 10-12.

Holotype: *Hercochitina turnbulli* Jenkins 1969, p. 27, pl. 8, fig. 12a, b.

Material: 3 specimens.

Dimensions: (3 specimens measured): L, mean: 136 μm , range: 131-138 μm ; Dp, mean: 85 μm , range: 84-87 μm ; L/Dp, mean: 1.59, range: 1.51-1.64.

Description: Conical to ovoid chamber with a short flaring neck. The vesicle is covered with multi-rooted spines. These can form very short longitudinal bars in the upper part of the vesicle. The aperture is covered with short simple and multi-rooted spines.

Discussion: *Hercochitina turnbulli* resembles *K. multispinata*. The difference is made based on the morphology, which is pear-shaped for the latter one. However, transitional forms can exist as described by De Backer (2017). *H. turnbulli* resembles *H. sp. 2* sensu De Backer (2017). They could be seen as one species based on the morphology and the fact that they occur in the same core. However, the distinction is made based on the fact that *H. turnbulli* does not form distinctive longitudinal bars. *H. turnbulli* resembles *H. pinguis* but the former is more densely ornamented.

Occurrence: *Hercochitina turnbulli* occurs at a depth of 521 ft.

Subfamily CONOCHITININAE Paris, 1981

Genus CONOCHITINA Eisenack, 1931 Emend. Paris, Grahn, Nestor and Lakova

Conochitina elegans Eisenack, 1931

Pl 8, fig. 1-6.

Holotype: *Conochitina elegans* Eisenack 1931, p. 87, pl.2, fig. 4.

Material: 119 specimens + 47 questionable identifications.

Dimensions: (40 specimens measured): L, mean: 334 μm , range: 169-642 μm ; Dp, mean: 89 μm , range: 65-143 μm ; L/Dp, mean: 3.79, range: 2.28-5.90.

Description: Conical to cylindrical vesicle. The oral tube can end in a slightly flaring collarette. It has a slender appearance. The flanks are straight, the basal margin is bluntly rounded and the base is flat. The wall is smooth.

Discussion: *Conochitina elegans* resembles *C. micracantha*, the difference is that the former has a more slender morphology and bears no ornamentation.

Occurrence: *Conochitina elegans* occurs in the interval between 519 ft and 523 ft depth.

Subfamily TANUCHITININAE Paris, 1981

Genus TANUCHITINA Jansonius, 1964

Tanuchitina bergstroemi Laufeld, 1967

Pl. 7, fig. 1-7.

Holotype: *Tanuchitina bergstroemi* Laufeld, 1967, p. 344, fig. 34A.

Material: 42 specimens.

Dimensions: (20 specimens measured): L, mean: 746 μm , range: 476-1163 μm ; Dp, mean: 141 μm , range: 119-157 μm ; L/Dp, mean: 5.30, range: 3.85-8.08.

Description: Very large, subcylindrical vesicle. Flexure inconspicuous and chamber and neck are not always easily differentiated from each other. The flanks are straight, the basal margin is rounded and the base generally flat. The greatest width can be obtained near the middle of the longitudinal axis when aboral swelling is present, or at the base when no aboral swelling is present. The basal margin carries membranous flange or small carina. The vesicle generally bears no ornamentation.

Discussion: Due to the bad preservation, the flange or carina is not always observed, but remains of it can be seen on the specimens. *T. bergstroemi* differs from *Tanuchitina ontariensis* by its slender morphology and greater length. *T. ontariensis* is identical to *Tanuchitina elongate* which is regarded as a senior synonym of *T. bergstroemi* (Paris, 1990).

Occurrence: *Tanuchitina bergstroemi* occurs in the interval between 519 ft to 523 ft depth.

Tanuchitina ontariensis Jansonius, 1964

Pl. 6, fig. 10.

Holotype: *Tanuchitina ontariensis* Jansonius, 1964, p. 914, pl. 1, fig. 6.

Material: 96 specimens + 11 questionable identifications.

Dimensions: (63 specimens measured): L, mean: 183 μm , range: 117-321 μm ; Dp, mean: 84 μm , range: 67-172 μm ; L/Dp, mean: 2.17, range: 0.87-3.18.

Description: Conical chamber with a (sub)cylindrical that slightly widens towards the aperture, which can be finely fimbriate. The flexure is generally not well developed, but can be conspicuous for some specimens. The flanks are straight, but can be slightly convex or concave. The basal margin can be bluntly rounded or angular and the base is flat. The wall is generally ornamented with small granules, but some smooth specimens are also present. The basal margin carries a short, thin carina.

Discussion: Variation in size and morphology of this species is observed. Some specimens have a more slender appearance while others have a more wider chamber. *Tanuchitina ontariensis* differs from *Cyathochitina hyalophrys* in length, the latter has a bigger size, and its neck does not widen near the aperture.

Occurrence: *Tanuchitina ontariensis* occurs at the interval between 542 ft and 545 ft depth. The questionable identifications occur at the interval between 530 and 532 ft depth.

Family LAGENOCHITINIDAE Eisenack, 1931 emend. Paris, 1981
Subfamily ANCYROCHITININAE Paris, 1981

Genus ANCYROCHITINA Eisenack, 1955

Ancyrochitina merga Jenkins, 1970

Pl. 7, fig. 8-9.

Holotype: *Ancyrochitina merga* Jenkins 1970, p. 267, pl. 47, fig. 12.

Material: 2 specimens.

Dimensions: (2 specimens measured): L, mean: 125 μm , range: 120-130 μm ; Dp, mean: 83 μm , range: 80-85 μm ; L/Dp, mean: 1.51, range: 1.50-1.53.

Description: Fungiform vesicle with a cylindrical or flaring neck. The flanks are straight and the flexure is well developed. The basal is convex and the basal margin is rounded, carrying 8-24 appendices, generally fewer than 15. They bifurcate up to 3 times, rarely up to 4 times. The chamber and neck bear small simple spines.

Discussion: *Ancyrochitina merga* differs from *Ancyrochitina corniculans*. The latter has a more conical morphology and generally has 4-6 simple or dichotomously branching appendices. *A. merga* differs from *Ancyrochitina spongiosa* by the morphology of the appendices. The former has slender appendices, while the appendices of the latter are sponge-like.

Occurrence: *Ancyrochitina merga* occurs at a depth of 536 ft.

Ancyrochitina nodifera Nestor, 1980

Pl. 6, fig. 11-14.

Holotype: *Ancyrochitina nodifera* Nestor, 1980, 9. 98-107, pl. 2, figs. 1a- 2.

Material: 32 specimens + 21 questionable identifications.

Dimensions: (29 specimens measured): L, mean: 129 μm , range: 100-173 μm ; Dp, mean: 81 μm , range: 60-104 μm ; L/Dp, mean: 1.60, range: 1.22-1.88.

Description: Conical vesicle with a cylindrical neck that slightly flares at the end. The length of the neck is variable, from less than half of the vesicle length to more than half of the vesicle length. The

base is flat to convex. The basal margin carries up to eight thick processes with irregular thickening, that can bifurcate. The chamber and neck can be smooth or covered with small spines or cones.

Discussion: Not every specimen is well preserved, but enough are with certainty identified as *Ancyrochitina nodifera*. *A. nodifera* resembles *A. clathrospinosa* but differs in the fact that the processes can thicken irregularly. *A. nodifera* differs from *A. spongiosa* in having appendices with irregular thickening.

Occurrence: *A. nodifera* occurs questionably at a depth of 482 ft, in the interval between 490 ft and 495 ft depth and in the interval between 506 ft and 510 ft depth.

Ancyrochitina spongiosa Achab, 1977b

Pl. 5, fig. 8-9, 10.

Holotype: *Ancyrochitina spongiosa* Achab 1977b, p. 2196, pl. 1, fig. 6.

Material: 4 specimens + 3 questionable identifications.

Dimensions: (4 specimens measured): L, mean: 132 μm , range: 112-167 μm ; Dp, mean: 77 μm , range: 67-90 μm ; L/Dp, mean: 1.75, range: 1.24-2.14.

Description: Conical chamber with a cylindrical neck that can be flaring at the end. The flexure is well developed. The flanks are straight to slightly convex, the basal margin is rounded and the base is flat. The basal margin carries 5-10 appendices. These are thick and sponge-like and can sometimes merge at their tips. The neck and chamber can be granulated or carry small spines.

Discussion: The ornamentation on the neck and chamber is not described in the type description, but De Backer (2017) describes *Ancyrochitina spongiosa* specimens with such ornamentation from the Gardner Kiln core of the Maquoketa Formation. Due to the bad preservation, only 1-2 appendices are preserved instead of 5-10 and no specimens with merging appendices are encountered. *A. spongiosa* differs from *A. merga* by the morphology of the appendices. The latter has slender appendices, while the appendices of the former are sponge-like. *A. spongiosa* differs from *A. nodifera* because the latter has appendices with irregular thickening.

Occurrence: *Ancyrochitina spongiosa* occurs at a depth of 512 ft and 532 ft.

Ancyrochitina sp. 1

Pl. 5, fig. 6-7.

Material: 3 specimens

Dimensions: (3 specimens measured): L, mean: 134 μm , range: 124-150 μm ; Dp, mean: 88 μm , range: 85-92 μm ; L/Dp, mean: 1.52, range: 1.46-1.63.

Description: Conical chamber with a short cylindrical or flaring neck. The flanks are convex and the flexure is well developed. The base is flat to convex and the basal margin is rounded. The basal margin carries a crown of small spines. The neck and chamber are granulated or ornamented with small spines.

Discussion: Only small parts of the appendices are reserved so it can not be observed if they branch or not. *Ancyrochitina* sp. 1 resembles some *Ancyrochitina* species, but the appendices of *A. sp. 1* are more densely spaced compared to other species.

Occurrence: *Ancyrochitina* sp. 1 occurs at a depth of 482 ft, 490 ft and 506 ft.

Subfamily ANGOCHITININAE Paris, 1981

Genus ANGOCHITINA Eisenack, 1931

Angochitina capillata Eisenack, 1937

Pl. 4, fig. 8, 12-15; Pl. 5, fig. 1.

Holotype: *Angochitina capillata* Eisenack, 1937, p.225, pl. 15 fig. 13.

Material: 284 specimens + 62 questionable identifications.

Dimensions: (54 specimens measured): L, mean: 154 μm , range: 124-185 μm ; Dp, mean: 75 μm , range: 40-102 μm ; L/Dp, mean: 2.11, range: 1.22-3.93.

Description: Conical to ovoid chamber with a cylindrical or flaring neck. The chamber is up to two-thirds of the total length, but this can be even more for some specimens. The aperture is generally serrate, but can also be straight or decorated with short spines. The neck and chamber carry spines. These can be simple, sometimes thorn-like and lambda-shaped.

Discussion: There is a strong variability in the shape and length of the spines. Some specimens display pseudo-alignment of the spines. The flexure is not always well developed making these specimens resemble the *Belonechitina* genus.

Occurrence: *Angochitina capillata* occurs sporadically in the interval between 490 and 495 ft depth and abundant in the interval between 530 ft and 545 ft depth.

Angochitina hansonica Soufiane and Achab, 2000

Pl. 4, fig. 6-7, 9-10.

Holotype: *Angochitina hansonica* Soufiane and Achab, 2000, pl. IV, fig. 5.

Material: 17 specimens + 5 questionable identifications.

Dimensions: (16 specimens measured): L, mean: 127 μm , range: 95-142 μm ; Dp, mean: 84 μm , range: 67-91 μm ; L/Dp, mean: 1.51, range: 1.12-1.90.

Description: Pear-shaped, conical to ovoid chamber with a short cylindrical or flaring neck. The flanks are straight to convex and the flexure is well developed. The basal margin is rounded and the base is flat or convex. The maximum width is obtained in the lower half of the chamber. The vesicle is ornamented with simple spines that decrease in size towards the neck.

Discussion: *Angochitina hansonica* resembles *Fungochitina illinoisensis*, but the latter has a much longer neck compared to the former. A lot of the specimens of *A. sp. 1* resemble *A. hansonica*. It is possible that some are indeed *A. hansonica* but the identification was complicated due to bad preservation of the specimens.

Occurrence: *Angochitina hansonica* occurs at a depth of 490 ft, in the interval between 500 ft and 506 ft depth and questionable in the interval between 500 and 506 ft depth.

Angochitina sp. 1

Pl. 4, fig. 2-5, 11.

Material: 273 specimens.

Dimensions: (79 specimens measured): L, mean: 135 μm , range: 100-205 μm ; Dp, mean: 83 μm , range: 61-105 μm ; L/Dp, mean: 1.64, range: 1.18-2.33.

Description: Species belonging to the *Angochitina* genus. The chamber is conical to ovoid. The neck is subcylindrical and can be flaring at the end. The general morphology of the specimens is similar but variability is possible due to deformation and bad preservation. The flexure is well developed and the neck and chamber can be easily distinguished from each other. The whole vesicle is covered with short spines which can be reduced to cones. These are in general simple but spines with a widened base are also present. Occasionally spines that coalesce at their tips can be seen. Some specimens display (pseudo-)longitudinal alignment of the spines.

Discussion: A lot of the specimens of *A. sp. 1* resemble *A. hansonica*. It is possible that some are indeed *A. hansonica* but the identification was complicated due to bad preservation of the specimens.

Occurrence: *Angochitina sp. 1* occurs in the interval between 472 ft and 510 ft depth.

Angochitina sp. 2
Pl. 3, fig. 9-11; Pl. 4, fig. 1.

Material: 112 specimens.

Dimensions: (28 specimens measured): L, mean: 132 μm , range: 91-159 μm ; Dp, mean: 62 μm , range: 54-73 μm ; L/Dp, mean: 2.13, range: 1.49-2.59.

Description: Conical, hemispherical to ovoid chamber with a long cylindrical or flaring neck, which makes up more than half of the vesicle length. The flexure is generally well developed. The flanks are straight to convex. The chamber and neck are granulated or ornamented with small spines.

Discussion: This is a morphological variable group with specimens that are not well preserved.

Occurrence: *Angochitina* sp. 2 occurs at a depth of 472 ft, 487 ft and 495 ft.

Angochitina sp. 3
Pl. 3, fig. 2-8.

Material: 17 specimens.

Dimensions: (11 specimens measured): L, mean: 142 μm , range: 125-168 μm ; Dp, mean: 77 μm , range: 64-92 μm ; L/Dp, mean: 1.84, range: 1.63-2.05.

Description: Ovoid chamber with a cylindrical neck. The flexure is conspicuous, the flanks are convex and the base is flat to convex. The chamber and neck are ornamented with lambda-shaped and complex spines.

Discussion: *Angochitina* sp. 3 resembles *Angochitina communis*, but the style of ornamentation differs. *A. communis* carries simple and wishbone spines while *A. sp. 3* carries more complex spines.

Occurrence: *Angochitina* sp. 3 occurs at a depth of 519 ft and 523 ft.

Genus FUNGOCHITINA Taugourdeau, 1966 restrict. Paris et al., 1999
Fungochitina illinoisensis Butcher et al., 2010
Pl. 5, fig. 2-5.

Holotype: *Fungochitina illinoisensis* Butcher et al., 2010, pl. II, fig. 1.

Material: 8 specimens + 7 questionable identifications.

Dimensions: (7 specimens measured): L, mean: 122 μm , range: 107-140 μm ; Dp, mean: 70 μm , range: 60-91 μm ; L/Dp, mean: 1.74, range: 1.53-1.98.

Description: Conical chamber with a cylindrical neck that can constitute up to half of the vesicle length. The flanks are straight and a flexure is developed. The basal margin is broadly rounded and the base is flat. The whole vesicle is covered with randomly distributed simple spines up to 7 μm in length.

Discussion: Some specimens have a neck that are only one third of the total vesicle length. *Fungochitina illinoisensis* resembles *A. hansonica*, but the latter has a shorter neck. *F. illinoisensis* differs from *Fungochitina kosovensis* in ornamentation which is much more dense for the latter. *F. kosovensis* also has a longer neck compared to the chamber than *F. illinoisensis*.

Occurrence: *Fungochitina illinoisensis* occurs in the interval between 472 and 477 ft depth, at a depth of 490 ft and 500 ft and questionably at a depth of 487 ft.

Subfamily CYATHOCHITININAE Paris, 1981

Genus CYATHOCHITINA Eisenack, 1955b emend. Paris et al., 1999
Cyathochitina campanulaeformis Eisenack, 1931
Pl. 2, fig. 1-5.

Holotype: *Conochitina campanulaeformis* Eisenack, 1931, pl. 2, fig. 1.

Material: 320 specimens + 96 questionable identifications.

Dimensions: (92 specimens measured): L, mean: 224 μm , range: 114-339 μm ; Dp, mean: 174 μm , range: 107-257 μm ; L/Dp, mean: 1.29, range: 0.87-2.00.

Description: Conical to hemispherical vesicle with a conical chamber. The neck can be cylindrical or flaring. The flexure is well developed and clear shoulders are present. The base is flat or weakly convex and the basal margin is sharp, carrying a short (<10 μm) carina.

Discussion: In the Silurian, some *C. campanulaeformis* species are a bit more elongated with a more cylindro-conical vesicle and a longer neck. Some are also slightly greater in size than species from the Ordovician. The general characteristics however are the same. *C. campanulaeformis* resembles *C. kuckersiana* but in theory, they can be easily distinguished by the clear shoulder and the short carina which are characteristic for *C. campanulaeformis*. In practice however, the distinction is more difficult due to intraspecific morphological variations. *C. kuckersiana* can also be slightly bigger *C. campanulaeformis*. In the analyzed samples, clear examples of both species are ob.

Occurrence: *Conochitina campanulaeformis* occurs throughout the whole core: at a depth of 482 ft, in the interval between 500 ft and 506 ft, at 512 ft, 519 ft and 524 ft depth, and in the interval between 530 ft to 545 ft depth with the exception of 541 ft depth.

Cyathochitina kuckersiana Eisenack, 1934

Pl. 1, fig. 1-5.

Holotype: *Conochitina kuckersiana* Eisenack, 1934, pl. 4, fig.14 a, b.

Material: 133 specimens + 34 questionable identifications.

Dimensions: (42 specimens measured): L, mean: 244 μm , range: 183-328 μm ; Dp, mean: 200 μm , range: 136-285 μm ; L/Dp, mean: 1.22, range: 0.95-1.88.

Description: Cylindro-conical vesicle with a conical chamber. The neck is cylindrical and most of the time also slightly flaring. The flanks can be both concave and straight but some specimens have even slightly convex flanks. The flexure is well developed and shoulders are absent. The base is flat or weakly convex and the basal margin is sharp, carrying a short (10-20 μm) carina. On well preserved specimens, parallel longitudinal wrinkles on the upper part of the chamber and latitudinal wrinkles on the base of the chamber can be seen. One specimen was found carrying radial thickenings.

Discussion: *C. campanulaeformis* resembles *C. kuckersiana* but in theory, they can be easily distinguished by the clear shoulder and the short carina which are characteristic for *C. campanulaeformis*. In practice however, the distinction is more difficult due to intraspecific morphological variations. *C. kuckersiana* can also be slightly bigger *C. campanulaeformis*. In the analyzed samples, clear examples of both species are found.

Occurrence: *Cyathochitina kuckersiana* occurs throughout the whole core: in the interval from 477 ft to 482 ft and 500 ft to 506 ft depth, at a depth of 512 ft and 524 ft, in the interval between 530 ft to 545 ft depth with the exception of 541 ft depth.

Cyathochitina calix Eisenack, 1931

Pl. 1, fig. 6-9.

Holotype: *Cyathochitina calix* Eisenack, 1931, pl. 23, fig. 1-3.

Material: 7 specimens.

Dimensions: (7 specimens measured): L, mean: 313 μm , range: 253-439 μm ; Dp, mean: 155 μm , range: 118-193 μm ; L/Dp, mean: 2.02, range: 1.80-2.27.

Description: Elongated vesicle with a cylindro-conical chamber. The neck is cylindrical. The flanks are straight to slightly convex. The flexure is present and the shoulders are absent. The base is flat, carrying a small carina. The surface of the vesicle is granulate. On well preserved specimens, longitudinal grooves on the neck and radial rings on the basal end of the chamber are present.

Discussion: *C. calix* differs from *C. campanulaeformis* as the latter has clear shoulders and a wider chamber. *C. calix* differs from *C. kuckersiana* as the latter has a much wider carina.

Occurrence: *Cyathochitina calix* occurs in the interval between 500 ft and 506 ft depth.

Cyathochitina? clepsydra Grahn, 1984

Holotype: *Cyathochitina? clepsydra* Grahn, 1984, pl. II, fig. H.

Material: 1 questionable identification.

Dimensions: (1 specimen measured): L: 125 μm ; Dp: 89 μm ; L/Dp: 1.40.

Description: Subconical vesicle with a flat base. The flanks are concave and widen towards the aperture. Slightly below the aperture, a characteristic lip is flaring. The basal margin carries a short carina.

Discussion: The attachment of the carina for this species is not typical for the *Cyathochitina* genus and is therefore questionably referred to this genus.

Occurrence: There is 1 questionable occurrence of *Cyathochitina? clepsydra* at 530 ft depth.

Cyathochitina hunderumensis Nölvak, Grahn & Paris, 1996

Pl. 2, fig. 10-12; Pl. 3 fig. 1.

Holotype: *Cyathochitina hunderumensis* Nölvak, Grahn & Paris, 1996, fig. 1 pl. 1.

Material: 15 specimens + 11 questionable identifications.

Dimensions: : (7 specimens measured): L, mean: 156 μm , range: 105-183 μm ; Dp, mean: 134 μm , range: 111-153 μm ; L/Dp, mean: 1.17, range: 0.95-1.35.

Description: Conical to bell-shaped vesicle with a short cylindrical neck which is shorter than half of the vesicle length. The base is flat to slightly convex and bears a short thickened carina. The maximum diameter is located near the base.

Discussion: *C. hunderumensis* differs from *C. campanulaeformis* in its smaller size and thickened carina.

Occurrence: *Cyathochitina hunderumensis* occurs at a depth of 524 ft, 530 ft, 536 ft and questionable at 512 ft depth.

Cyathochitina latipatagium Jenkins, 1969

Pl. 2, fig. 6-9.

Holotype: *Cyathochitina kuckersiana latipatagium* Jenkins, 1969, p. 19, pl. 4, fig. 5

Material: 23 specimens.

Dimensions: : (12 specimens measured): L, mean: 264 μm , range: 100-375 μm ; Dp, mean: 196 μm , range: 107-267 μm ; L/Dp, mean: 1.35, range: 0.93-1.84.

Description: Conical chamber and a cylindrical neck. The flanks are straight to convex. The flexure is well developed and the shoulder can be both inconspicuous as conspicuous. The base is usually flat. On well preserved specimens, longitudinal grooves on the neck and radial rings on the basal end of the chamber are present. The basal edge carries a wide carina (> 30 μm and sometimes almost up to 50 μm).

Discussion: *C. latipatagium* can be easily distinguished from *C. campanulaeformis* and *C. kuckersiana* by its very wide carina. *C. latipatagium* differs from *Cyathochitina vaurelensis* by the different shape of the test and the very wide carina.

Occurrence: *Cyathochitina latipatagium* occurs at a depth of 524 ft and in the interval between 530 ft and 545 ft depth with the exception of 541 ft depth.

Cyathochitina patagiata Jenkins, 1969

Pl. 1, fig. 10-11.

Holotype: *Cyathochitina kuckersiana patagiata* Jenkins, 1969, p. 19, pl. 5, figs. 6-9-14, 17.

Material: 4 specimens.

Dimensions: : (3 specimens measured): L, mean: 256 μ m, range: 206-346 μ m; Dp, mean: 171 μ m, range: 122-207 μ m; L/Dp, mean: 1.50, range: 1.17-1.69.

Description: Conical chamber and a short cylindrical neck. The flanks are usually straight but can also be slightly convex or concave. Flexure is present and the shoulder can be both inconspicuous as conspicuous. On well preserved specimens, longitudinal grooves on the neck are present. The basal edge carries a rather short carina (5-12 μ m).

Discussion: *C. patagiata* is a subspecies of *C. kuckersiana* and the shape and dimensions are rather similar. The difference however is the size of the carina. *C. patagiata* has a smaller carina than *C. kuckersiana*. This is why these specimens are classified as a different species. *C. patagiata* also has similar shape and dimensions of *C. latipatagium*, but there is a clear difference in size of the carina. The latter has a much wider carina.

Occurrence: *Cyathochitina patagiata* occurs at a depth of 512 ft and 524 ft.

Annex III

PLATE 1

All scale bars are 200 μm unless indicated otherwise and placed on the right side of the vesicle.

1. *Cyathochitina kuckersiana*, sample IGS-527-512
2. *Cyathochitina kuckersiana*, sample IGS-527-536
3. *Cyathochitina kuckersiana*, sample IGS-527-536
4. *Cyathochitina kuckersiana*, sample IGS-527-545, scale bar = 100 μm
5. *Cyathochitina kuckersiana*, sample IGS-527-545
6. *Cyathochitina calix*, sample IGS-527-500
7. *Cyathochitina calix*, sample IGS-527-506
8. *Cyathochitina calix*, sample IGS-527-500
9. *Cyathochitina calix*, sample IGS-527-506
10. *Cyathochitina patagiata*, sample IGS-527-512
11. *Cyathochitina patagiata*, sample IGS-527-512

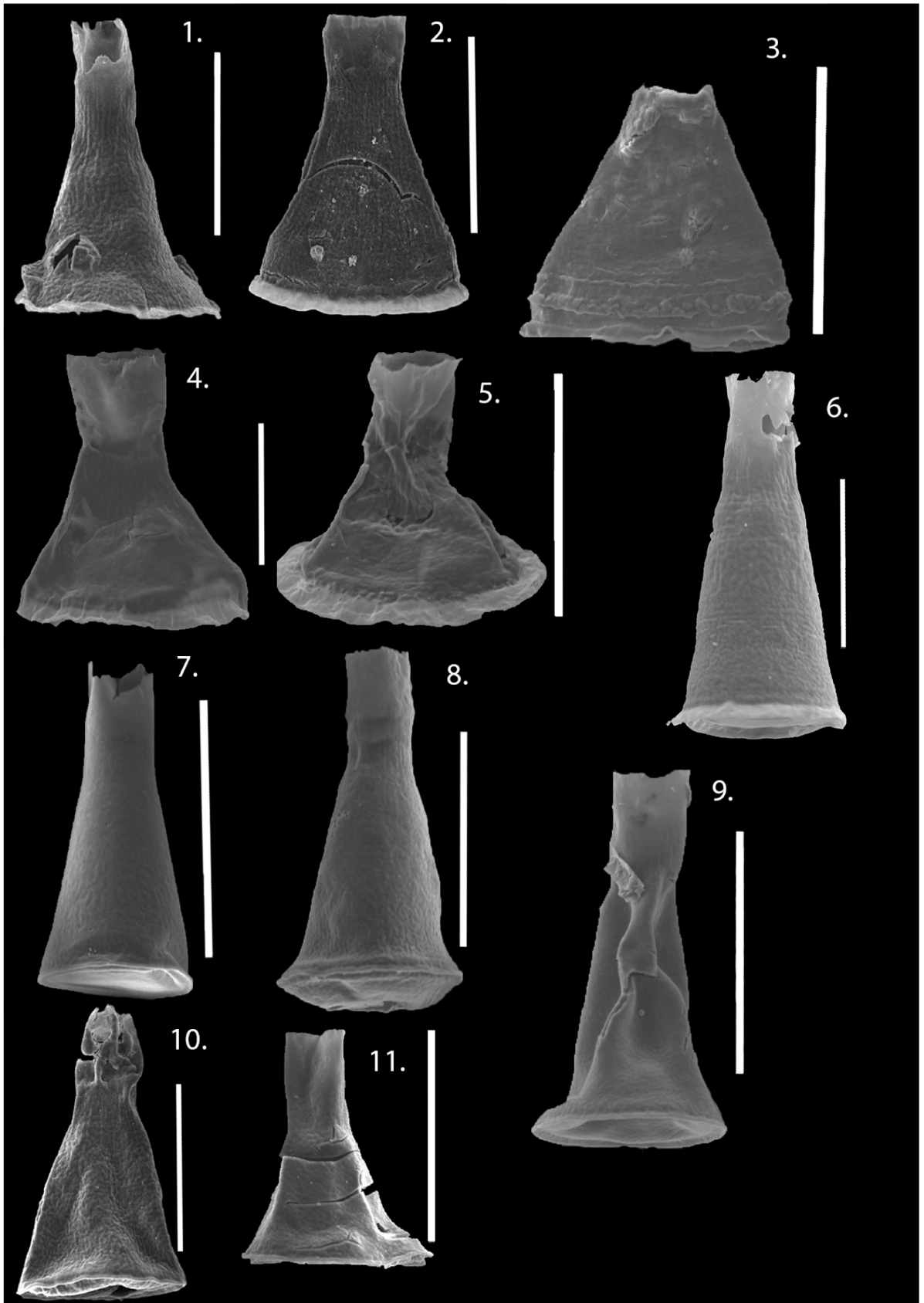


PLATE 2

All scale bars are 200 μm unless indicated otherwise and placed on the right side of the vesicle.

1. *Cyathochitina campanulaeformis*, sample IGS-527-512
2. *Cyathochitina campanulaeformis*, sample IGS-527-536, scale bar = 100 μm
3. *Cyathochitina campanulaeformis*, sample IGS-527-545
4. *Cyathochitina campanulaeformis*, sample IGS-527-545
5. *Cyathochitina campanulaeformis*, sample IGS-527-512
6. *Cyathochitina latipatagium*, sample IGS-527-530
7. *Cyathochitina latipatagium*, sample IGS-527-545
8. *Cyathochitina latipatagium*, sample IGS-527-545
9. *Cyathochitina latipatagium*, sample IGS-527-545
10. *Cyathochitina hunderumensis*, sample IGS-527-536, scale bar = 100 μm
11. *Cyathochitina hunderumensis*, sample IGS-527-536, scale bar = 100 μm
12. *Cyathochitina hunderumensis*, sample IGS-527-536, scale bar = 100 μm

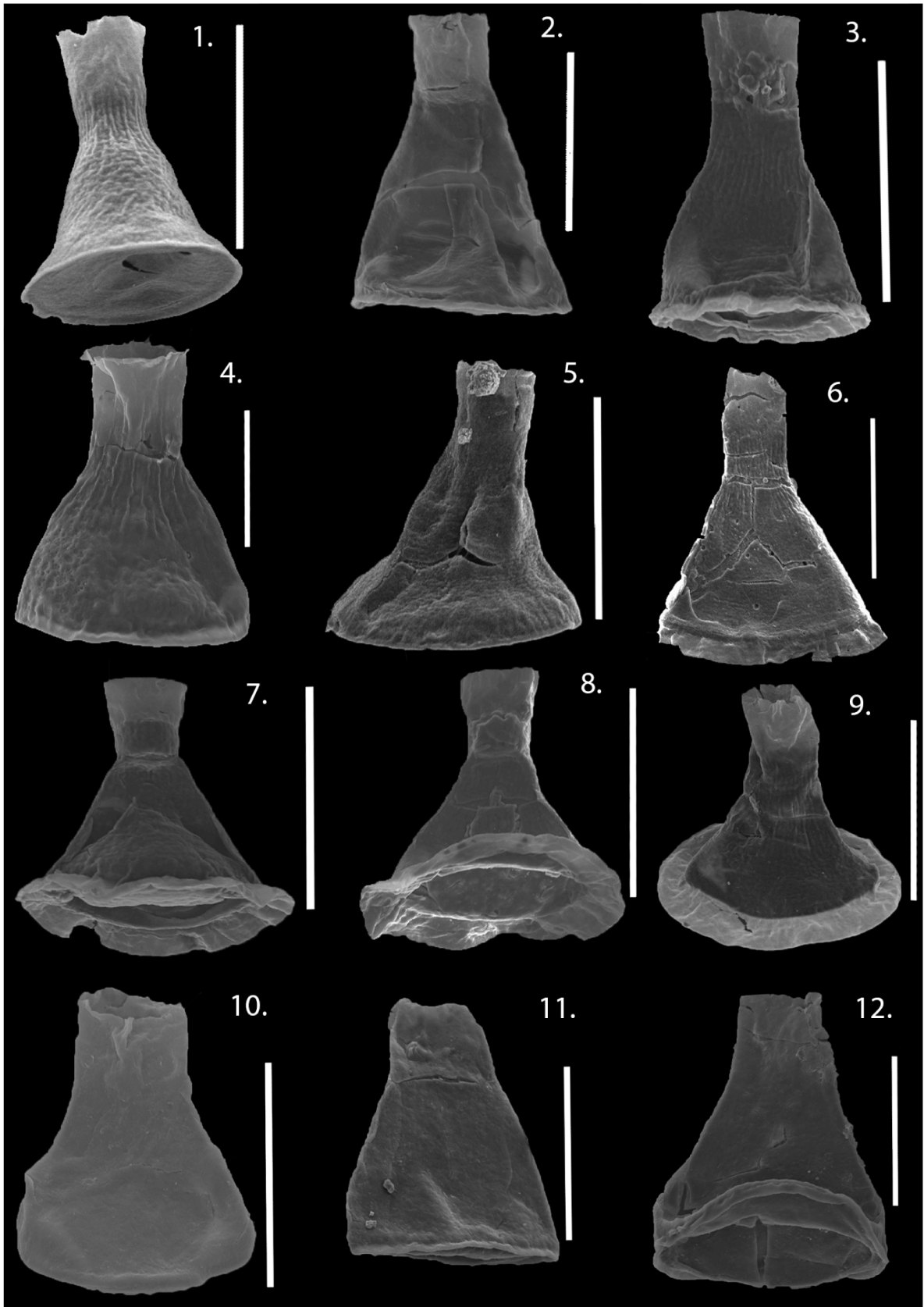


PLATE 3

All scale bars are 100 μm unless indicated otherwise and placed on the right side of the vesicle.

1. *Cyathochitina hunderumensis*, sample IGS-527-536
2. *Angochitina* sp. 3, sample IGS-527-519
3. *Angochitina* sp. 3, sample IGS-527-523
4. *Angochitina* sp. 3, sample IGS-527-523
5. *Angochitina* sp. 3, sample IGS-527-523
6. *Angochitina* sp. 3, sample IGS-527-523
7. *Angochitina* sp. 3, sample IGS-527-523, scale bar = 50 μm
8. *Angochitina* sp. 3, sample IGS-527-523
9. *Angochitina* sp. 2, sample IGS-527-472
10. *Angochitina* sp. 2, sample IGS-527-472
11. *Angochitina* sp. 2, sample IGS-527-487

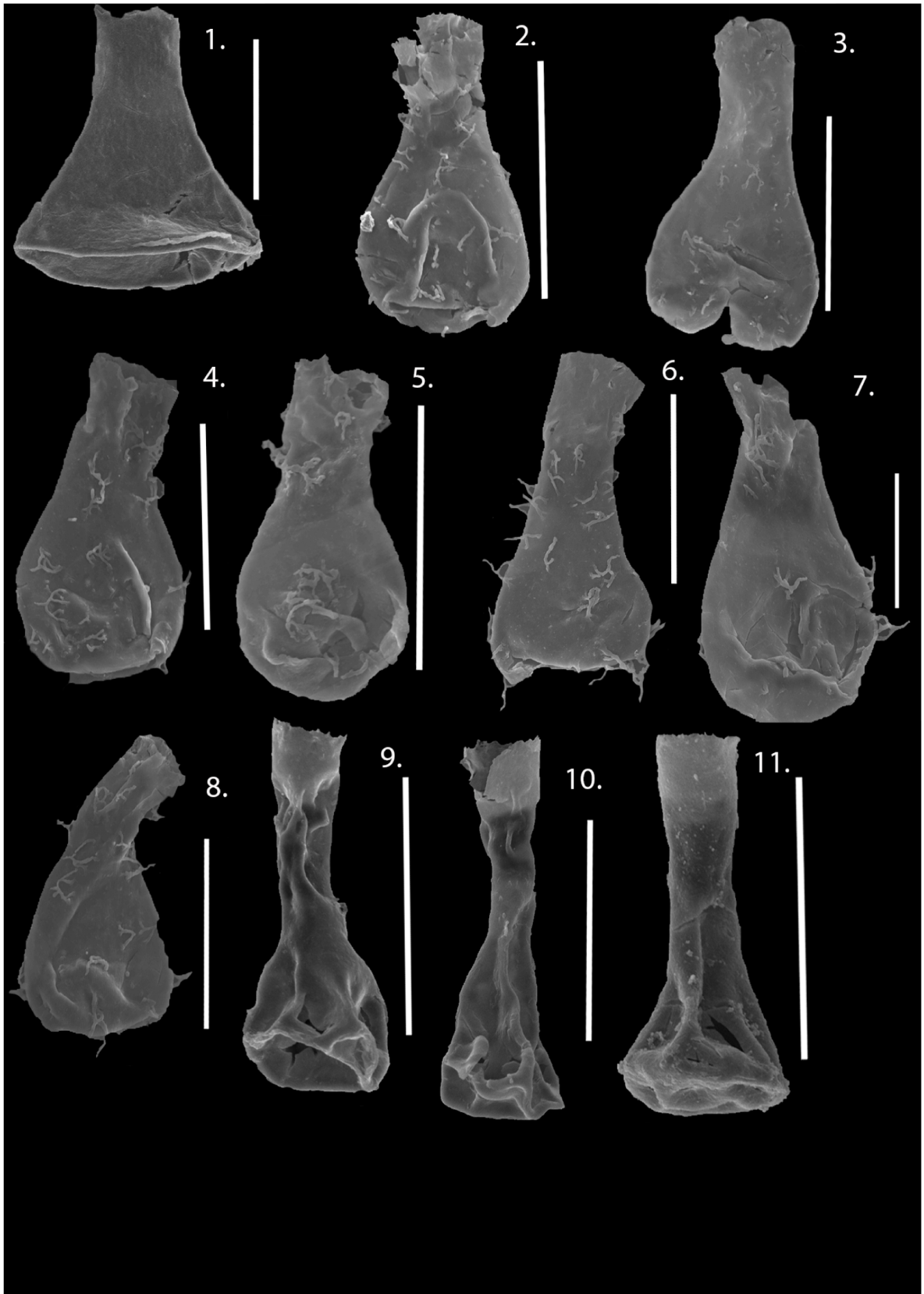


PLATE 4

All scale bars are 100 μ m unless indicated otherwise and placed on the right side of the vesicle.

1. *Angochitina* sp. 2, sample IGS-527-487
2. *Angochitina* sp. 1, sample IGS-527-477
3. *Angochitina* sp. 1, sample IGS-527-477
4. *Angochitina* sp. 1, sample IGS-527-490
5. *Angochitina* sp. 1, sample IGS-527-510
6. *Angochitina hansonica*, sample IGS-527-490
7. *Angochitina hansonica*, sample IGS-527-490
8. *Angochitina capillata*, sample IGS-527-545
9. *Angochitina hansonica*, sample IGS-527-490
10. *Angochitina hansonica*, sample IGS-527-490
11. *Angochitina* sp. 1, sample IGS-527-477
12. *Angochitina capillata*, sample IGS-527-541
13. *Angochitina capillata*, sample IGS-527-545
14. *Angochitina capillata*, sample IGS-527-541
15. *Angochitina capillata*, sample IGS-527-541

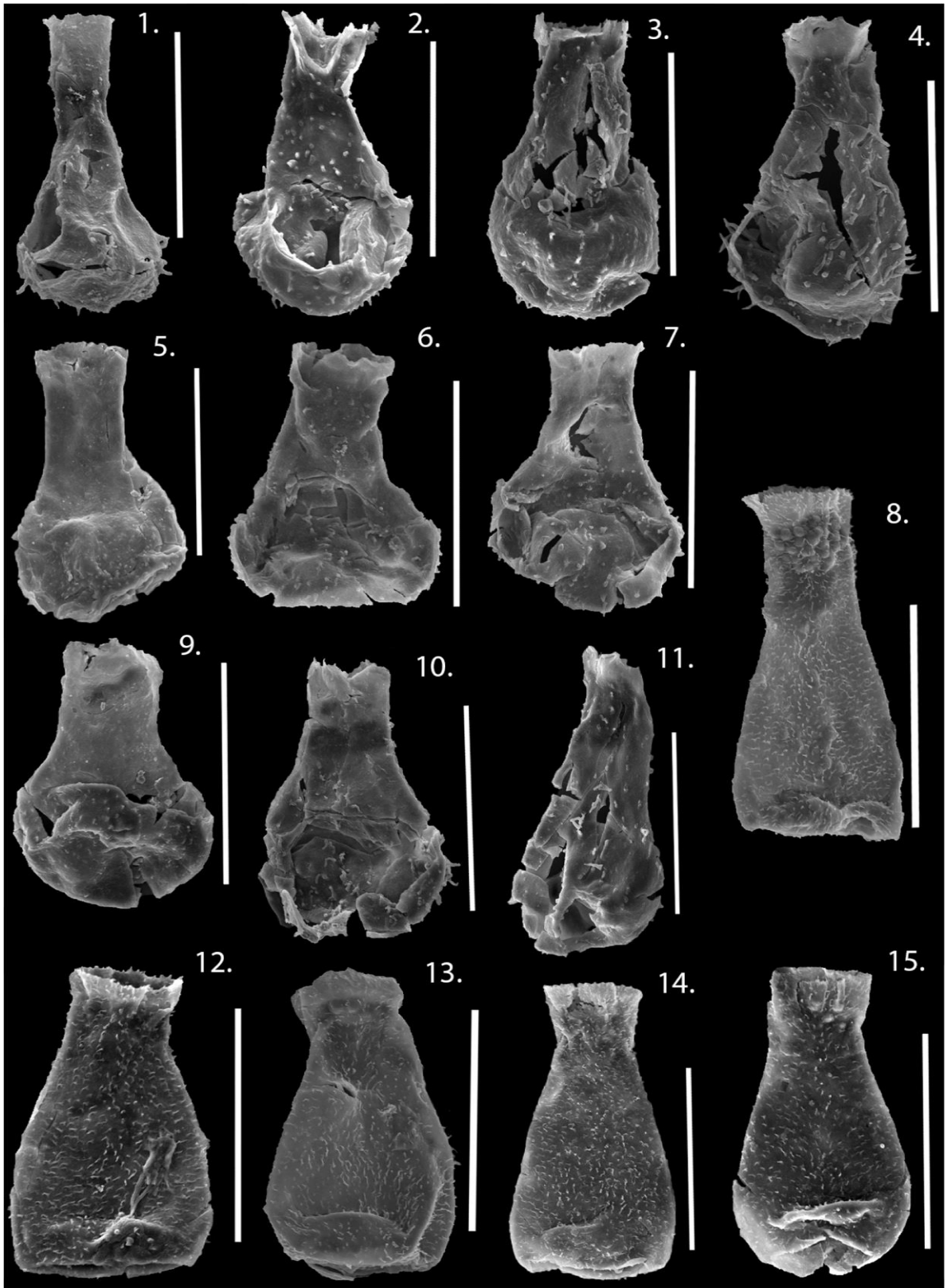


PLATE 5

All scale bars are 100 μm unless indicated otherwise and placed on the right side of the vesicle.

1. *Angochitina capillata*, sample IGS-527-545
2. *Fungochitina illinoisensis*, sample IGS-527-472
3. *Fungochitina illinoisensis*, sample IGS-527-477
4. *Fungochitina illinoisensis*, sample IGS-527-477
5. *Fungochitina illinoisensis*, sample IGS-527-490
6. *Ancyrochitina* sp. 1, sample IGS-527-482
7. *Ancyrochitina* sp. 1, sample IGS-527-490
8. *Ancyrochitina spongiosa*, sample IGS-527-512
9. *Ancyrochitina spongiosa*, sample IGS-527-512
10. *Strange looking specimen*, sample IGS-527-521, scale bar = 200 μm
11. *Strange looking specimen*, sample IGS-527-521, scale bar = 200 μm
12. *Ancyrochitina spongiosa*, sample IGS-527-512

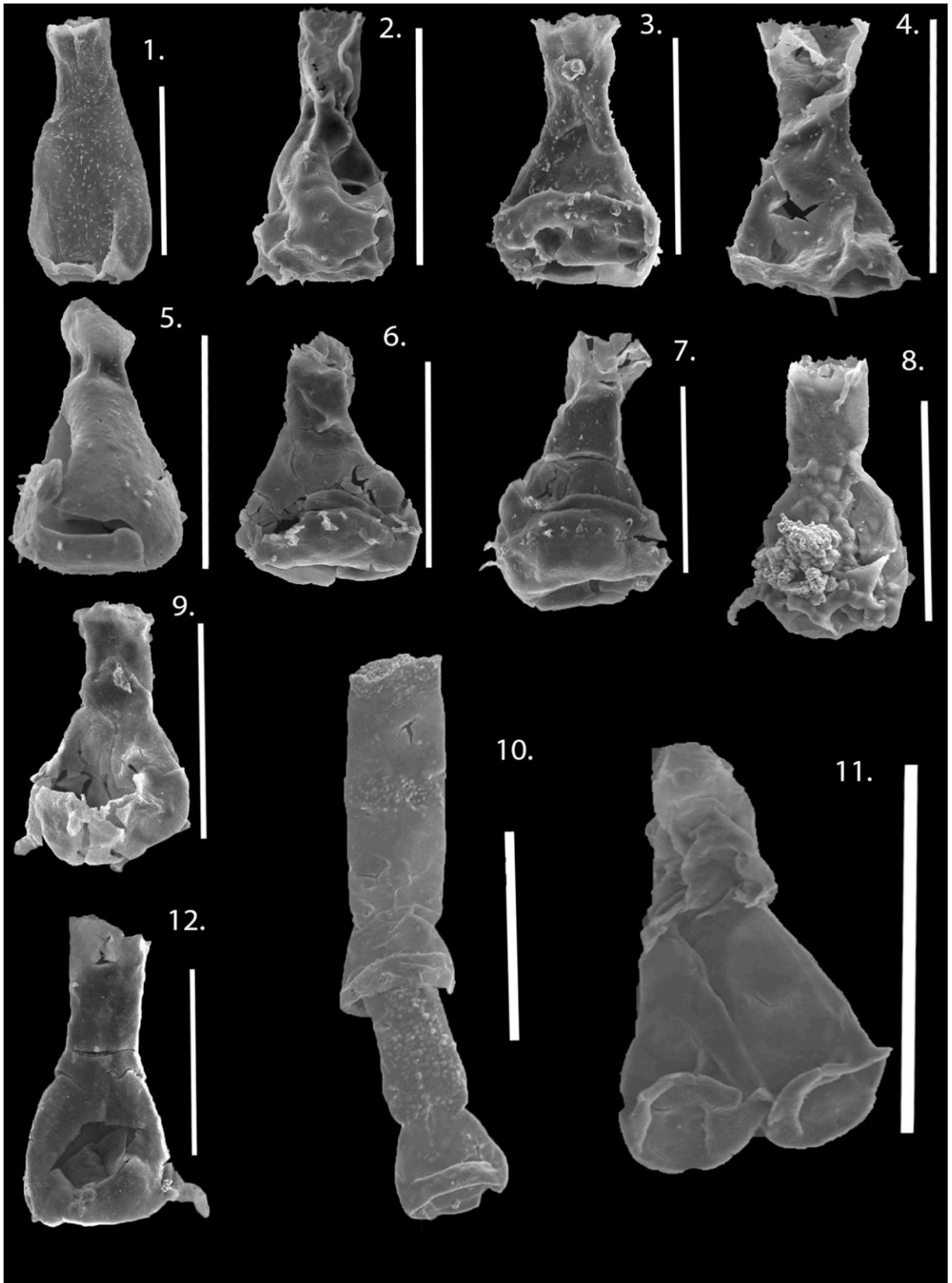


PLATE 6

All scale bars are 100 μm unless indicated otherwise and placed on the right side of the vesicle.

1. *Tanuchitina ontariensis*, sample IGS-527-545
2. *Tanuchitina ontariensis*, sample IGS-527-545, scale bar = 50 μm
3. *Tanuchitina ontariensis*, sample IGS-527-541
4. *Tanuchitina ontariensis*, sample IGS-527-541
5. *Tanuchitina ontariensis*, sample IGS-527-541
6. *Tanuchitina ontariensis*, sample IGS-527-541
7. *Tanuchitina ontariensis*, sample IGS-527-543
8. *Tanuchitina ontariensis*, sample IGS-527-545
9. *Tanuchitina ontariensis*, sample IGS-527-545
10. *Tanuchitina ontariensis*, sample IGS-527-545, scale bar = 50 μm
11. *Ancyrochitina nodifera*, sample IGS-527-506
12. *Ancyrochitina nodifera*, sample IGS-527-495
13. *Ancyrochitina nodifera*, sample IGS-527-495
14. *Ancyrochitina nodifera*, sample IGS-527-510

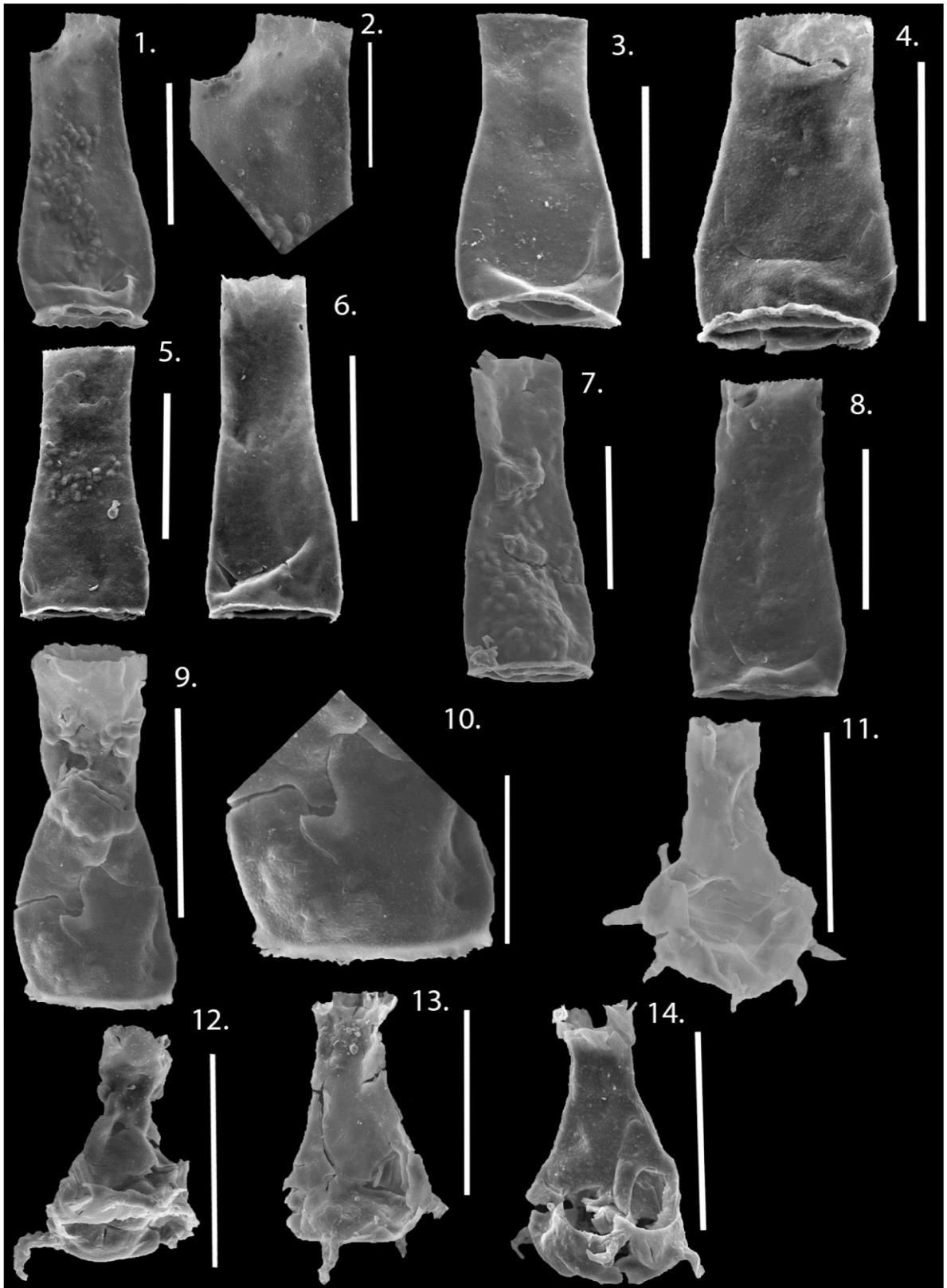


PLATE 7

All scale bars are 500 μm unless indicated otherwise and placed on the right side of the vesicle.

1. *Tanuchitina bergstroemi*, sample IGS-527-519
2. *Tanuchitina bergstroemi*, sample IGS-527-519
3. *Tanuchitina bergstroemi*, sample IGS-527-519, scale bar = 200 μm
4. *Tanuchitina bergstroemi*, sample IGS-527-521
5. *Tanuchitina bergstroemi*, sample IGS-527-521
6. *Tanuchitina bergstroemi*, sample IGS-527-521, scale bar = 200 μm
7. *Tanuchitina bergstroemi*, sample IGS-527-523
8. *Ancyrochitina merga*, sample IGS-527-536, scale bar = 50 μm
9. *Ancyrochitina merga*, sample IGS-527-536, scale bar = 100 μm
10. *Hercochitina turnbulli*, sample IGS-527-521, scale bar = 100 μm
11. *Hercochitina turnbulli*, sample IGS-527-521, scale bar = 100 μm
12. *Hercochitina turnbulli*, sample IGS-527-521, scale bar = 100 μm

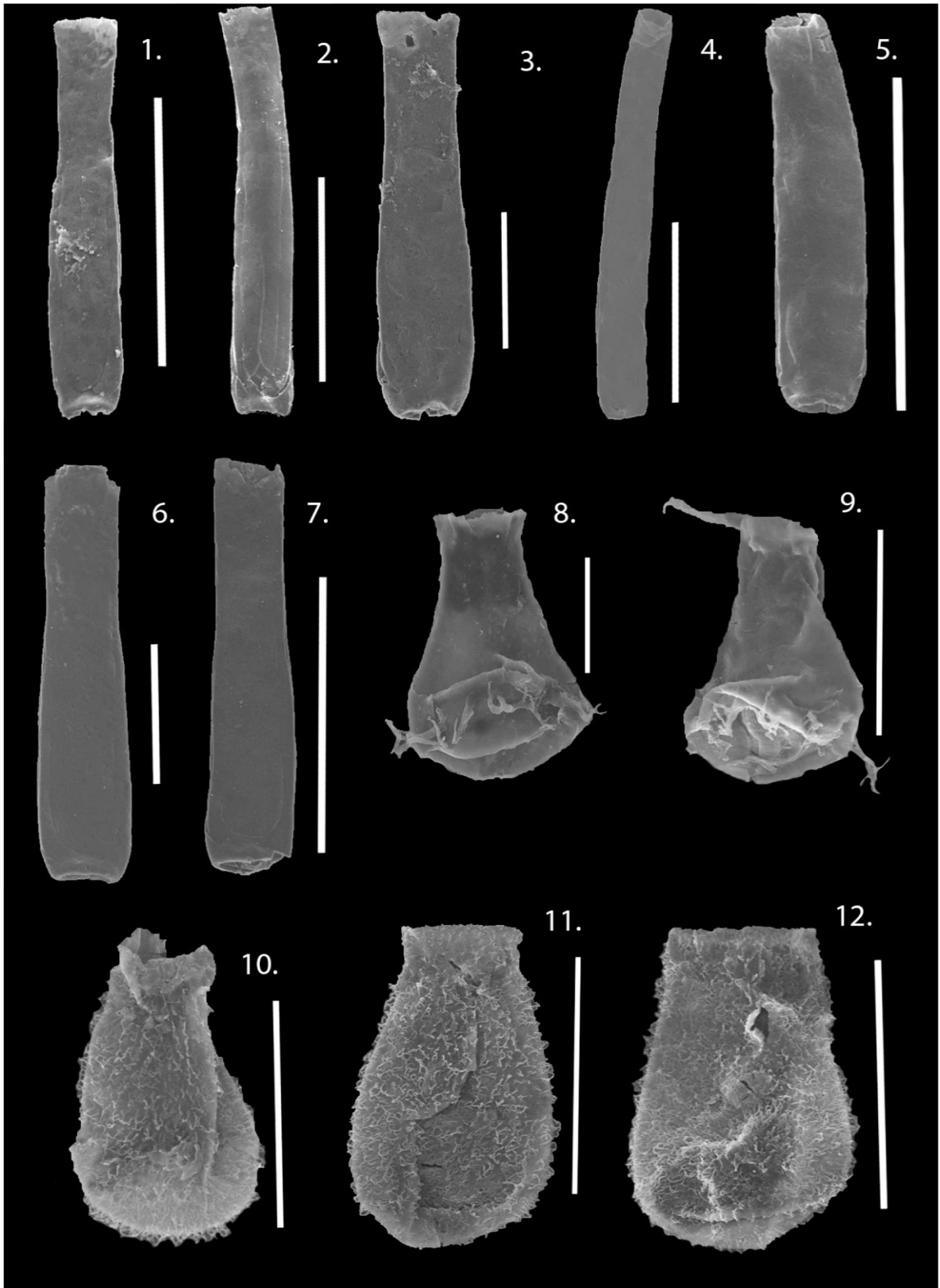


PLATE 8

All scale bars are 200 μm unless indicated otherwise and placed on the right side of the vesicle.

1. *Conochitina elegans*, sample IGS-527-519, scale bar = 500 μm
2. *Conochitina elegans*, sample IGS-527-519
3. *Conochitina elegans*, sample IGS-527-521
4. *Conochitina elegans*, sample IGS-527-521
5. *Conochitina elegans*, sample IGS-527-521
6. *Conochitina elegans*, sample IGS-527-523
7. *Hercochitina longi* sensu De Backer (2017), sample IGS-527-536, scale bar = 100 μm
8. *Hercochitina longi* sensu De Backer (2017), sample IGS-527-536
9. *Hercochitina longi* sensu De Backer (2017), sample IGS-527-536
10. *Belonechitina* sp. 1, sample IGS-527-512, scale bar = 100 μm
11. *Belonechitina* sp. 1, sample IGS-527-512, scale bar = 50 μm
12. *Belonechitina* sp. 1, sample IGS-527-512, scale bar = 100 μm
13. *Belonechitina* sp. 1, sample IGS-527-512, scale bar = 50 μm

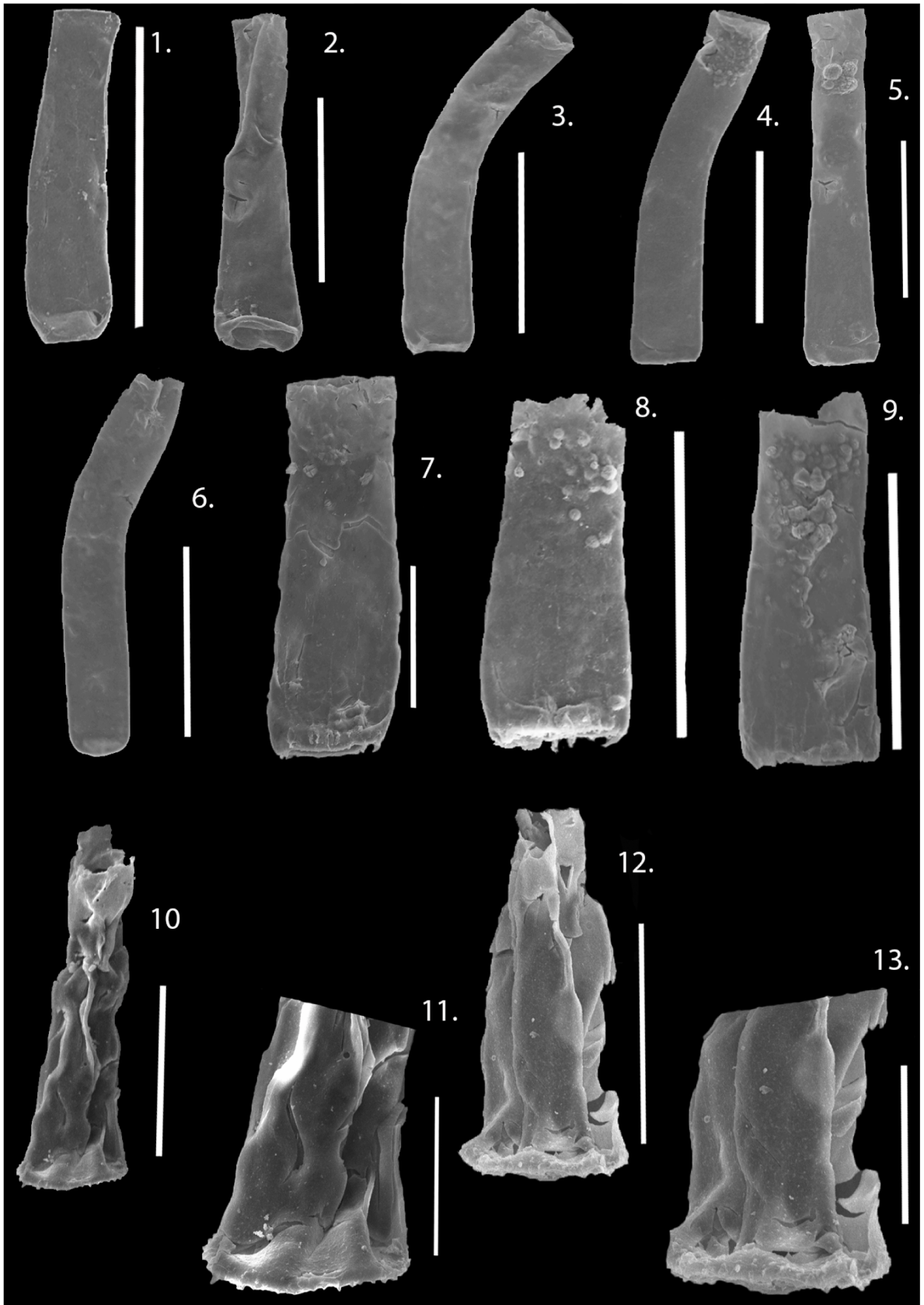


PLATE 9

All scale bars are 100 μm unless indicated otherwise and placed on the right side of the vesicle.

1. *Belonechitina* sp. 1, sample IGS-527-512
2. *Belonechitina* sp. 1, sample IGS-527-512, scale bar = 50 μm
3. *Hercochitina* sp. 2 sensu De Backer (2017), sample IGS-527-521
4. *Hercochitina* sp. 2 sensu De Backer (2017), sample IGS-527-521
5. *Hercochitina* sp. 2 sensu De Backer (2017), sample IGS-527-523
6. *Hercochitina* sp. 2 sensu De Backer (2017), sample IGS-527-523
7. *Hercochitina* sp. 2 sensu De Backer (2017), sample IGS-527-536
8. *Hercochitina* sp. 2 sensu De Backer (2017), sample IGS-527-536
9. *Kalochitina multispinata*, sample IGS-527-523
10. *Kalochitina multispinata*, sample IGS-527-523
11. *Kalochitina multispinata*, sample IGS-527-523

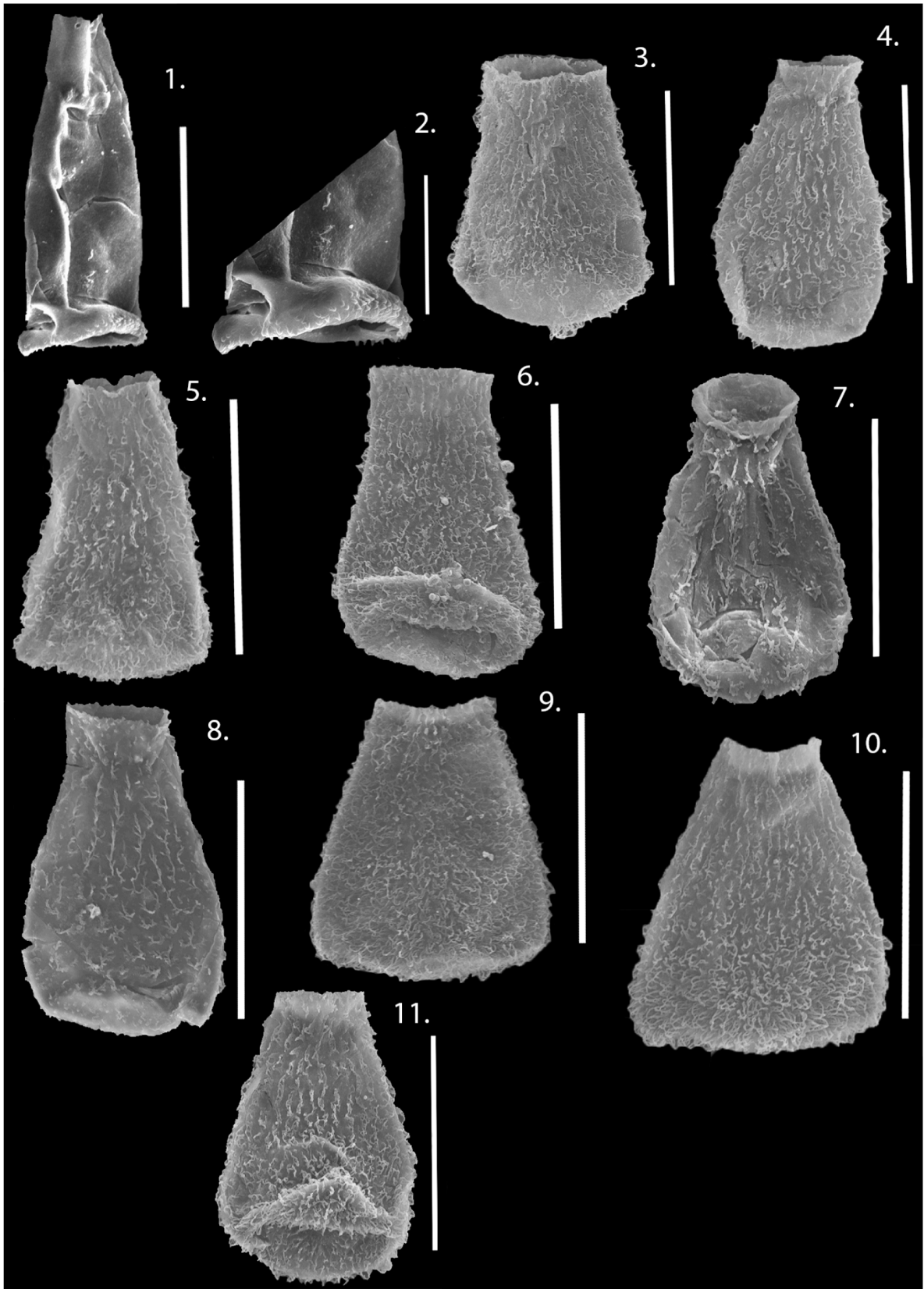


PLATE 10

All scale bars are 100 μm unless indicated otherwise and placed on the right side of the vesicle.

1. *Nevadachitina cf. praevininica*, sample IGS-527-530
2. *Nevadachitina cf. praevininica*, sample IGS-527-530
3. *Nevadachitina cf. praevininica*, sample IGS-527-530
4. *Nevadachitina cf. praevininica*, sample IGS-527-530
5. *Nevadachitina cf. praevininica*, sample IGS-527-530
6. *Nevadachitina cf. praevininica*, sample IGS-527-530
7. *Nevadachitina cf. praevininica*, sample IGS-527-530
8. *Nevadachitina cf. praevininica*, sample IGS-527-536, scale bar = 200 μm
9. *Nevadachitina cf. praevininica*, sample IGS-527-530
10. *Nevadachitina cf. praevininica*, sample IGS-527-530
11. *Nevadachitina cf. praevininica*, sample IGS-527-536



PLATE 11

All scale bars are 100 μm unless indicated otherwise and placed on the right side of the vesicle.

1. *Kalochitina multispinata*, sample IGS-527-536
2. *Kalochitina multispinata*, sample IGS-527-536
3. *Hercochitina pinguis*, sample IGS-527-536
4. *Hercochitina pinguis*, sample IGS-527-536
5. *Hercochitina pinguis*, sample IGS-527-536
6. *Hercochitina pinguis*, sample IGS-527-536
7. *Hercochitina pinguis*, sample IGS-527-536
8. *Belonechitina* sp. 3, sample IGS-527-519
9. *Belonechitina* sp. 3, sample IGS-527-521
10. *Belonechitina* sp. 3, sample IGS-527-523
11. *Belonechitina* sp. 3, sample IGS-527-523
12. *Belonechitina* sp. 3, sample IGS-527-523
13. *Belonechitina* sp. 3, sample IGS-527-523, scale bar = 50 μm

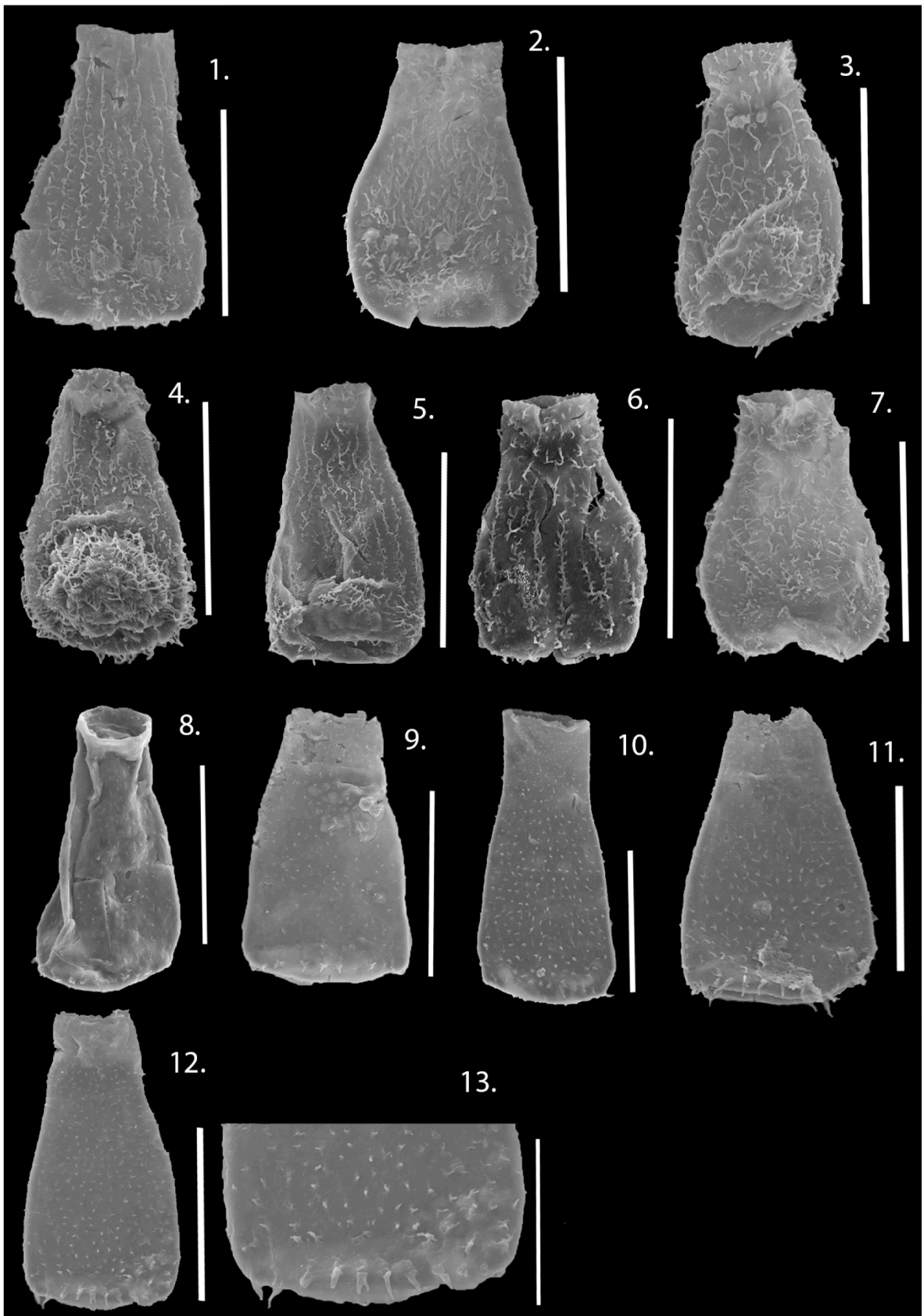


PLATE 12

All scale bars are 100 μm unless indicated otherwise and placed on the right side of the vesicle.

1. *Belonechitina micracantha*, sample IGS-527-521
2. *Belonechitina micracantha*, sample IGS-527-521
3. *Belonechitina micracantha*, sample IGS-527-523, scale bar = 200 μm
4. *Belonechitina micracantha*, sample IGS-527-523
5. *Belonechitina micracantha*, sample IGS-527-523, scale bar = 20 μm
6. *Belonechitina micracantha*, sample IGS-527-523
7. *Belonechitina* cf. *cactacea*, sample IGS-527-524, scale bar = 50 μm
8. *Belonechitina* cf. *cactacea*, sample IGS-527-524

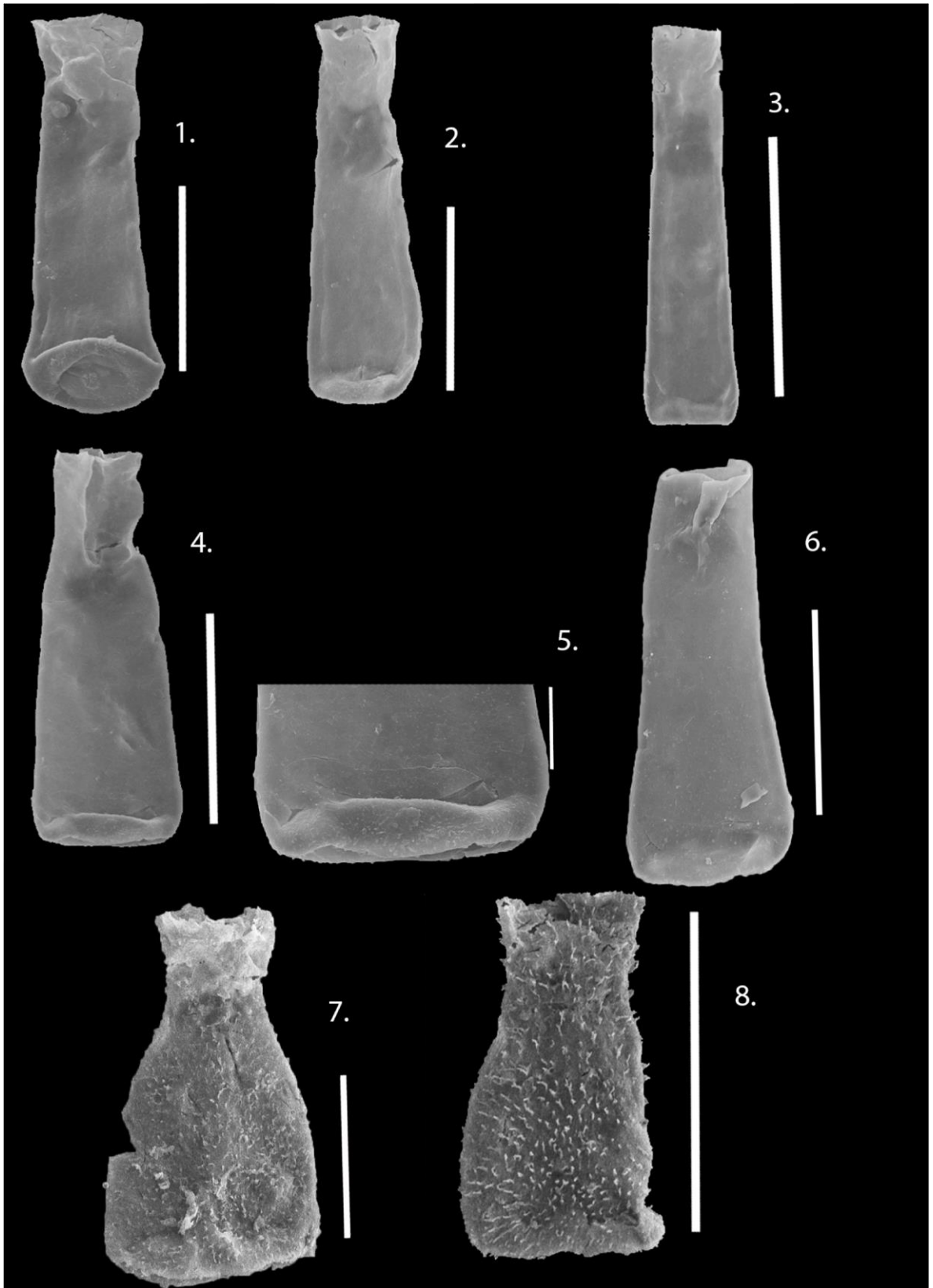


PLATE 13

All scale bars are 100 μ m unless indicated otherwise and placed on the right side of the vesicle.

1. *Belonechitina* sp. 2 sensu Meyvisch (2018), sample IGS-527-530
2. *Belonechitina* sp. 2 sensu Meyvisch (2018), sample IGS-527-530
3. *Belonechitina* sp. 2 sensu Meyvisch (2018), sample IGS-527-524
4. *Belonechitina* sp. 2 sensu Meyvisch (2018), sample IGS-527-530
5. *Belonechitina* sp. 2 sensu Meyvisch (2018), sample IGS-527-530
6. *Belonechitina* sp. 2 sensu Meyvisch (2018), sample IGS-527-530
7. *Belonechitina* sp. 2 sensu Meyvisch (2018), sample IGS-527-530
8. *Belonechitina* sp. 2 sensu Meyvisch (2018), sample IGS-527-530
9. *Belonechitina* sp. 2 sensu Meyvisch (2018), sample IGS-527-530
10. *Belonechitina* sp. 2 sensu Meyvisch (2018), sample IGS-527-530
11. *Belonechitina* sp. 2 sensu Meyvisch (2018), sample IGS-527-530

